A Hydroecological Assessment of Hydraulic Connectivity: Phase 3 Field Investigation at Otter Park, Langley

Adam J. Mitton, Diana M. Allen, and Alexandre H. Nott

September 2024

BRITISH COLUMBIA

SFU SIMON FRASER UNIVERSITY
THINKING OF THE WORLD

Author's Affiliation:
Adam J. Mitton, PhD student
Department of Earth Sciences
Simon Fraser University

Diana M. Allen, P.Geo.
Department of Earth Sciences
Simon Fraser University

Alexandre Nott, MSc student
Department of Earth Sciences
Simon Fraser University

Cover Photograph: Bertrand Creek at Otter Park in Langley, B.C. by Adam Mitton

EXECUTIVE SUMMARY

This report summarizes an investigation of how hydrological variability influences instream habitat and stream organisms in Bertrand Creek at Otter Park in Langley Township, British Columbia. This project is an extension of a multi-year study focused on aquifer-stream exchange. Phase 2 of the study focused on the hydrological response of the aquifer, the stream, and their interactions during pumping. Two pumping tests were carried out to analyze and quantify the potential impacts of groundwater pumping on streamflow (i.e., streamflow depletion). This ecological study compliments the Phase 2 study because the results provide context to understand potential ecological impacts of streamflow depletion caused by groundwater pumping. This study was primarily motivated by observations of the stream going completely dry at Otter Park during the period between the two pumping tests. Stream drying is a unique hydrological behaviour relative to most stream sites in the region. Therefore, it is important to understand the distinct hydroecological characteristics at the site as they are hypothesized to be key factors for managing groundwater. Stream drying is associated with hotter and drier conditions that typically prevail during the summer; therefore, this study focused on the period from May through the end of September of 2020 and 2021.

The hydrological monitoring network installed at Otter Park in 2018 used to characterize hydrological variability consisted of groundwater monitoring wells, a pumping well, instream piezometers, and hydrometric stations. Although this study focused on 2020 and 2021, streamflow data for all years were analyzed to examine whether stream drying was a rare occurrence. Habitat and macroinvertebrate sampling began in 2020 to characterize how habitat conditions and benthic communities varied with hydrological variables as conditions became drier over the summer. Macroinvertebrates samples were collected each month from June through September using a Surber net at eight sites spaced throughout the reach between riffle habitat and pool habitat. Benthic samples were followed by measurement of water quality variables (DO, pH, EC,) and hydraulic habitat variables (velocity, depth, substrate) at each location.

Hydrometric data revealed that stream drying observed in 2018 was consistent with dominant hydrological patterns at Otter Park. Stream drying is proceeded by flow cessation, which occurred each year. However, the intensity of channel drying that occurred in 2018 did not occur in other years, aside from in 2021 which experienced the greatest intensity of channel drying. Drier and hotter conditions also drove earlier onset and longer duration of flow cessation events. While the occurrence of flow cessation was consistent over the four years of study in the upstream segment of the Otter Park study reach, flow was persistent in the downstream segment through each period of flow cessation, excluding a short period of flow cessation in the downstream reach that occurred in 2019. A dominantly positive upward mean hydraulic gradient for the upstream segment suggested that groundwater contribution to the stream helped maintain streamflow in the downstream reach through these dry periods. The regular (annual) occurrence of flow cessation at Otter Park likely extends even further than these data, as reports of regular flow cessation date to before 2010 (Avery-Gomm 2013).

Macroinvertebrate and habitat sampling data revealed important ecological consequences of the recurrence of flow cessation and drying. Extremely low richness and diversity of the benthic macroinvertebrate community assemblages in riffle habitat and pool habitat is likely due the loss of many taxa in response to adverse changes in habitat conditions associated with flow cessation and drying since the few taxa present at Otter Park are extremely well adapted to these systems and thus are often some of the most dominant taxa in non-perennial systems. Despite being well adapted, substantial declines in abundance and even total loss of some taxa due to flow cessation was likely reflective of the habitat preferences of different invertebrate taxa and their ability to avoid adverse

changes in habitat conditions by seeking out refuge habitats, such as wetted interstitial spaces in the hyporheic zone or in perennial pools.

Modelling of relationships between benthic macroinvertebrate abundance and habitat variables suggested that DO and velocity were the significant drivers of spatial and temporal variability in benthic macroinvertebrate abundance. Both DO and velocity conditions were generally better in riffle habitat than pool habitat. As such, riffles consistently had more prey for the riffle-dwelling Nooksack Dace than pool habitat. However, analysis of relationships between depth, velocity, and stream temperature with discharge revealed far greater sensitivity of these variables to changes in discharge in riffle habitat than in pool habitat. This sensitivity results in riffle habitats drying and heating more quickly, which likely adversely affects macroinvertebrate populations, a phenomenon already observed in the Nooksack Dace. However, the maintenance of standing pools, which has been shown to help Nooksack Dace to persist through dry periods, likely provides refuge for their macroinvertebrate prey as well.

Unfortunately, the maintenance of habitat at zero discharge is one of the unique characteristics of hydrological and habitat variability in non-perennial systems that challenges and likely precludes the routine application of many common environmental flow assessment methodologies in these systems. This was evidenced by the failure of a common habitat modelling approach to capture and convey the true patterns in habitat availability in the stream. However, non-zero y-intercepts for curves generated using the wetted width method suggested that the wetted width method may in fact be useful for flow assessments. However, the scarcity of literature on non-perennial systems, especially for Canada, and especially in relation to the transferability of ecological concepts and environmental flow assessment methodologies, necessitates future studies to be able to incorporate non-perennial systems into our management frameworks and adequately address their unique hydroecological characteristics.

Bertrand Creek, particularly at Otter Park, is an intermittent stream, often experiencing periods where it dries up, a pattern that has been consistent for over two decades. However, it is unclear how much of this dryness is due to natural cycles versus human activities because detailed data on water use and historical streamflow records are lacking. Our study highlights that habitat changes in Bertrand Creek are not uniform; different sections respond differently to environmental shifts. In particular, pools are crucial for the survival of both fish and benthic macroinvertebrates, serving as refuge habitats during dry spells. Recognizing that intermittent streams like Bertrand Creek remain biologically active even when they are not flowing challenges traditional assumptions and underscores the need for careful water management during both flowing and non-flowing periods to protect the stream's diverse and vital ecosystems.

CONTENTS

1. <u>INTRODUCTION</u>

Groundwater discharge to stream systems has an important functional role in stream ecology. For example, groundwater discharge can act as a buffer to droughts or hot weather by stabilizing streamflow and moderating stream temperature fluctuations. These effects of groundwater on the stream can promote habitat availability and maintain values of habitat characteristics within ranges to which aquatic species are adapted (Brunke and Gonser 1997; Poff et al. 1997; Poole and Berman 2001; Boulton and Hancock 2006). Therefore, human activities, such as groundwater abstraction, which can alter the direction and magnitude of aquifer-stream exchanges, can adversely impact aquatic ecosystems (de Graaf et al. 2019). Deteriorating ecological health due to the effects of anthropogenic hydrological alterations is a pervasive issue in developed watersheds and likely will be exacerbated by increasing drought frequency and groundwater demand (Kløve et al. 2014; de Graaf et al. 2019). However, predicting the potential ecological impacts of anthropogenic alterations to the groundwater system remains a challenge due to a lack of understanding of the nature of aquifer-stream exchanges and how aquatic ecosystems depend on them (Boulton and Hancock 2006; Arthington et al. 2018).

Complex spatial and temporal variability in aquifer-stream exchanges can result in varying degrees of groundwater dependency that are difficult to quantify (Brunke and Gonser 1997; Boulton and Hancock 2006). At the reach scale, local flow systems interact with land surface topography, streambed topography, and streambed roughness features to determine whether a stream reach is gaining groundwater or losing water to the groundwater system (Harvey and Bencala 1993; Cardenas et al. 2004). A single stream reach may even have alternating gaining and losing sections, especially in smaller watersheds (Sophocleous 2002). As the direction of the streambed flux is controlled by the height of the groundwater table relative to the stream stage, changes in precipitation, recharge, and surface and subsurface water withdrawals may cause a stream or stream reach to switch from gaining or losing over time (Sophocleous 2002).

In many regions, especially those with seasonal patterns of hot and dry weather, temporal variability in aquifer-stream exchange dynamics may lead to the cessation of streamflow, or the complete drying of the channel. Ecological responses to flow and aquifer-stream exchange variability are especially not well understood in these systems because studies of flow-ecology relationships have focused largely on perennial systems. Therefore, studies involving monitoring and characterizing variability in streamflow and aquifer-stream exchange and associated dynamics of instream habitat and biota in intermittent streams are crucial to building a holistic understanding of these unique environments.

This study was carried out in Bertrand Creek at Otter Park in Langley, British Columbia (B.C.) (Figure 1). The regional climate of the Lower Fraser Valley is temperate with dry summers (Peel et al. 2007). Based on climate normals (1981-2010) for the Environment and Climate Change Canada (ECCC) station at the Abbotsford International Airport (Climate ID: 1100030), located 13 km from the field site, over 400 mm of precipitation (mostly rain) falls during the winter months (December to February), while summers (June to August) see just over 150 mm. July and August are the driest and hottest months, each with just over 40 mm of precipitation and average daily air temperatures topping just over 18°C. September typically has more precipitation, but the first half of the month is often as dry as August.

The Abbotsford-Sumas Aquifer is the unconfined aquifer underlying the site. It is a late glacial outwash aquifer composed of sand and gravel (Aquifer 15; https://apps.nrs.gov.bc.ca/gwells/aquifers/15). The aquifer extends from Abbotsford and Langley, B.C. into Washington State, USA. Bertrand Creek is hydraulically connected to the Abbotsford-Sumas Aquifer. In some reaches streamflow is maintained throughout the summer by groundwater discharge (Berg and Allen 2007). Precipitation is the primary source of recharge to the aquifer, so variability in precipitation and associated variability in recharge can

impact streamflow (Scibek and Allen 2005). In addition, groundwater pumping tests at the Otter Park field site demonstrated that pumping causes streamflow depletion and thereby impacts the spatial and temporal variability of streamflow (Allen et al. 2020).

Highly valued ecological components in Bertrand Creek are the two endangered fish species, the Nooksack Dace (Fisheries and Oceans Canada 2008, 2019) and the Salish Sucker (Fisheries and Oceans Canada 2020). Bertrand Creek holds critical habitat for both fish species, and Otter Park itself is considered critical habitat for the Nooksack Dace (Fisheries and Oceans Canada 2008, 2019). Avery-Gomm et al. (2014) list a number of co-occurring fish species in Bertrand Creek, including coastal cutthroat trout (*Oncorhynchus clarkia*), rainbow and steelhead trout (*Oncorhynchus mykiss*), and coho salmon (*Oncorhynchus kisutch*). However, it is unclear if these larger fishes frequent Otter Park and reaches further upstream because connectivity to upstream reaches may be limited by the characteristically low flows at Otter Park (Avery-Gomm 2013). Meteorological drought and the related low flows are leading threats to both the Salish Sucker (Fisheries and Oceans Canada 2020) and Nooksack Dace (Fisheries and Oceans Canada 2008, 2019). Water quality is also a concern for both these fishes and likely also for the macroinvertebrate prey of the Nooksack Dace (Fisheries and Oceans Canada 2018, 2019, 2020; Hilsenhoff 1987). Flow cessation and seasonal channel drying of Bertrand Creek near Otter Park motivated the decision to use Otter Park for this study.

Figure 1: Bertrand Creek Watershed in the Lower Fraser Valley of British Columbia. The location of the Otter Park field study site is shown.

1.1 Previous Research at Otter Park and Bertrand Creek Watershed

This study constitutes Phase 3 of a multi-year project aimed at investigating aquifer-stream interactions and streamflow response to groundwater pumping. Phase 1 consisted of a targeted field study in Langley, B.C. (Union Creek at Steele Park) to determine the impacts of pumping on aquifer-stream interactions in an unconfined aquifer. The study included testing various analytical methods for quantifying streamflow depletion from groundwater pumping (Hall et al. 2017). Phase 1 yielded valuable data and provided critical knowledge surrounding how to conduct a field study to assess hydraulic connectivity. Phase 2 was carried out at Otter Park from May 2018 to October 2018 (Allen et al. 2020). Phase 2 had four main objectives 1) Estimating the hydraulic conductivity (K) of the aquifer and streambed sediments using grain size analysis and slug testing; 2) Estimating the transmissivity (T), hydraulic conductivity, and specific yield (Sy) of the aquifer from pumping test data; 3) Characterizing the hydraulic connectivity between the stream and the aquifer; and 4) Quantifying streamflow depletion during pumping and evaluating against a streamflow depletion model.

Over the past several years, staff from the B.C. Ministry of Water, Land and Resource Stewardship (WLRS) observed that Otter Park was prone to flow cessation and channel drying. These observations motivated Phase 3 of this study. In 2018, the year pumping tests were conducted, streamflow at Otter Park ceased and large portions of the reach completely dried (Figure 2). This raised the questions: why does Otter Park dry in the summer?

Using a steady-state numerical groundwater flow model, Nott and Allen (2020) found that Otter Park is likely prone to drying because reaches upstream of Otter Park are dominantly losing, while downstream of Otter Park are both gaining and losing reaches (Figure 3). However, data from 2018 suggested that Otter Park might vary between gaining and losing over the course of the summer (Allen et al. 2020). This finding motivated a detailed look at spatial and temporal variability in aquifer-stream exchange, groundwater level, and streamflow. With these unique hydrological characteristics and Otter Park being one of five reaches in Bertrand Creek hosting critical habitat for the endangered Nooksack Dace, Otter Park was the ideal site to study potential linkages between hydrological processes and ecological responses, which are important to understand for defining minimum flow requirements of a stream. Moreover, seasonal lack of water is a key management concern for the preservation of Nooksack Dace and the endangered Salish Sucker (Kerr Wood Leidal Associates Ltd. 2009; Avery-Gomm 2013; Fisheries and Oceans Canada 2019, 2020); therefore, Otter Park was ideal for studying ecological responses to low flows and drying in intermittent streams.

Figure 2: (a) Pool habitat in the upstream segment of the Otter Park reach in May 2018 and (b) August 2018. (c) Riffle habitat in the upstream segment of the Otter Park reach in May 2018 and (d) August 2018.

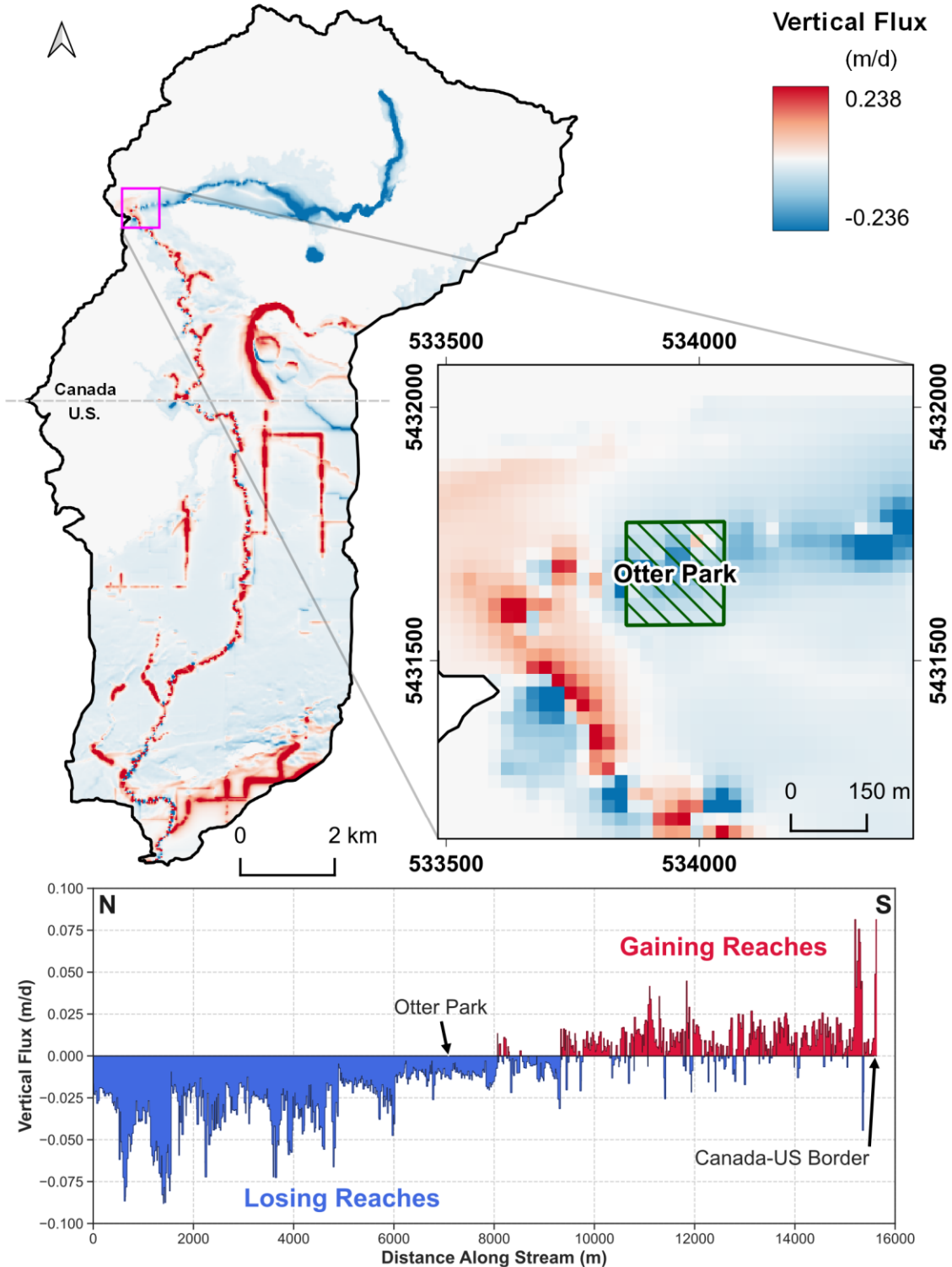*Figure 3: Vertical flux map of the Bertrand Creek Watershed within the first model layer of the non-pumping groundwater flow model described by Nott and Allen (2020). Areas in blue indicate a negative flux down into the aquifer (groundwater recharge) while areas in red indicate a positive flux up out of the aquifer (groundwater discharge). Areas in white have no component of vertical flux. Figure from Nott and Allen (2020).*

1.2   Purpose and Objectives of Study

The purpose of this study was to develop a better understanding of how streamflow, groundwater flow, and aquifer-stream exchange influence instream habitat and stream organisms within an intermittent stream. In addition, the study explored how ecological and hydrological tools might be used to assess how groundwater pumping might influence streamflow and the consequences on instream habitat.

The objectives included:

1) Design, instrument, and carry out sampling of various physical, chemical, and biological parameters at the Otter Park field site continuously over two successive summer low flow periods.
2) Examine the relationships among the parameters (e.g., correlations among the various parameters, trends or distinct differences between the seasons, thresholds that might serve as useful indicators of responses of aquatic communities to changing instream conditions) and develop potential response graphs for each parameter in relation to changes in streamflow.
3) Use analytical and numerical groundwater models to investigate how groundwater pumping (scenario modeling) influences streamflow (i.e., streamflow depletion) and, consequently, habitat.

The study at Otter Park focused on the period from May 2020 to October 2020 but included hydrological data for the period from May 2018 to October 2021. Variability in habitat conditions was characterized over the summer to observe how changes in streamflow impacts the spatial variability of physical and chemical parameters. Macroinvertebrate community dynamics were monitored to examine how communities responded to changes in habitat. Macroinvertebrates were selected for this study because of their ubiquity and widespread use in biomonitoring.

2.   THE FIELD PROGRAM

2.1   Hydrological Monitoring Network

Otter Park was first instrumented in 2018 for the field investigation of pumping impacts on streamflow conducted in Phase 2 (Allen et al. 2020). One pumping well and three groundwater monitoring wells (Figure 4a) were installed in March 2018. The pumping well, PW01, is screened from 16.8 – 19.8 m depth, MW02 and MW01 are screened from 16.8 – 18.3 m depth and monitoring well MW03 is screened from 27.4 – 29.0 m depth. This original network also incorporated instream piezometer pairs and hydrometric stations (Figure 4b); however, the piezometers and hydrometric stations were removed in October 2018 to avoid damage over the winter months.
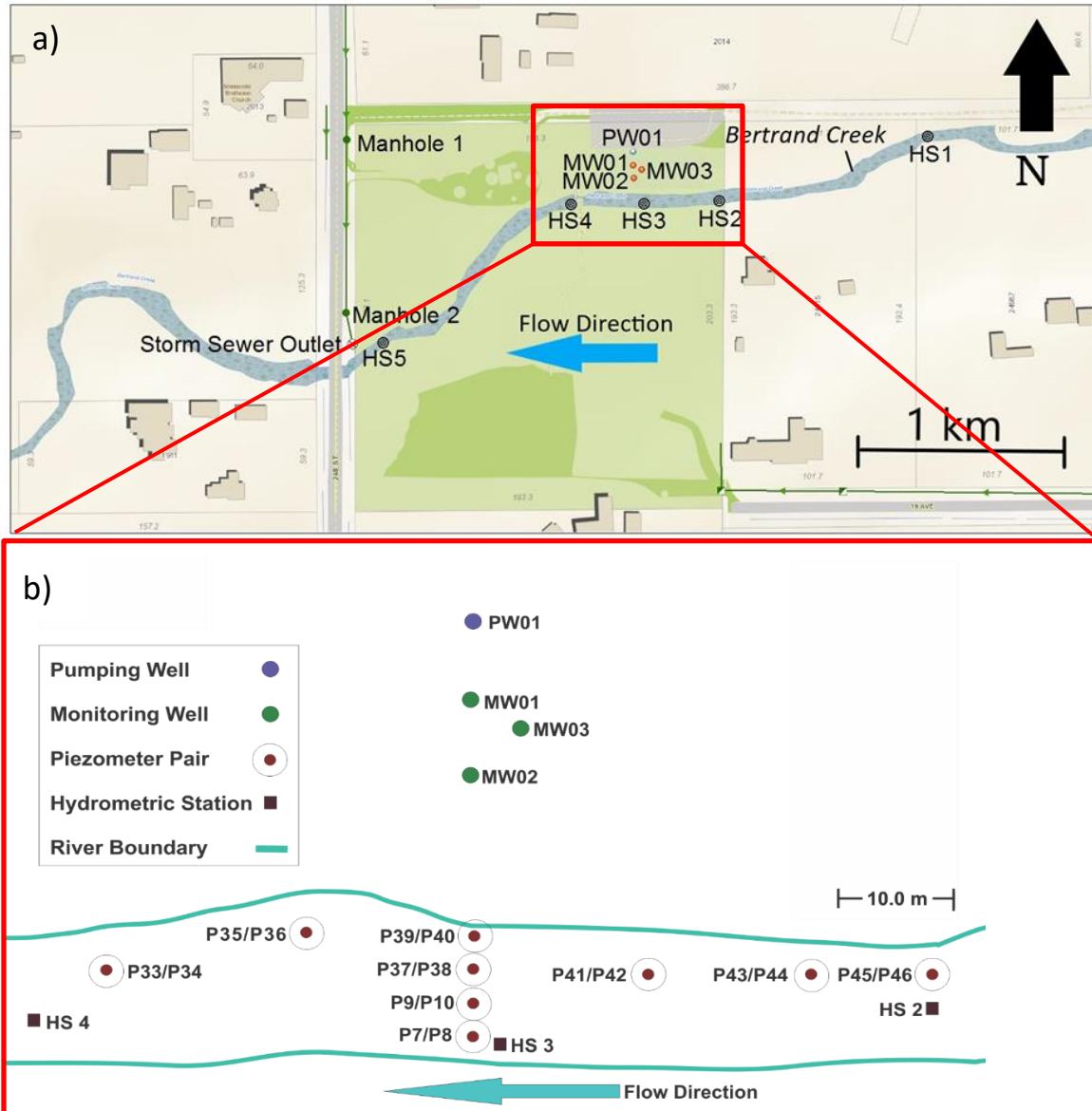
Figure 4: (a) Hydrological monitoring network configuration in 2018 at Otter Park for Phase 2 of the field study. Shown are the locations of the pumping well (PW01) and the monitoring wells (MW01, MW02, and MW03) along with the site hydrometric stations (HS1, HS2, HS3, HS4, and HS5). (b) Network of intream piezometers used in Phase 2.

The site was re-instrumented for Phase 3 in May 2019 (Figure 5). Two hydrometric stations, one upstream from the wells in a pool, HS2, and one downstream in a riffle, HS5, were installed on May 9th, 2019. Over the study period, discharge measurements were made by WLRS staff to develop station-specific rating curves to calculate streamflow from the continuous stage data. Rating curve development was done using AQUARIUS software by WLRS staff.

Seven nested instream piezometer pairs (i.e., one deep and one shallow) were installed, with the deeper piezometers (denoted by lower numbers in Figure 5) screened at depths of around 1.05 m and the shallow piezometers (denoted by higher numbers in Figure 5) screened at depths of around 0.4 m to create a separation of around 0.65 m for each pair. Piezometer D37 was knocked down during winter

high flows, so D36/D37 data are omitted from this study. Solinst Leveloggers were deployed in each of the instream piezometers, and Onset HOBO loggers were installed in the groundwater wells and hydrometric stations to log water levels and temperatures continuously. Temperature recorded by the HOBO loggers installed at hydrometric stations and groundwater wells was used to represent stream temperature and groundwater temperature, respectively. Canopy coverage for the area around the hydrometric stations was visually assessed and recorded as a percentage of the stream section adjacent to each station with overhead canopy cover (Environment Canada 2011). One HOBO TidbiT v2 temperature logger was attached to a tree adjacent to the site to monitor air temperature. On the bank opposite the air temperature logger, loggers were hung from trees to measure barometric pressure. All instruments were set to record data continuously at 15-minute intervals with some short interruptions due to data downloads.
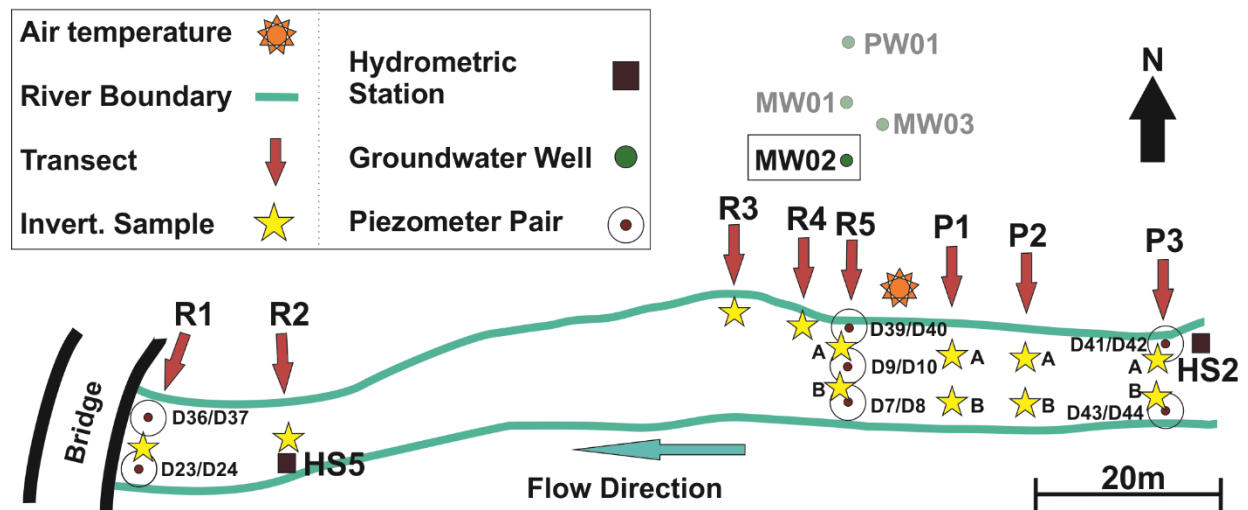
Figure 5: Hydrological monitoring network configuration and locations of macroinvertebrate and habitat sampling sites for Phase 3. The macroinvertebrate sampling sites (yellow stars) are numbered the same as the flow transects (red arrows). Where there are two sampling sites along a flow transect, the north location is A and the south location is B. Stream width is representative of wetted width in June.

2.2 Macroinvertebrate and Habitat Sampling

Macroinvertebrate and habitat sampling was carried out in 2020 and 2021 to characterize spatial and temporal variability in macroinvertebrate communities and habitat variables as flows declined from late spring to early fall. Selection of sampling locations involved identifying a similar number of sites in riffles (areas with turbulent, fast-flowing water) and pools (areas of slower, deeper water) in order to cover a broad range of habitat characteristics (Johnston and Slaney 1996).

Sampling occurred once per month in June, July, August, and September of 2020. In 2021, sampling only took place in June due to channel drying. Site visits occurred roughly 30 days apart to allow for recolonization of the disturbed substrate by macroinvertebrates. Sampling was carried out at 12 sites, labeled P1-P3 (pools) and R1-R5 (riffles) in Figure 5. Each visit began at site R3 and progressed upstream to avoid disturbing other sites during sampling. The two furthest downstream sites, R1 and R2, were sampled last because the channel length and complex channel features between R2 and R3 likely prevented disturbance from upstream activity. In the upstream area where the wetted width was greater, two macroinvertebrate samples were collected along each transect (Figure *5*). The sample location to the north is denoted with an A, while the south location is denoted with a B.

For each macroinvertebrate sample, the 30.5 cm x 30.5 cm frame of a 500 μm mesh Surber sampler was centered next to the site marker and the substrate within the frame was disturbed vigorously for two minutes to dislodge macroinvertebrates into the net on the downstream end. After two minutes, the net was removed, and its contents were placed in sample containers and preserved with isopropyl alcohol. Pool sites in September had insufficient flow to direct dislodged macroinvertebrates into the net, so the sediments within the Surber frame were scooped by hand into the net. Macroinvertebrate specimens were stored and identified within two weeks after their collection to the family level using a taxonomic key (Bouchard 2004).

After each macroinvertebrate sample was taken, discharge measurements were made using the Sontek FlowTracker2 along the transect crosscutting the site or pair of sites. Depth and velocity were measured in equal increments along each transect for a total of approximately 23 measurements per transect. By keeping the number of measurements relatively constant for all transects, the spacing of measurements was smaller for transects with smaller wetted widths. The depth and velocity measurements made on either side of the Surber net were averaged to assign a two-point average to each macroinvertebrate sample. Velocity data were missing for sites R3 and R4 in September 2020 because the water was not deep enough to measure velocity with the FlowTracker2. The missing values were estimated by multiplying the measured September depths by the average velocity:depth ratios for each corresponding site. Depth measurements were not available to replace missing June 2020 data for sites P2A and P2B. Discharge for each transect was calculated in the FlowTracker2 desktop application (Version 1.7) using the mean-section method (SonTek 2019).

After each flow transect was completed, dissolved oxygen, pH, and conductivity were measured with a YSI 600 XLM multiparameter water quality sonde at the macroinvertebrate sampling points. Data missing from June 2020 due to a malfunctioning DO probe were replaced with values recorded 10 days after the June macroinvertebrate sampling event.

A streambed survey was conducted in May 2020 (Appendix A) primarily to provide a baseline dataset for future studies at the site. A substrate survey was also conducted in May 2020 for inclusion in analysis of hydraulic habitat variables. Turbid water at some of the upstream sites prevented visual assessment of the substrate composition. Instead, the 100-stone count used by the Canadian Aquatic Biomonitoring Network (CABIN) to characterize substrate at the mesohabitat scale was adapted to characterize substrate for smaller habitat sizes (Environment Canada 2011). Twenty random stones were selected from the 50 cm radius surrounding each site marker and the intermediate axis of the stone was measured and recorded. The intermediate axis is perpendicular to the longest axis of a stone and the measurement is taken at the point resulting in the longest intermediate axis measurement (Environment Canada 2011). A substrate index was calculated to capture the variability in substrate sizes (Jowett et al. 1991). To calculate the substrate index, stones comprising each 20-stone sample were classified using the modified Wentworth particle size scale (Bovee and Milhous 1978) adjusted to include a fine gravel category (Jowett et al. 1991). The weighted percentages of each size class were then summed to get the final substrate index (Jowett et al. 1991):

$$\text{Subbstrate index} = \ 0.08 \ \text{bedrock\%} \ + \ 0.07 \ \text{boulder\%}$$

$$+0.06 \ \text{cobble\%} + 0.05 \ \text{coarse gravel\%} \ + \ 0.04 \ \text{fine gravel\%} \ + \ 0.03 \ \text{sand\%}. \tag{1}$$

2.3 Water Chemistry Sampling and Analysis

Surface water samples were collected at site R5A after each macroinvertebrate and habitat sampling event in 2020. One groundwater sample was collected from MW01 after the June 2020 sampling event. These samples were analyzed at Simon Fraser University for cations using Inductively coupled plasma mass spectrometry (ICP-MS) with a Thermofisher iCAP Qc. Anions were analyzed using Ion Chromatography (IC) with a Dionex ICS-3000. Bicarbonate concentrations for each sample were estimated by assuming a neutral charge balance for major cations (Ca^{2+}, Mg^{2+}, Na^+, K^+) and major anions (SO_4^{2-}, Cl^-, HCO_3^-). A Piper diagram was generated using Geochemist's Workbench Community Edition 15.0.

3. RESULTS

3.1 Temperature and Precipitation

Each year, precipitation declined from May to August and increased in September. In 2020, the year when the bulk of the macroinvertebrate and habitat data were collected, the period from May to August was much wetter than other years (Figure 6a). However, relative to 2020, September precipitation was substantially greater in 2018, 2019, and 2021. Years 2018 and 2021 were the driest, with 2018 having the lowest total precipitation for the entire period from May to September. In 2021, total precipitation from May to September was just slightly greater than in 2018, with zero precipitation in July.

In addition to having the lowest precipitation across the study period, 2018 and 2021 were also the hottest years, with the greatest contrast in mean monthly temperatures being attributed to the heatwave that occurred in June 2021 (Figure 6b). Mean monthly temperatures in 2020 were more similar to the temperature normal (Figure 6b). For the normals period and for all study years, mean monthly temperature increased from May to July. Mean monthly temperatures in August were generally similar to July, and September was cooler than August each year.
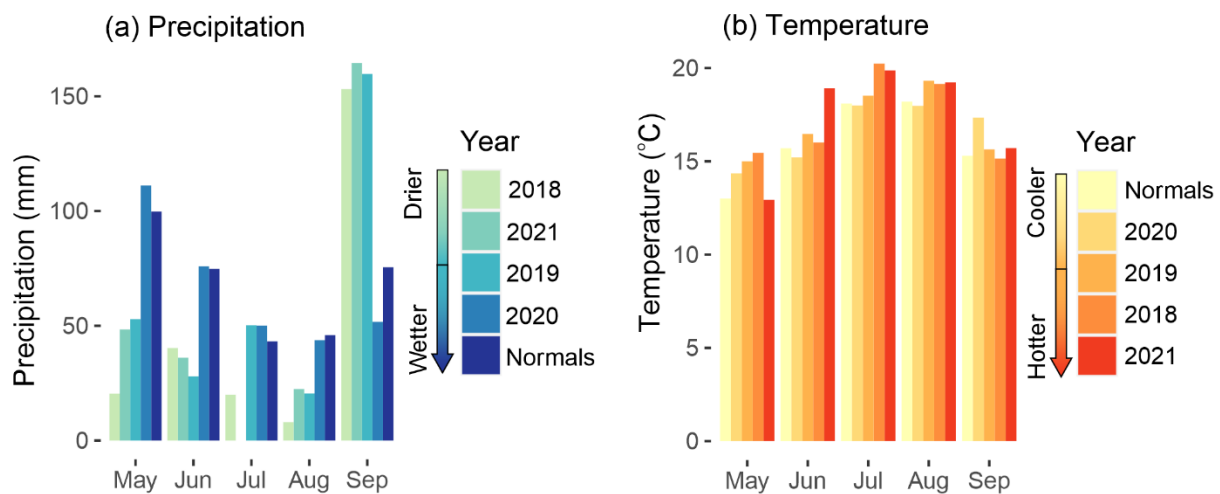

Figure 6: Monthly mean (a) precipitation and (b) temperature recorded at the Abbotsford International Airport for each month of the focal study period (May, June, July, August, September) from 2018 – 2021, along with the climate normals (1981-2010). Lighter colours represent lower values for (A) total precipitation and (B) mean temperature across the focal period.

The observed patterns of precipitation and temperature during the study period provide crucial context for understanding the streamflow intermittency in the years examined. The following section will delve deeper into the streamflow data, illuminating how these climatic factors influenced the hydrological conditions leading to periods of ceased flow and stream drying.

3.2   Hydrological Analysis

Hydrological monitoring network data were analyzed to characterize the hydrological system and how aquifer-stream exchanges varied with streamflow and groundwater levels. Analyses focused on the period from May 1st to September 30th in 2020 and 2021. Background streamflow data for 2018 and 2019 were also analyzed, as detailed in the following section. Data manipulation, visualization, and analysis were carried out in R Version 4.0.3 through the integrated development environment R-Studio Version 1.3.1093 (R Core Team 2020). The R packages *ggplot2* (Wickham 2016), *ggfortify* (Tang et al. 2016), *RcolorBrewer* (Neuwirth 2014), *dplyr* (Wickham et al. 2020), and *tidyr* (Wickham 2021) were used frequently.

3.2.1   Streamflow

Streamflow analyses incorporated streamflow data from 2018 to 2021 to develop an understanding of hydrological variability. Streamflow data for the focal period (May-September) for 2018-2021 were evaluated against temperature and precipitation data from the Abbotsford International Airport Station. Streamflow variability was characterized for all four years to help identify consistent hydrological patterns and help understand how relationships identified in this study might be impacted by interannual hydrological variability. As flow cessation and stream drying were identified as key issues in other studies, a focus of the analysis was to characterize low flows and zero-flow variability. Discharge data from the two hydrometric stations, HS2 and HS5, were plotted on a pseudo-log scale using the R package *scales* (Wickham and Seidel 2020).

Highlighting the link between precipitation, temperature, and streamflow, mean streamflow from May through September was greater in years with cooler temperatures and higher precipitation (Table 1). Mean streamflow at the downstream station, HS5, was proportional to total precipitation for each year. For station HS2, while a similar trend may be present, data quality for 2018 was compromised post-early July, likely due to interference from beaver activity (Allen et al., 2020). The temporary removal of stations in Fall 2018 resulted in underdeveloped rating curves, introducing uncertainty in the 2018 data for both stations compared to the data from 2019 through 2021.

Table 1: Summary statistics for streamflow (m^3/s) at hydrometric stations HS2 and HS5 for the period from May to the end of September for 2018 – 2021. Mean and standard deviation (St. Dev.) are missing at HS2 for 2018 due to impaired data quality during low flows. Timing of zero flow (TOZF) is the date when discharge declined to zero and remained at zero for at least 12 hours. Duration of zero flow (DOZF) is the number of days with zero discharge following TOZF. Brief periods of non-zero discharge that interrupted zero flow events are not included in the total for DOZF.

Year	Hydrometric Station - HS2				Hydrometric Station - HS5			
	Mean (m^3/s)	St.Dev.	TOZF	DOZF	Mean (m^3/s)	St.Dev.	TOZF	DOZF
2018			July 26th*	48.0*	3.97×10^{-2}	9.52×10^{-2}		
2019	8.37×10^{-2}	1.76×10^{-1}	Aug 5th	31.5	9.61×10^{-2}	1.94×10^{-1}	Aug 7th	29.6
2020	1.46×10^{-1}	2.16×10^{-1}	Sep 7th	13.3	1.52×10^{-1}	2.17×10^{-1}		
2021	8.52×10^{-2}	2.83×10^{-1}	Jul 7th	69.5	6.49×10^{-2}	1.85×10^{-1}		

Extremely low flows and subsequent flow cessation and drying were consistent annual occurrences. Streamflow at both hydrometric stations hovered around 1×10^{-1} m^3/s in May, declining below 1×10^{-2} m^3/s over the summer (Figure 7). Each year, streamflow eventually ceased at HS2. Streamflow cessation also occurred at HS5 in 2019, but flow at HS5 persisted for the entire study period in other years, despite flow cessation at HS2. Although reliable streamflow data are missing for 2018, photographs taken at Otter Park on August 8th of that year confirm that the upstream segment of the study reach was already mostly dry (Figure 2b). Therefore, flow cessation likely occurred at least a few days prior to August 8th, which is near when flow stopped being recorded at HS2 (Table 1). During the period for which reliable HS2 data are missing in 2018, streamflow patterns at HS5 mirrored the patterns that occurred at HS5 during periods of flow cessation in other years. Based on this similarity in streamflow patterns, as well as the underlying weather patterns, the beginning and end of the missing data period of 2018 are likely close to the times when flow ceased and resumed, respectively.

By assuming zero values for most missing 2018 discharge data, it is inferred that flow cessation commenced earlier and endured longer during hotter and drier years (Table 1). Although mean precipitation for the study period was greater in 2021 than 2018, the earliest and longest period of flow cessation was in 2021 (Table 1). The onset of flow cessation in 2021 followed a record heat wave at the end of June, which was amplified by a complete lack of precipitation for the month of July. In contrast, 2020 was the wettest and coolest and thus had the latest and shortest duration of flow cessation at HS2. In 2020, the final event of sampling benthic macroinvertebrates and measuring habitat variables occurred one day after flow resumed briefly following an approximately 10-day long period of flow cessation.

Visual assessments during site visits indicated a correlation between the intensity of stream drying, and precipitation and temperature variables. In 2018, most of the upstream channel segment (between transect R5 and P3; see Figure 5) was dry by late July. This segment was mostly dry in mid-July in 2021, and completely dry by late August. However, stagnant pools persisted for some time following flow cessation in both 2018 and 2021 (Appendix A). Due to wetter and cooler conditions in 2020, the upstream pool between R5 and P3 persisted through the entire period of flow cessation, but the riffle where R4 and R3 were located likely dried for a short period of time.
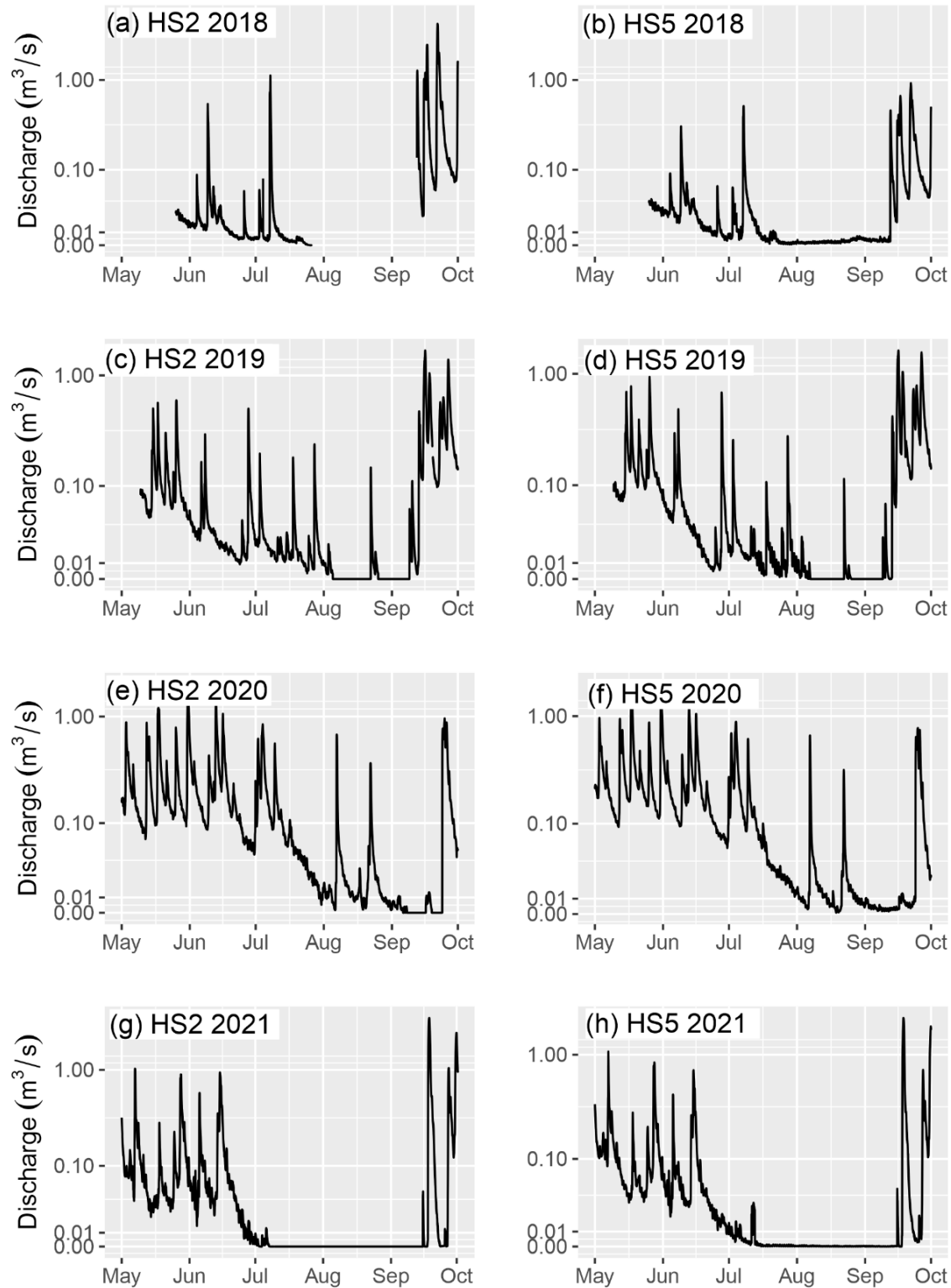
Figure 7: Streamflow at (a) HS2 and (b) HS5 in 2018, (c) HS2 and (d) HS5 in 2019, (e) HS2 and (f) HS5 in 2020, and (g) HS2 and (h) in 2021.

3.2.2 Groundwater

Groundwater level data for MW02 and MW03 (see Figure 5 for locations) were plotted for 2020 and 2021 with daily precipitation data for Abbotsford International Airport to examine how groundwater level varied with precipitation and how changes in groundwater level compared to changes in streamflow. Data from MW01 and the pumping well, PW01, were omitted (due to their proximity to MW02 and MW03) to simplify the analysis.

Mean daily groundwater levels in the shallow monitoring well, MW02, and the deep monitoring well, MW03, varied with daily precipitation (Figure 8). Groundwater level fluctuations in both monitoring wells reflected variations in the water table; however, the response in MW02 was more rapid because it is screened across dominantly very coarse sand, while MW03 is screened partially over fine sand and silt, which resulted in a more sluggish response in that well. In both wells, the recession in groundwater level occurred from May to September. The rate of recession was more rapid in 2021 than in 2020. Minimum groundwater levels for MW02 and MW03 were lower in 2021 than in 2020 by 0.34 m and 0.20 m, respectively.
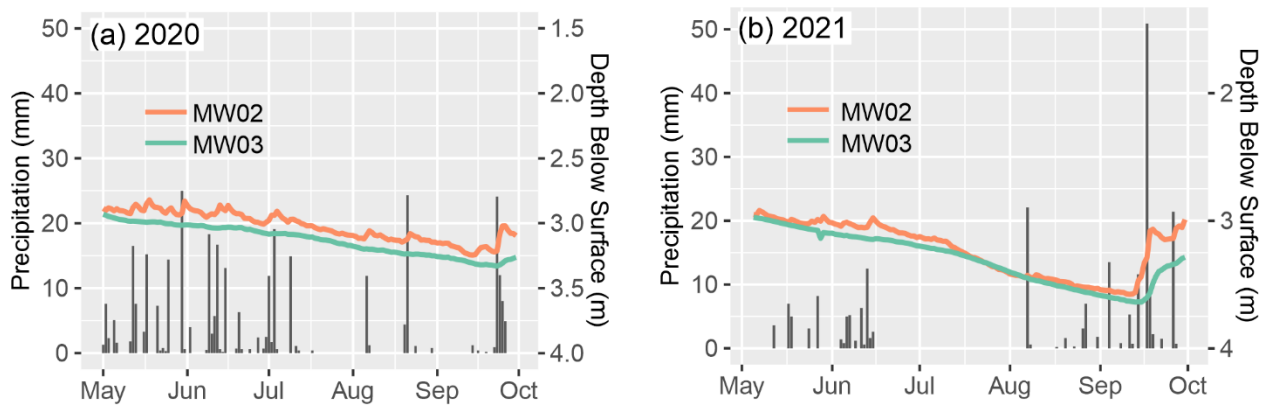
Figure 8: Depth to groundwater level below ground surface in MW02 and MW03 in (a) 2020 and (b) 2021.

3.3   Vertical Hydraulic Gradient

Vertical hydraulic gradient was calculated at each 15-minute time step for each piezometer pair by taking the difference in water levels between the nested pair and dividing by the difference in their depth (Appendix B). The average hydraulic gradient for the upstream segment between R5 and P3 (see Figure 5 for locations) was calculated using the piezometer pairs in the upstream segment (D39/D40, D41/D42, and D43/D44), excluding D7/D8 and D9/D10 because of their anomalous data.

Between transects R5 and P3, the vertical hydraulic gradient averaged across piezometer pairs D39/D40, D41/D42, and D43/D44 was highly temporally variable (Figure 9). In 2020, the mean vertical gradient was 4.5×10^{-3}. Precipitation events caused frequent large magnitude downward spikes in hydraulic gradient. However, hydraulic gradient was mostly positive during periods when it was not raining, suggesting that the segment of the Otter Park study reach between transects R5 and P3 was mostly gaining in 2020. The upward spike in hydraulic gradient during the period when flow ceased at HS2 suggests groundwater contribution increased with streamflow decline. In 2021, the hydraulic gradient was neutral for most of May and the first half of June. Negative hydraulic gradient values suggest that losing conditions prevailed from mid-June to mid-July. However, when streamflow ceased in mid-July, gaining conditions began to prevail until heavy rains brought an end to the period of flow cessation and

drying in mid-September. This extended gaining period resulted in a mean vertical gradient for the study period of 1.6×10^{-3}. The prevalence of gaining conditions during the periods of flow cessation that occurred each summer suggests that groundwater discharge helped maintain streamflow at the downstream hydrometric station, HS5, while flow ceased at HS2.
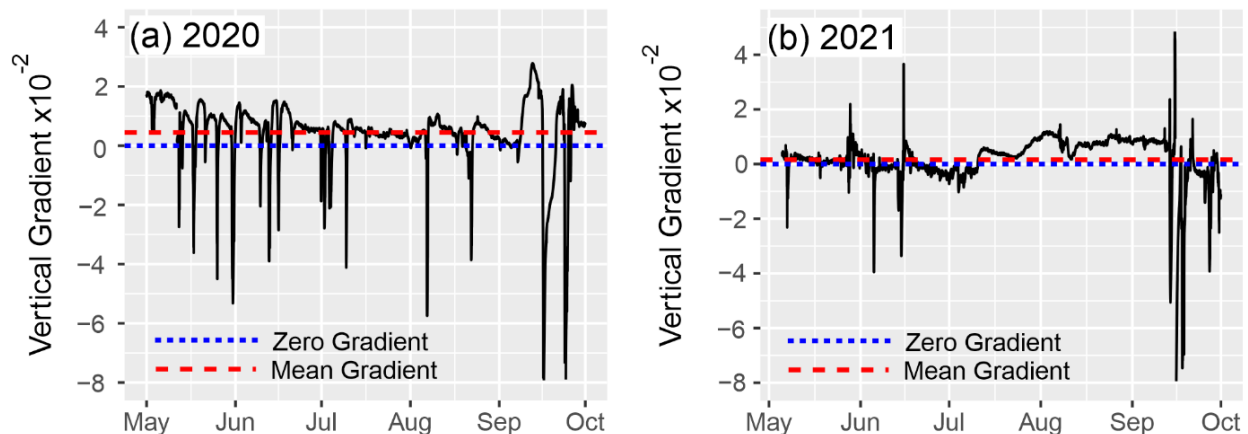

Figure 9: Average vertical flow across the streambed between transect R5 and transect P3 as estimated from the vertical gradients in D39/D40, D41/D42, and D43/D44 in (a) 2020 and (b) 2021. Positive values above the blue line indicate upward flow (gaining stream), and negative values below the blue line indicate downward flow (losing stream). The mean vertical gradient during the critical period for each year is shown as a horizontal red line.

3.4 Hydraulic Habitat Variables

Hydraulic habitat variables (depth, velocity, and substrate) were analyzed to see how they varied throughout the stream reach and through time with changes in hydrological conditions over the focal period. Analyses focused on 2020 due to extremely dry conditions in 2021. Relationships between depth and velocity with discharge (measured at 12:00 pm at HS2 on the day of sampling) were compared between riffle habitat and pool habitat. One-way ANOVA tests were used to examine differences between sites for velocity, depth, and substrate. Velocity was transformed using Tukey's Ladder of Powers transformation through the R package *rcompanion* (Mangiafico 2020). Post-hoc Tukey's Honestly Significant Difference (HSD) tests were used to test for significant differences between all possible levels of each factor (i.e., month, site). A Welch's Two Sample t-test was used to see if substrate differed between all sites in pools and all sites in riffles. For all parametric tests, Levene's test of homogeneity of variance was performed through the R package *car* (Fox and Weisberg 2019), and diagnostic plots were visually inspected to ensure that the assumptions of the tests were met. Diagnostic plots are provided in Appendix C.

In the results that follow, Tukey's HSD results are reported in brackets, with $p < 0.05$ indicating significant differences and $p > 0.05$ indicating no significant differences. The degrees of freedom (df) and p-values (p) are reported in brackets for the t-test. Note that the monitoring and analysis of hydraulic habitat variables conducted in 2020 could not be replicated in 2021 due to the more rapid and intense stream drying that occurred in that year.

ANOVA tests revealed significant spatial and temporal differences in velocity, depth, and substrate size (Table 2). Velocity was significantly higher in riffles than in pools (Table 2; Tukey's HSD: $p < 0.05$). Velocities also differed among the 12 individual sites (Table 2).

Table 2: Degrees of freedom (df), sample size (n), F-statistic (F), and p-value for each factor in the leftmost column in bolded font. A p-value less than $5x10^{-2}$ indicates that the factor was a significant predictor of the corresponding habitat variable listed in the heading rows. Site was a predictor variable in the one-way ANOVA tests conducted for each habitat variable. Habitat type, month, and the interaction between habitat type and month were predictor variables in the two-way ANOVA tests conducted for each habitat variable.

	Velocity				Depth				Substrate			
	df	n	F	p	df	n	F	p	df	n	F	p
Site	11	34	10.0	$8.5x10^{-8}$	11	34	10.0	$1.5x10^{-10}$	11	228	2.40	$7.67x10^{-3}$
Habitat Type	1	38	34.6	$8.2x10^{-7}$	1	38	34.6	$3.1x10^{-9}$				
Month	3	38	2.97	$4.4x10^{-2}$	3	38	2.97	$7.0x10^{-2}$				
Habitat Type and Month Interaction	3	38	0.91	$4.4x10^{-1}$	3	38	0.91	$9.8x10^{-1}$				

Stream velocities at site R3 were greater than the riffle site R5B and all pool sites (Figure 10a; Tukey's HSD: p<0.05). Site R2 velocities exceeded those at R5B, P1A, P3A, and P3B (Figure 10a; Tukey's HSD: p<0.05). Conversely, velocities were low across pool sites and thus there were no significant differences in velocity between pool sites (Figure 10a; Tukey's HSD: p>0.05). Low velocities at pool sites were also generally consistent through time relative to riffles (Figure 10a).

Stream velocity increased as a function of discharge in both riffles and pools, but the relationship between discharge and velocity varied more between riffle sites than pool sites (Figure 10b). From June to September, the average decrease in velocity across riffle sites was 0.154 ± 0.132 m/s, while pool velocities decreased by an average of 0.039 ± 0.007 m/s. While all sites had lower velocity in September relative to June, the only significant difference in velocity across all sites was between July and September (Figure 10a; Tukey's HSD: p<0.05).

Figure 10: (a) Two-point average for velocity at each site in June, July, August, and September. Sites are ordered downstream (left) to upstream (right) for each of pools and riffles. (b) Change in velocity as a function of discharge for riffle (dashed) and pool (solid) habitat.

Pools were deeper than riffles (Table 2; Tukey's HSD: p<0.05). Depth also varied among the 12 individual sites (Table 2; Figure 11a). Sites R4 and R3 had lower depths than all six pool sites (Figure 11a; Tukey's HSD: p<0.05). The only pairwise differences in depth between just the riffle sites were R5A and R5B, and 19 and R5B (Figure 11a; Tukey's HSD: p<0.05). In contrast to spatial patterns in velocity, there was more between-site variability in depth for pool sites than there was for riffles (Figure 11a). Depths at all pool sites were greater than all riffle sites other than R5B in June, and most pool sites were deeper than all riffle sites for the following months as well. On average, riffle depths differed between June and September by 0.087 ± 0.022 m. Across pool sites, there was no consistency in the month that was associated with the greatest depth. However, September depths were shallowest across all pool sites other than R3B (Figure 11a).

Although depth decreased linearly with discharge in pools and riffles (Figure 11b), there were no significant differences in depths between months across all of the sites (Table 2).
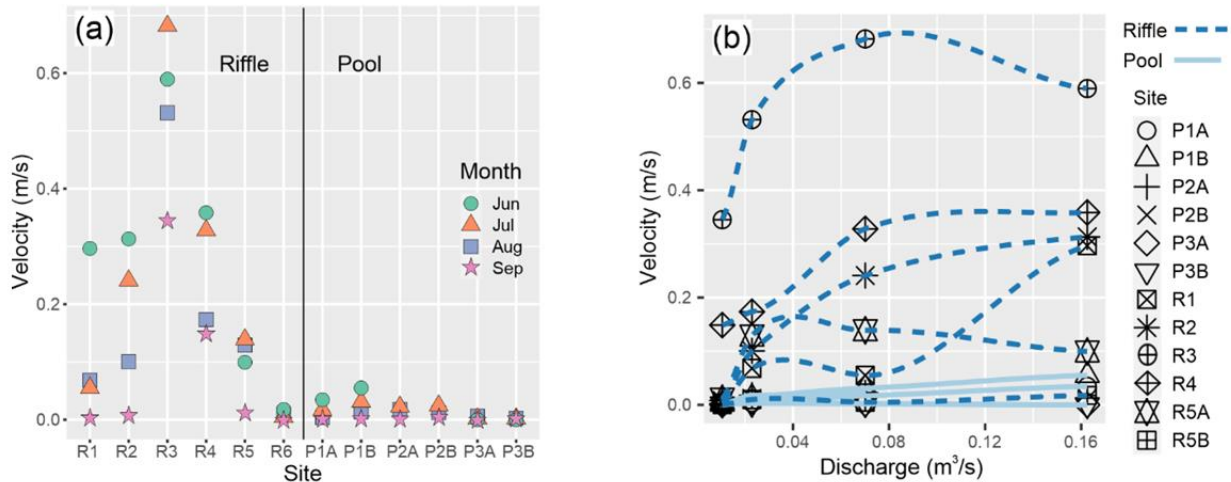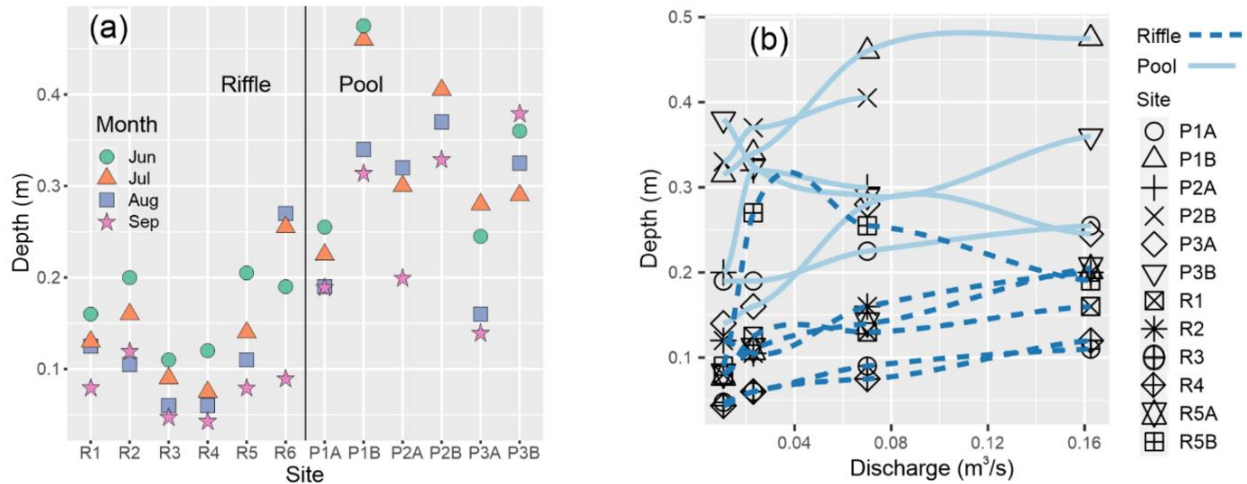
Figure 11: (a) Two-point average for depth at each site in June, July, August, and September. Sites are ordered downstream (left) to upstream (right) for each of pools and riffles. (b) Change in depth as a function of discharge for riffle (dashed) and pool (solid) habitat.

For substrate, there was variability among sites, but there were no significant pairwise differences between sites (Table 2; Tukey's HSD: p>0.05). Mean substrate size was significantly higher in riffle habitat than pool habitat (df = 237.26, p= 2.09x10^{-2}). Variability in substrate size was similar across all sites other than R1 (Figure 12).
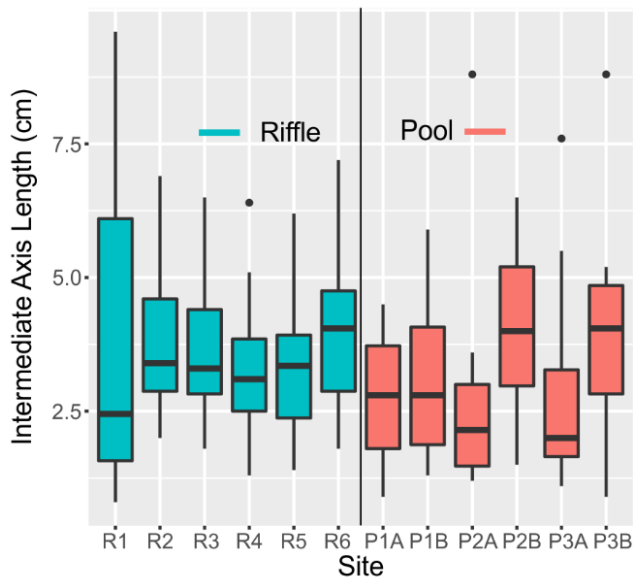
Figure 12: Variability of intermediate axis length of the 20 stones collected at each site in June 2020. Lines extending from each box indicate the range; top and bottom of boxes indicate the upper and lower quartiles, respectively; horizontal lines crossing each box indicate the median; and single points indicate potential outliers. Sites are ordered downstream (left) to upstream (right) for each of pools and riffles.

3.5   Water Chemistry

Water chemistry generally fluctuated little from June to September of 2020. Nitrate was notably higher in June and July, but concentrations remained below the guidelines for acute toxicity to aquatic life. All other measured parameters were within guidelines (refer to citations in Table 3). Groundwater from MW01-1 closely mirrored surface water composition, with most constituents, apart from silicon (Si) and magnesium (Mg), present in lower concentrations in the June groundwater sample compared to the surface water sample from the same period. The major ion chemistry for the study period is depicted in the Piper plot in Figure 13.

Table 3: Water Chemistry for surface water samples collected in June (SW01), July (SW02), August (SW03), and September (SW04) at Otter Park, as well as one groundwater sample collected in June (MW01-1). Guideline values accepted in B.C. are listed with the original reference for each guideline. nd = not detected. CCME = Canadian Council of Ministers of the Environment. ECCS = Environment and Climate Change Strategy.

	Units	SW01	SW02	SW03	SW04	MW01-1	Guideline	Citation
Na	(mg/L)	11.0	13.6	9.6	12.6	5.7	NA	
Mg	(mg/L)	6.6	8.4	6.9	9.6	8.6	NA	
Al	(mg/L)	<0.01	<0.01	<0.01	<0.01	<0.01		
Si	(mg/L)	3.6	3.8	3.0	3.6	8.6	NA	
K	(mg/L)	3.8	4.7	4.8	7.7	2.0	NA	
Ca	(mg/L)	15.6	19.9	16.5	22.4	10.4	1000 mg/L	Livestock (CCME, 2022)
Mn	(mg/L)	<0.001	<0.001	<0.001	<0.001	<0.001	0.65 mg/L (Acute)	Aquatic Life (ECCS, 2021)
Fe	(µg/L)	17.5	13.7	9.1	<0.01	<0.01	0.35 mg/L	Aquatic Life (ECCS, 2021)
Zn	(µg/L)	2.2	2.6	1.5	1.4	1.2	7.5 mg/L	Aquatic Life (ECCS, 2021)
Sr	(µg/L)	102.9	131.3	110.2	152.9	43.7	7 mg/L	Drinking Water (ECCS, 2020)
Zr	(µg/L)	<0.01	<0.01	<0.01	<0.01	<0.01	NA	
Ba	(µg/L)	20.0	18.1	19.0	24.1	10.4	1 mg/L	Aquatic Life (Haywood and Drinnan, 1983)
F⁻	(mg/L)	nd	nd	nd	nd	nd	1.17 mg/L @ 66.1 mg/L hardness (as CaCO3)	Aquatic Life (ECCS, 2021)
Cl⁻	(mg/L)	16.9	20.4	13.2	16.9	7.6	600 mg/L (acute) 150 mg/L (chronic)	Aquatic Life (ECCS, 1981)
Br⁻	(mg/L)	nd	nd	nd	nd	nd		
NO₃⁻	(mg/L)	12.0	11.2	2.8	0.6	1.6	550 mg/L (acute) 13 mg/L (chronic)	Aquatic Life (CCME, 2012)
PO₄³⁻	(mg/L)	nd	nd	nd	nd	nd	15 µg/L (Total P)	Aquatic Life (ECCS, 2021)
SO₄²⁻	(mg/L)	14.7	19.1	20.7	31.0	13.7	128 mg/L	Aquatic Life (ECCS, 2021)
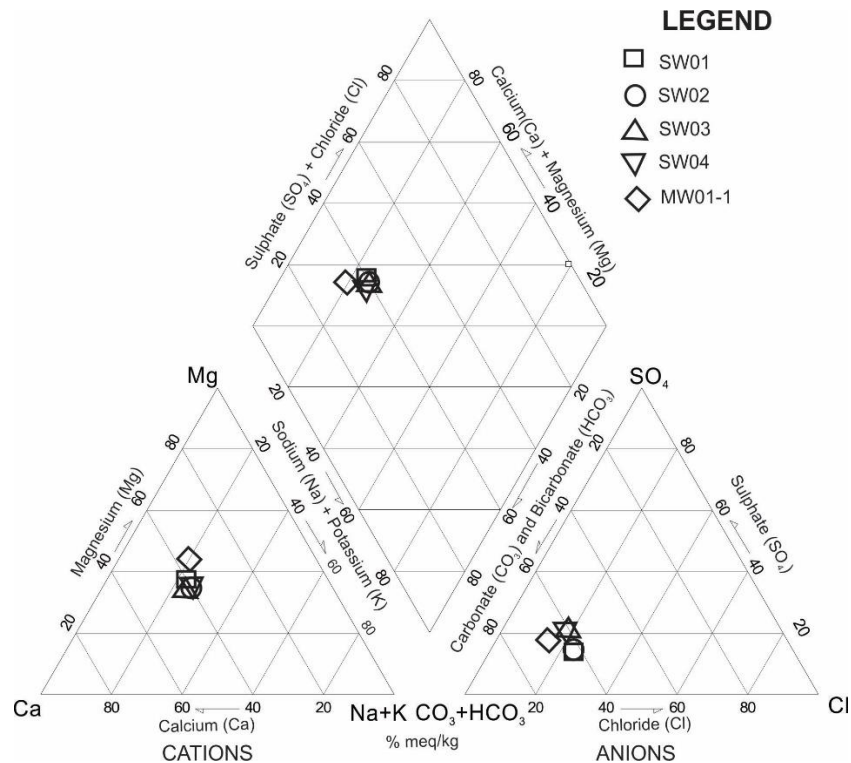
Figure 13: Piper diagram for surface water samples collected in June (SW01), July (SW02), August (SW03), and September (SW04) at Otter Park, as well as one groundwater sample collected in June (MW01-1).

3.6   Water Quality Variables

Water quality variables (dissolved oxygen (DO), pH, electrical conductivity (EC), and temperature) were analyzed to characterize spatial and temporal variability in water quality. Analyses focused on 2020 due to extremely dry conditions in 2021. The effects of month and site were analyzed using one-way ANOVA when the assumptions could be met. Kruskal Wallis tests were used when the assumptions of ANOVA were violated. DO-discharge relationships were compared between riffle habitat and pool habitat. Discrete DO and pH data, and stream temperature time series data from HS2 and HS5, were evaluated against water quality guidelines (ECCS 2019, 2021). EC was evaluated against the typical values of EC found in freshwater streams.

From June through September, pH, EC, and DO differed significantly between months, but not between sites (Table 4). However, of these discretely measured variables, only DO exceeded water quality guidelines (Table 5).

Table 4: Degrees of freedom (df), sample size (n), F-statistic (F), and p-value for each one-way ANOVA test of the effect of month on electrical conductivity (EC), pH, and dissolved oxygen (DO). For Kruskal Wallis tests of the effect of site on each water quality variable, the chi-square (X^2) statistic is given instead of an F-statistic. A p-value less than 5×10^{-2} indicates that the factor was a significant predictor of the corresponding water quality variable listed in the heading rows.

	pH					EC					DO				
	df	n	F	X^2	p	df	n	F	X^2	p	df	n	F	X^2	p
Site	11	34	10.0	7.43	1.00	11	34	10.0	0.934	1.00	11	228	2.40	1.54	1.00
Month	3	42	78.7		2.0×10^{-16}		42		41.6	5.0×10^{-9}	3	42	320		2.0×10^{-16}

Table 5: Summary statistics for water quality variables and evaluation against water quality guidelines. Mean weekly maximum temperature (MWMT) is the average of the warmest daily short-term temperatures for 7 consecutive days. SD = standard deviation, HRC = hourly rate of change.

	Min	Max	Mean	SD	Guideline	Source	Meets Guideline?
pH	7.0	7.7	7.4	0.22	6.5 – 9.0	(ECCS, 2019)	Yes
EC (µS/cm)	206	270	242	24	50-1500		Yes
Temperature @ HS2 (°C)	11.4	20.0	16.6	1.0	MWMT<18°C HRC<1°C/hour	(ECCS, 2019)	No Yes
Temperature @ HS5 (°C)	10.3	22.5	15.7	2.2	MWMT<18°C HRC<1°C/hour		No No
DO (mg/L)	4.3	12.9	9.1	3.3	>5.0	(Canadian Council of Resource and Environment Ministers [CCREM], 2015)	No

DO levels were mostly above 6 mg/L from June to August. DO dropped to below the guideline of 5.0 mg/L in September for all but two sites (R3 and R4) (Figure 14a). DO in September and August was lower than DO in June, and DO in September was the lowest of all months (Table 4; Tukey's HSD: p<0.05). While DO decreased over the study period, the relationship between DO and discharge was non-linear in both riffle habitat and pool habitat (Figure 14b).
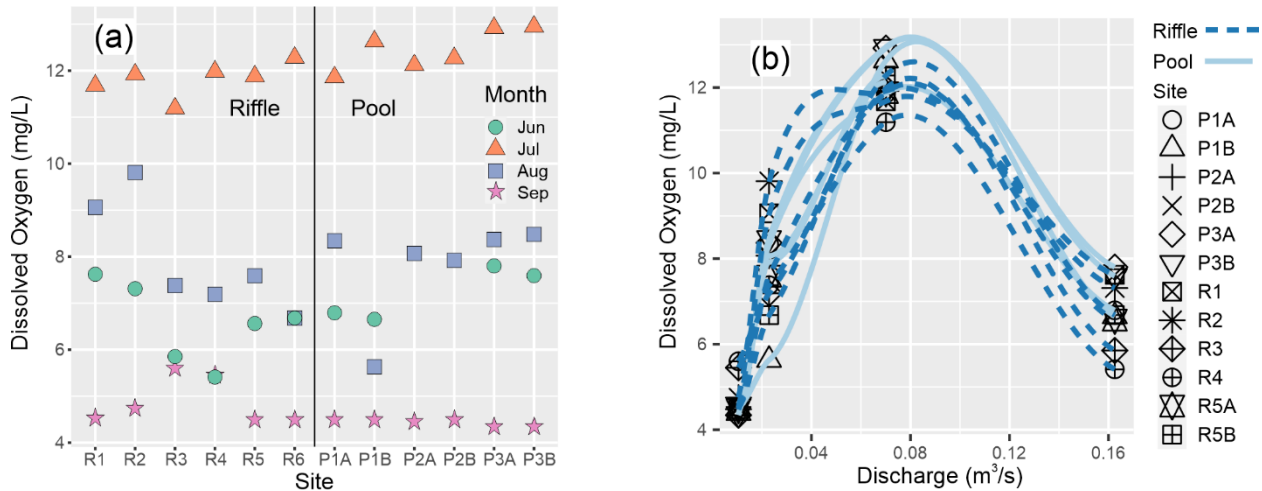
Figure 14: (a) Dissolved oxygen in June, July, August, and September at each site, which are listed in order from downstream (left) to upstream (right). (b) Dissolved oxygen as a function of discharge in riffle (dashed) and pool (solid) habitat.

Stream temperature guidelines for B.C. streams with unknown fish distributions were exceeded at the two hydrometric stations, HS2 and HS5 (Table 5). The mean weekly maximum temperature (MWMT), which is the average of maximum daily temperatures for seven consecutive days, frequently exceeded the 18°C guideline at the upstream hydrometric station, HS2. The MWMT guideline was exceeded more frequently at the downstream hydrometric station, HS5. The 1°C/hour change in stream temperature guideline was exceeded at HS5 once on August 16th, 2020 (Table 5).

Stream temperature at both stations followed air temperature, but the response in temperature at HS2 was muted relative to HS5 (Figure 15). In 2020, the mean daily variability in stream temperature of 3.0°C at HS5 was ten times greater than the mean daily variability of 0.3°C at HS2. Despite greater variability in stream temperature at HS5, stream temperature averaged across the study period was higher at HS2 (16.4 °C) than at HS5 (15.9 °C). Groundwater temperatures were lower than stream temperatures for most of the critical period but surpassed stream temperatures near the end of September. Implications for Nooksack Dace are discussed in Section 4.2.1.
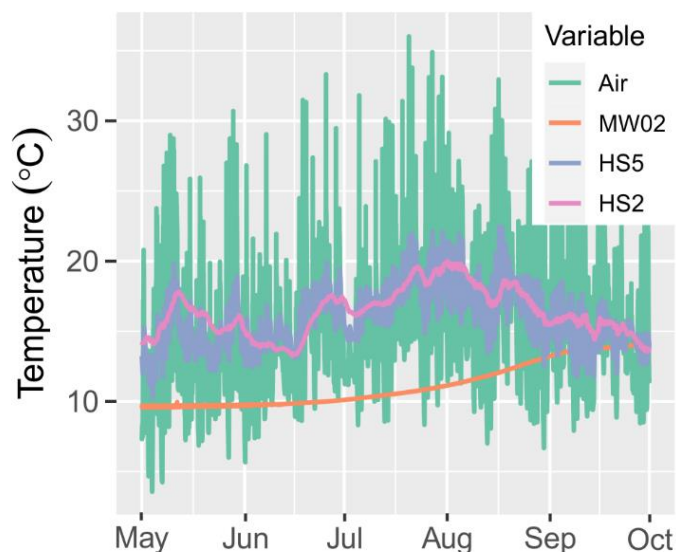

Figure 15: Air (teal lines), groundwater (MW02) (orange line), and stream temperatures at upstream HS2 (pink) and downstream (purple) HS5 over the critical period in 2020.

3.7 Benthic Macroinvertebrates

3.7.1 Benthic Macroinvertebrate Communities in 2020

Counts of macroinvertebrate taxa from each Surber sample were analyzed to assess how macroinvertebrate communities varied throughout the study reach and over the study period. Analyses focused on 2020, but the results of the sampling event in June 2021 were used to assess interannual variability in community compositions. A focus of the analysis of 2020 data was identifying potential changes related to streamflow and associated changes in habitat for the purpose of understanding how macroinvertebrates might be used for flow monitoring. While macroinvertebrates are critical ecosystem components and thus useful tools for biomonitoring regardless of the presence of predators, macroinvertebrates were also considered in the context of being an important food source for fish. Total macroinvertebrate abundance or dried biomass of benthic samples are sometimes taken as indicators of prey availability for fish (Bovee 1986). However, this assumes that all taxa in a sample are equally available as prey and disregards how behavioral adaptations to avoid predators or palatability of different taxa might influence a specific taxon's status as a prey item (Bovee 1986). Because the study reach at Otter Park contains critical habitat for Nooksack Dace, studies on the gut contents and foraging patterns of Nooksack Dace were consulted to group taxa that are likely prey for Nooksack Dace into a group henceforth referred to as Dace prey.

Chironomids (*Chironomidae)* were the most abundant of benthic macroinvertebrate taxon (Figure 16). Gammarids (*Gammaridae)* and black flies (*Simuliidae*) were nearly equal in abundance. *Baetidae* (baetid mayflies) was the only benthic macroinvertebrate family of the mayflies (*Ephemeroptera)*, stoneflies (*Plecoptera*), and caddisflies (*Trichoptera*) to have an abundance that accounted for at least 5% of the total number of specimens collected across the study period. In fact, the only other specimens belonging to these orders, which are abbreviated EPT, were a few specimens of *Heptageniidae.*
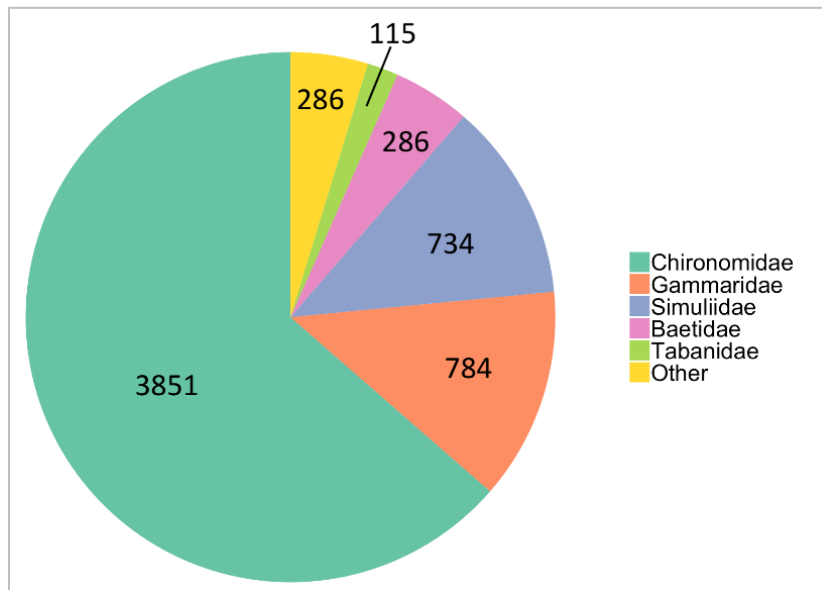

Figure 16: Abundance of the five most abundant benthic macroinvertebrate families and all "Other" taxa displayed as a proportion of the total abundance collected in June, July, August, and September 2020.

Regarding spatial and temporal patterns amongst the individual macroinvertebrate families, chironomids were generally the most abundant in riffles and pools from June to August. Aside from chironomids, gammarids generally dominated pools (Figure 17). At least a few black flies or baetids were also found at a minimum of one pool site in each month prior to September, but abundances of these families were much higher in riffles (Figure 17). In September, Site P1A and Site P1B were the only sites in the pool habitat with macroinvertebrates remaining. The only non-chironomids remaining at P1A and P1B in September were a few gammarids and a few non-insects from the "Other" group. In riffles, black flies were the second most abundant taxon aside from chironomids and they were mainly found at sites R3 and R4 where the majority of baetids were also found (Figure 17). Baetid and gammarid abundances were generally similar and were lower than black fly abundances (Figure 17). By September, however, there were no baetids or black flies, leaving gammarids as the dominant taxon in riffles (Figure 17). As baetid mayflies, free swimming gammarids, and other taxa available to Dace prey were mostly found in riffles, Dace prey abundance was higher in riffle habitat than pool habitat throughout the study period, including immediately following the resumption of streamflow in September.
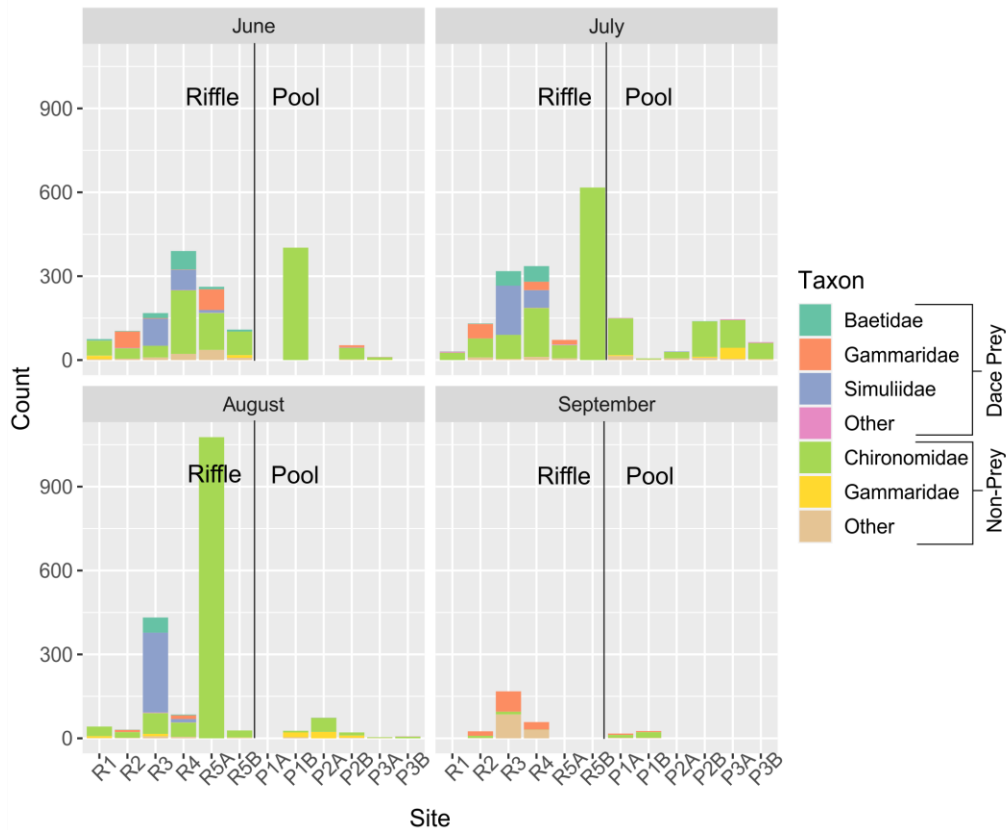
Figure 17: Raw macroinvertebrate taxonomic counts for each site in 2020 for June, July, August and September. Dominant Dace Prey and non-prey groups are shown. Gammaridae are shown in both groups because Gammaridae associated with filamentous algae were characterized as non-prey, while free swimming Gammaridae were characterized as Dace Prey.

3.7.2 Benthic Macroinvertebrate-Habitat Relationships

Generalized additive models (GAMs) were used to analyze the potential effects of habitat variables (e.g., EC, DO, pH, velocity, substrate, depth) on spatial and temporal variability in abundance for different benthic macroinvertebrate taxa. GAMs are generalized linear models in which the response variable depends on the sum of smooth functions of one or more predictor variables (Wood 2017). Potential complex non-linear relationships between habitat variables and abundance justified the use of GAMs over linear models. Diagnostic plots that were used to evaluate the fit of the GAMs and whether they met assumptions are provided in Appendix C. Further details on model construction and model selection are provided in Appendix D.

First, two GAMs were built to model and evaluate potential relationships of total macroinvertebrate abundance and Dace prey abundance with EC, pH, DO, velocity, depth, and substrate size. For each of the four most abundant benthic macroinvertebrate families, GAMs were used to model and evaluate potential relationships between family abundance and the habitat variable that was the most significant predictor of total abundance and Dace prey abundance.

Figure 18 shows the partial effect of each habitat variable on Dace prey abundance. The smooth functions represent the estimated effect of each habitat variable on Dace prey abundance while accounting for the influence of the other variables in the model. Therefore, the y-axis of each plot represents the partial effect of the habitat variable on abundance, with values above or below zero

indicating positive or negative effects, respectively. Non-linear trends in these plots suggest that the relationship between the variable and abundance is not simply linear but involves more complex interactions.

Total macroinvertebrate abundance varied significantly with velocity (Figure 18a) and DO (Figure 18b). The GAM had an adjusted r^2 of 0.39 and the relationships between total abundance and each of velocity and DO were positive and non-linear. Dace prey abundance was only significantly correlated with velocity (Figure 18c), but the model had an adjusted r^2 of 0.77. The model indicated that the relationship between DO and Dace prey abundance was insignificant and uncertain (Figure 18d).
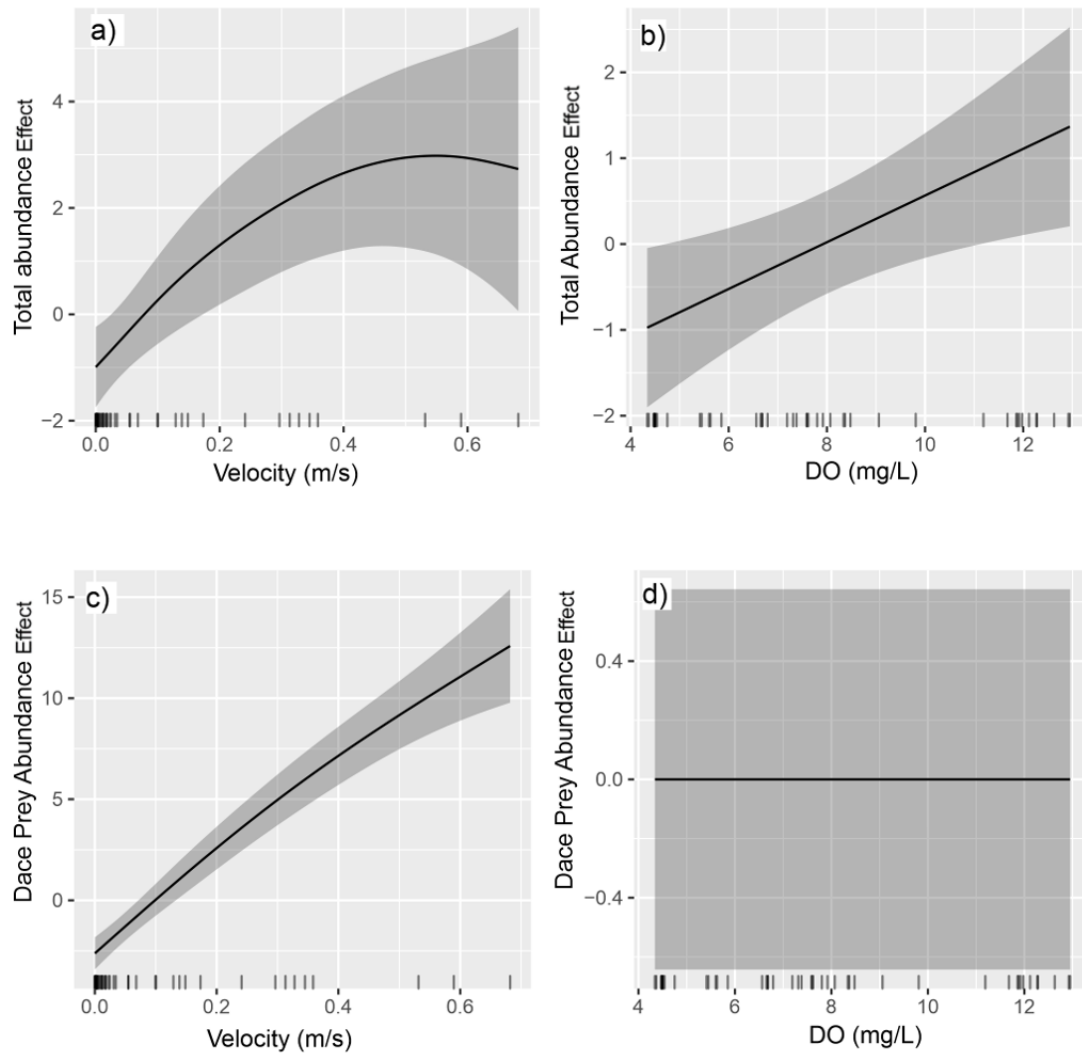
Figure 18: Partial effect of (a) velocity and (b) dissolved oxygen (DO) on total macroinvertebrate abundance. Partial effect of (c) velocity and (d) dissolved oxygen (DO) on Dace prey abundance. Dace prey abundance was square-root transformed and total abundance was cube-root transformed to satisfy model assumptions, which is reflected in the magnitudes of the partial effects on the y-axis of each plot.

For individual taxa, modelling the abundance of black flies (*Simuliidae*) as a function of velocity each month explained most variability in black fly abundance, as the adjusted r^2 was 0.95. Black fly abundance increased non-linearly with velocity, and the relationship between abundance and velocity was similar each month, indicating a consistent preference of black flies for higher velocity habitats (Figure 19). In September, however, the relationship is insignificant and uncertain due to the absence of black flies in all samples.
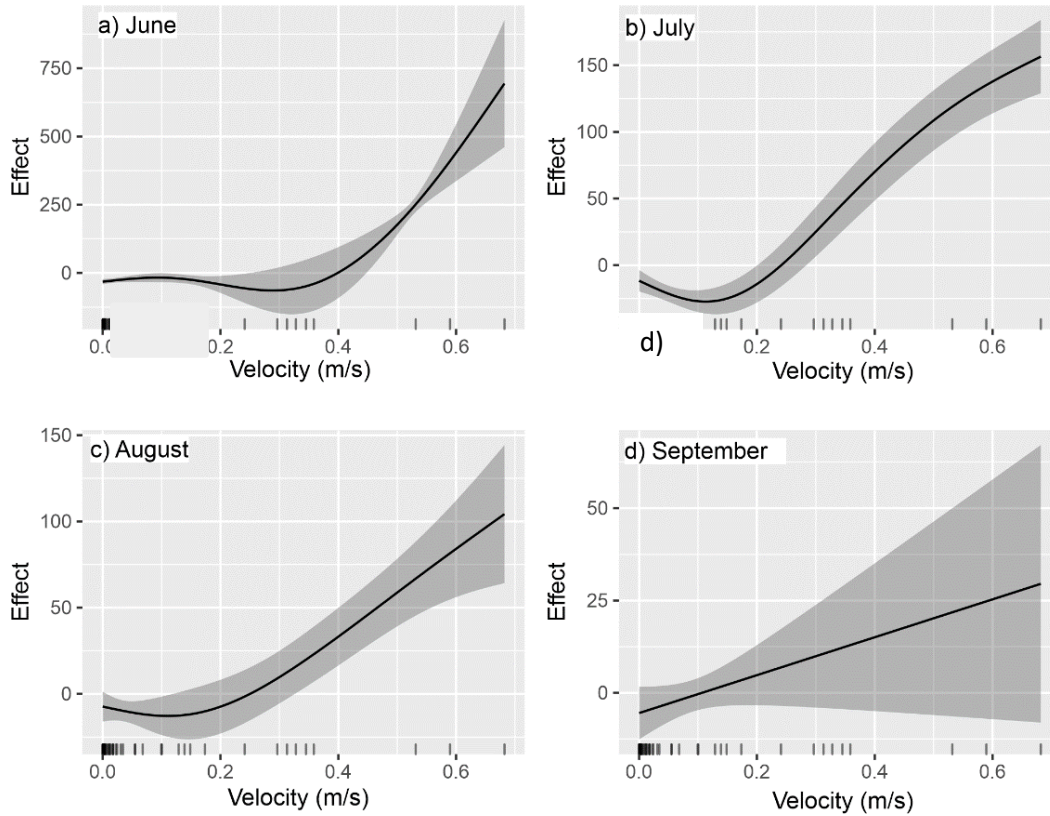
Figure 19: Patial effect of velocity on total abundance of black flies in (a) June, (b) July, (c) August, and (d) September.

For baetid mayflies, the relationship between abundance and velocity was more linear than for black flies (Figure 20). The relationship between baetid mayfly abundance and velocity also varied month to month to a greater degree than black flies. By September, the absence of baetid mayflies resulted in insignificant and uncertain relationships. The adjusted r^2 was 0.64.

Figure 20: Patial effect of velocity on total abundance of Baetidae in (a) June, (b) July, (c) August, and (d) September.

For chironomids, the model had an r^2 value of 0.18 and thus did a poor job of explaining variability in chironomid abundance. Velocity was only significantly related to abundance in June, but velocity had a negative effect on chironomids abundance (Figure 21).
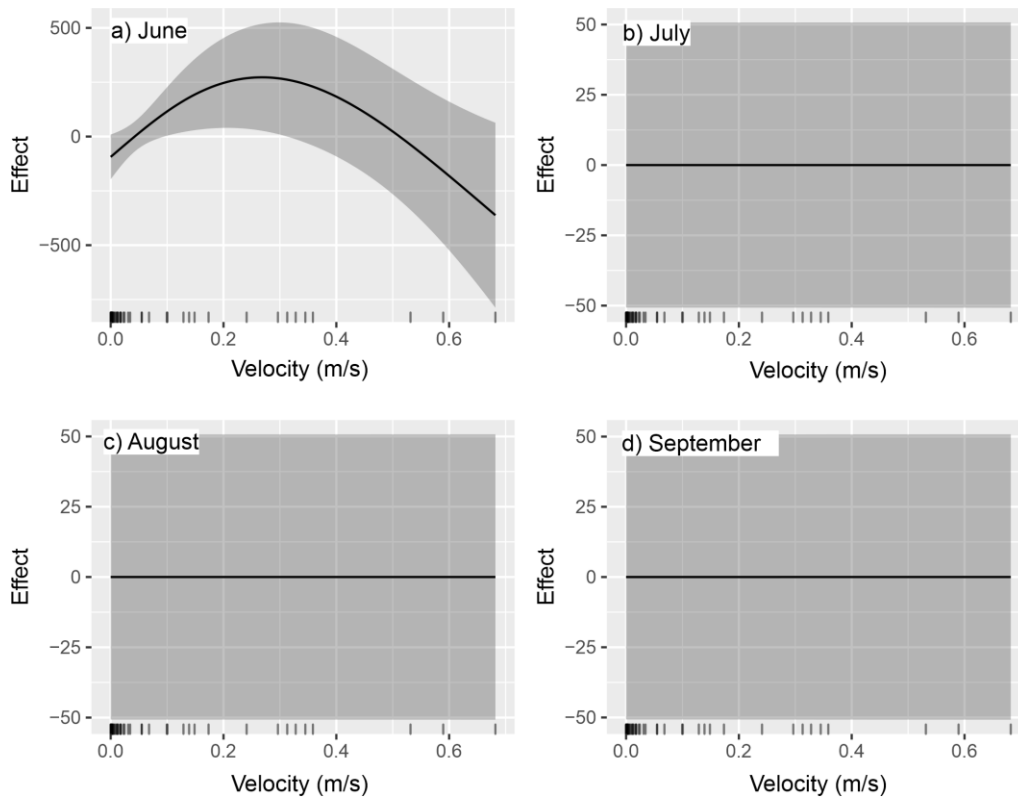
Figure 21: Patial effect of velocity on total abundance of chironomids in (a) June, (b) July, (c) August, and (d) September.

For gammarids, the model had an r^2 value of 0.15 and velocity was only significantly related to abundance in September (Figure 22). However, unlike chironomids, the change to a positive relationship between abundance and velocity may indicate an increase in the importance of velocity with decreasing discharge.

3.7.3 Benthic Macroinvertebrate Communities in 2021

Relative to June 2020, the dominance of chironomids was greater in 2021 (Figure 23). In contrast to the high abundances of black flies and baetid mayflies at riffle sites in 2020, just a few specimens of these taxa were found across all riffle sites in 2021. As black flies and baetid mayflies constituted large portions of total abundances at R3 and R4, abundances at these sites were lower in 2021. However, riffle sites generally maintained higher abundances than pool sites. Across all sites, total abundance increased from 1592 in 2020 to 2290 in 2021. In contrast, diversity was lower in 2021, with chironomid and gammarid specimens constituting 97% of the total abundance.
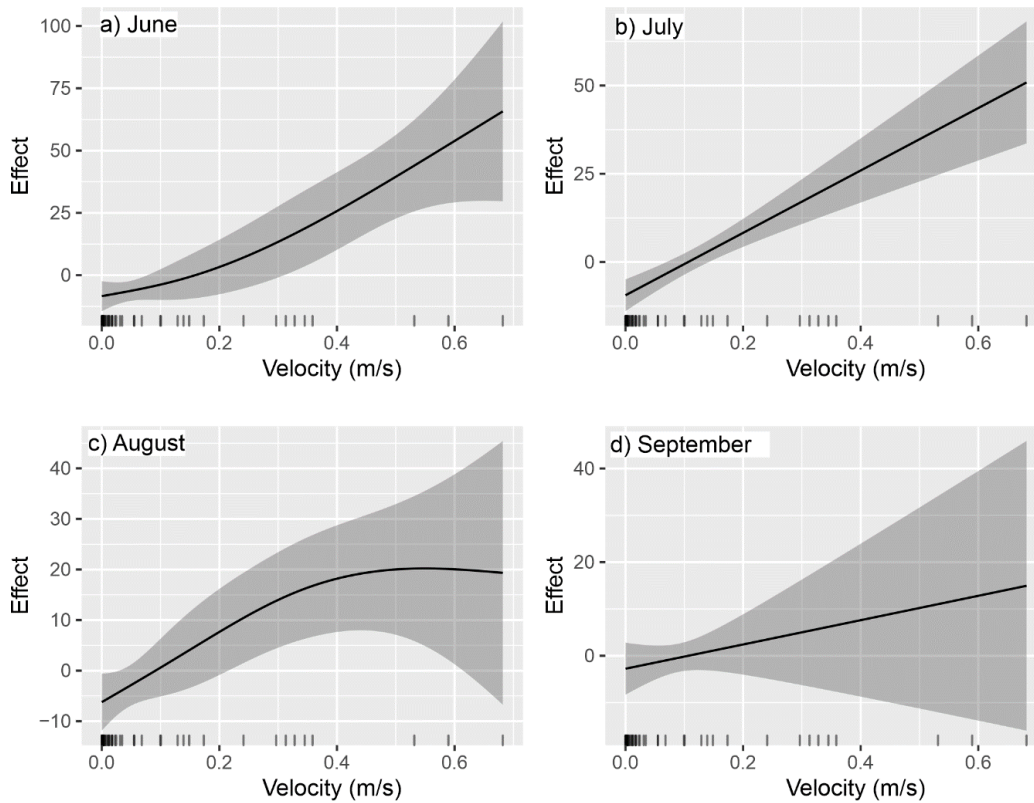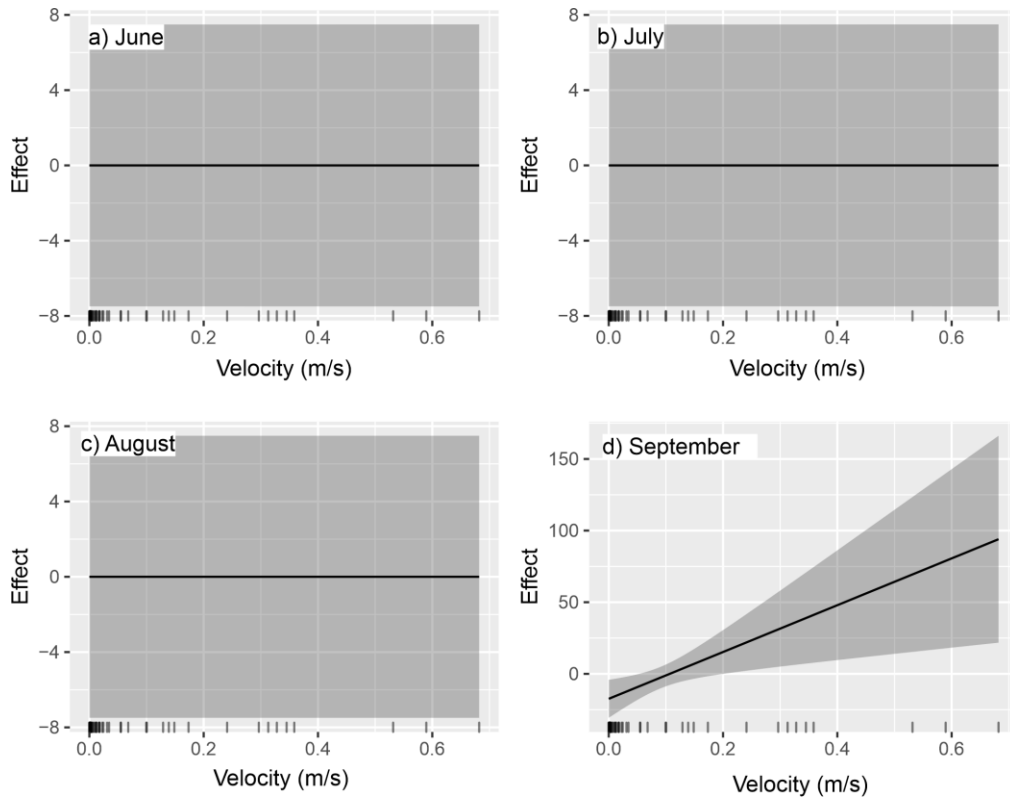
Figure 22: Patial effect of velocity on total abundance of Gammarids in (A) June, (B) July, (C) August, and (D) September.

Figure 23: Raw macroinvertebrate taxonomic counts for each site in June 2021. Dominant Dace Prey and non-prey groups are shown. Gammaridae are shown in both groups because Gammaridae associated with filamentous algae were characterized as non-prey, while free swimming Gammaridae were characterized as Dace Prey.

3.8 Habitat Suitability Models

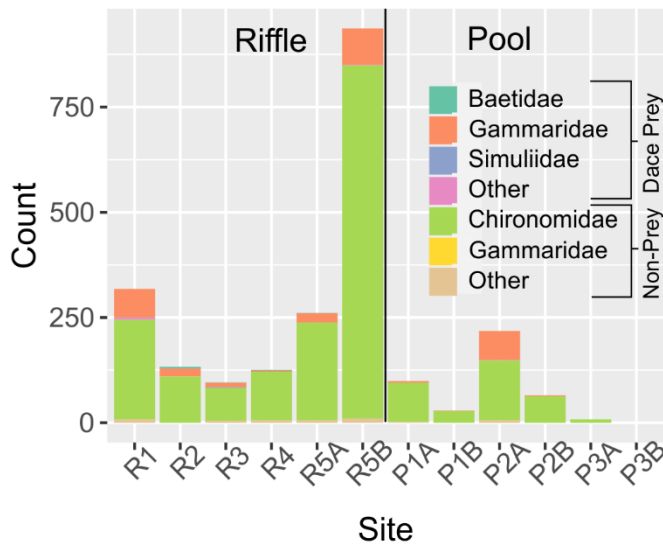Like GAMs, habitat suitability index (HSI) models can be used to relate changes in habitat parameters to changes in biotic variables. While GAMs are likely more statistically powerful, they are rarely used in environmental flows studies (Jowett and Richardson 2007). Conversely, HSI models are a key component of habitat simulation methodologies, which are one of the most widely used classes of environmental flow methodologies in the world, including in North America (Tharme 2003; Linnansaari 2012). To test these methodologies at Otter Park, HSI models were constructed for Dace Prey and for Nooksack Dace, which were used to generate useable width (WUW) models for each organism.

Depth and velocity HSI models were constructed for Dace Prey using the same taxonomic and habitat data used to construct the Dace Prey GAM. HSI curves for depth and velocity for Nooksack Dace at Otter Park were recreated from those published by Inglis and Pollard (1994) for Nooksack Dace from a double-pass electrofishing survey of Nooksack Dace habitat utilization in Bertrand Creek. Inglis and Pollard (1994) followed the closed-site electrofishing approach of Platts et al. (1983) and during the day surveyed 20 sites in Bertrand Creek, each made up of one habitat type (i.e., riffle, glide, or pool). Inglis and Pollard's (1994) calculation of the "weighting factors", or HSI scores, for incremental bins of depth and velocity in which Nooksack Dace were captured, followed the guidelines associated with the Instream Flow Incremental Methodology (IFIM) (Bovee and Cochnauer 1977; Bovee 1986). These same guidelines were used to develop the HSI models for Dace Prey in this study.

Constructing HSI curves for Dace Prey followed the frequency analysis methodology detailed by (Bovee and Cochnauer 1977):

1) Two-point average depths and velocities associated with each macroinvertebrate sample were split into incremental bins of 0.05 m and 0.1 m/s, respectively (Table 6).
2) The number of Dace Prey captured within each bin was tallied, and the total number of Dace Prey in each bin was divided by the number of samples belonging to each bin (Table 6).
3) The corrected number of Dace Prey in each bin was divided by the number of Dace Prey in the bin with the highest abundance, known as the optimum (Bovee and Cochnauer 1977; Bovee 1986), to assign relative suitability scores for each bin ranging from zero to one (Table 6).
4) Linear interpolation using the scores of neighbouring bins was performed to assign a suitability score to an empty velocity bin (0.4-0.5 m/s).

*Table 6: Data used in each step of calculating of HSI scores for velocity bins. *Asterisk indicates the HSI score was calculated through linear interpolation using the two neighbouring bins because no specimens were captured in that specific bin.*

Velocity Range (m/s)	Observations	Specimens	Specimens/Observations	HSI Score
0.0 0.1	31	81	2.61	0.011
0.1 - 0.2	6	181	30.2	0.132
0.2 - 0.3	2	60	30.0	0.132
0.3 - 0.4	4	426	106.5	0.467
0.4 - 0.5		No observations		0.569*
0.5 - 0.6	3	459	153	0.671
0.6 - 0.7	1	228	228	1.000

3.8.1 *Nooksack Dace*

Habitat suitability index (HSI) curves for depth and velocity for Nooksack Dace at Otter Park were recreated from those published by Inglis and Pollard (1994) for Nooksack in Bertrand Creek. Nooksack Dace abundance, and in turn, habitat suitability, increased with velocity until reaching values typically measured (~0.35 m/s) at riffle site R3 (Figure 24a). Extremely low velocities (0.05 m/s) and extremely high velocities (0.45 m/s) were associated with few Nooksack Dace (Figure 24a). Depths characteristic of riffles (0.1 – 0.25 m) were associated with relatively high abundance (Figure 24b). Conversely, depths greater than 0.25 m, which characterize pool habitat at Otter Park, were associated with lower abundance (Figure 24b).
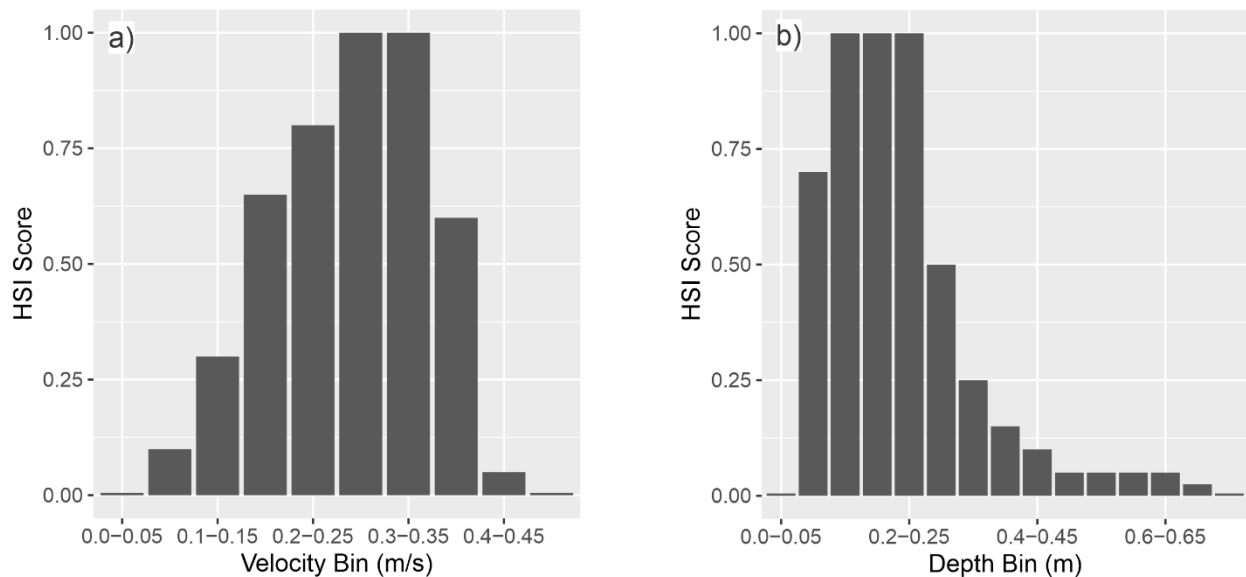
Figure 24: Habitat Suitability Indices for (a) velocity and (b) depth for Nooksack Dace based on an electrofishing survey conducted in Bertrand Creek by Inglis and Pollard (1994).

Dace Prey

The HSI curve for Dace Prey abundance showed increasing suitability with increasing velocity to the highest velocities measured in this study, concurrent with the strong positive relationship between Dace prey abundance and velocity that was revealed through the GAM analysis in Section 3.7.1. Dace Prey were largely limited to depths between 0.05 – 0.1 m, which are only found in riffle habitat, or pool habitat during events of flow cessation and drying (Figure 25).
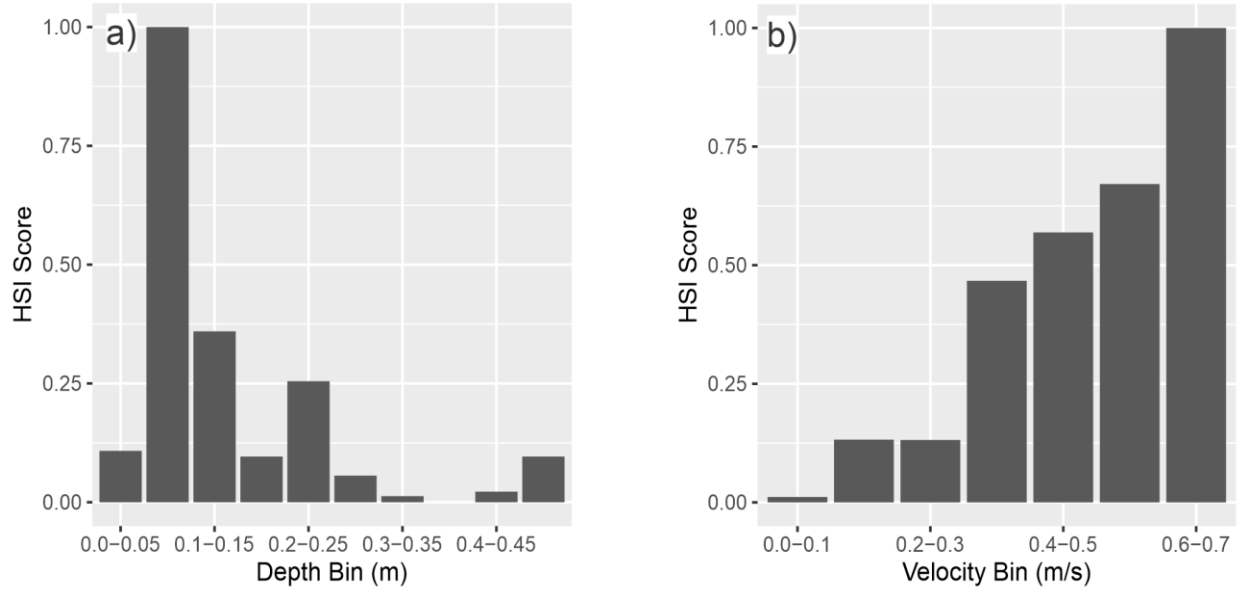
Figure 25: Habitat Suitability Indices for (a) depth and (b) velocity for Dace Prey based on data collected at each transect at Otter Park monthly from June to September 2020.

3.9 Weighted Usable Width

Weighted usable width (WUW) models were constructed using stream transect data following the steps used in IFIM and its software component PHABSIM to calculate WUA (Bovee 1986), except the calculations were performed on transect panels rather than simulated grid cells following WUW approaches used in British Columbia (Lewis et al. 2004; Okanagan Nation Alliance 2020).

First, a combined suitability score, CS_i, was calculated for each panel i of each transect according to:

$$CS_i = D_i \times V_i \tag{2}$$

where D_i and V_i are the HSI scores (as determined by the respective HSI curves for each of Nooksack Dace and Dace Prey) that are associated with the depth and velocity of each transect panel i. Then, WUW was calculated for each transect made up of n panels according to:

$$WUW\ (m) = \sum_{i=1}^{n} CS_i \times W_i \tag{3}$$

where W_i is the panel width [m] and CS_i is the combined suitability score for each panel i. This resulted in a WUW score for Nooksack Dace and Dace Prey for each transect for each month that flow data were recorded. The WUW scores for Nooksack Dace and Dace Prey are henceforth denoted WUW_{ND} and WUW_{DP}, respectively.

After WUW_{ND} and WUW_{DP} were calculated for each transect, reach-averaged WUW_{ND} and WUW_{DP} values were calculated by averaging the WUW_{ND} and WUW_{DP} values across all transects at the study site for each month. In theory, these monthly reach-averaged values reflect how relative habitat suitability changed on average throughout the study reach as flows declined from June to September in 2020. However, WUW_{ND} and WUW_{DP} had to be estimated for some transects for certain months. Data were missing for pool transects P2 and P1 for June and September, respectively, due to data loss. Data were also missing for riffle transects R3 and R4 for September because the depths at both riffle sites were too

low to measure velocity. For these few instances, estimates of WUW_{ND} and WUW_{DP} values were made using the average percent change in WUW_{ND} and WUW_{DP} of transects in the same habitat type (i.e., riffle or pool).

WUW-discharge curves were fit to the four WUW_{ND} and WUW_{DP} values to produce continuous functions that predict WUW_{ND} and WUW_{DP} as a function of discharge. The instantaneous discharge values recorded at the upstream hydrometric station, HS2, at noon of each respective day when flow transects were conducted were used for the analysis. Curve fitting was done in Python 3.8.8 through the integrated development environment Spyder 4.2.5 using Python libraries *SciPy* (Virtanen et al. 2020), *NumPy* (Harris et al. 2020), and *Matplotlib* (Hunter 2007). The Ricker Curve (Equation 4) and a log-normal curve (Equation 5) were fit for each WUW-discharge relationship using least-squares, following other studies of flow-ecology relationships (Lewis et al. 2004; Bolker 2007; Okanagan Nation Alliance 2020):

$$WUW = m \times Q \times e^{(-b \times Q)} \tag{4}$$

$$WUW = m \times \ln(Q) + b \tag{5}$$

where *m* and *b* are constants estimated by the least squares method that relate discharge (*Q*) to WUW.

The tangent method (Jowett and Briggs 2006) was implemented using each of the WUW-discharge curves. For the tangent method, tangents of the curve from the maximum and minimum WUW values are drawn and the intersection point is used to represent the point at which habitat begins to degrade rapidly with discharge (Jowett and Biggs 2006). The critical threshold discharge values produced through the tangent method are often used to set minimum instream flows, so the values resulting from these analyses were evaluated in terms of whether they were reasonable minimum flow values.

Similarities in the HSI curves for Nooksack Dace and Dace Prey resulted in nearly identical log-normal WUW-discharge curves, each with a good fit to the data (Figure 26). The log-normal curves suggest rapid increases in suitable habitat availability (WUW) with discharge from the point of flow cessation to just under 0.3 m³/s, which is near the magnitude of streamflow at HS2 in June. The tangent method suggests that habitat suitability starts to rapidly decline with discharge below 0.029 m³/s for Dace Prey and 0.032 m³/s for Nooksack Dace (Figure 26).
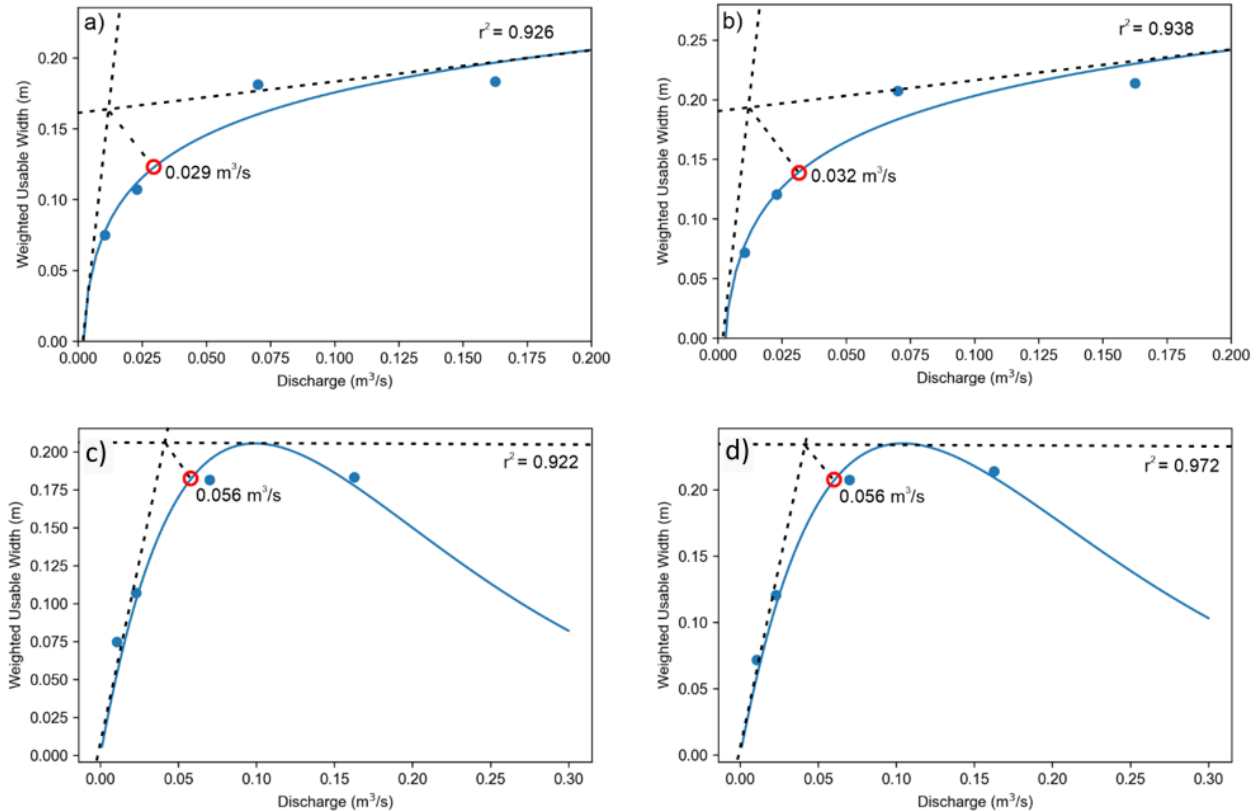
Figure 26: Weighted Usable Width for (a) Dace Prey (WUW$_{DP}$) and (b) Nooksak Dace (WUW$_{ND}$) as a function of discharge using a log-normal fit. Weighted Usable Width for (c) Dace Prey (WUW$_{DP}$) and (d) Nooksak Dace (WUW$_{ND}$) as a function of discharge using a Ricker curve. The r^2 values indicate the goodness of fit for each curve. From June to September, months occurring later are closer to zero along the x-axis. The point on the curve circled in red indicates the point at which the tangent method suggests habitat quality rapidly diminishes.

Since the same HSI curves were used as input, the Ricker curves were also similar for Dace Prey and Nooksack Dace (Figure 26). Instead of a constant increase in available suitable habitat as suggested for the log-normal curves, the Ricker curves suggest a peak in WUW near a discharge of 0.1 m^3/s. In contrast to the log-normal WUW$_{DP}$-discharge curve, the Ricker curve predicts that WUW$_{DP}$ started to decrease at discharge values greater than 0.1 m^3/s (Figure 26). As the Ricker curves have shallower slopes at low discharge relative to the log-normal curves, the thresholds suggested by the tangent method are larger. The tangent approach for this Ricker curve also suggests a threshold of 0.056 m^3/s, which is nearly double that for the log-normal curve (Figure 26). At flows below the critical threshold, WUW$_{DP}$ declines more rapidly for the Ricker curve than the log-normal curve. However, while the goodness of fit of both curves is nearly equal for Dace Prey, the Ricker curve has a higher r^2 than the lognormal curve for Nooksack Dace. The likely extent to which these curve types accurately capture observable changes in biological response metrics as a function of discharge is discussed in Section 4.3 below.

3.10 Change in Wetted Width

The wetted width method is one of the most used environmental flow methodologies globally, including in Canada and the United States (Gippel and Stewardson 1998; Tharme 2003; Linnansaari 2012). It is

regarded as the simplest field-based site-specific method for determining minimum flow requirements (Gippel and Stewardson 1998). The wetted width method was tested for Otter Park using wetted widths extracted from site-visit data for HS2 and HS5, which were plotted as a function of discharge at each respective hydrometric station. Like the thresholds identified using the tangent method with WUW-discharge curves, a "breakpoint" of each curve is interpreted as a critical discharge threshold below which habitat conditions rapidly degrade for the target organism (Gippel and Stewardson 1998). The point of maximum slope and the point of unit slope are commonly used breakpoints, so both options were evaluated for each model.

In the riffle at HS5, wetted width decreased non-linearly with decreasing discharge (Figure 27). Additional wetted width measurements at intermediate flows will reduce uncertainty in the relationship, but the shallow slope of the wetted-width-discharge relationship is expected for low-gradient streams with flat streambed morphology, which characterizes Bertrand Creek at Otter Park (Gippel and Stewardson 1998). As the wetted-width discharge relationship is used to reflect change in habitat availability, the non-zero y-intercept is reflective of the maintenance of isolated pools in the riffle during periods of flow cessation like what occurred in 2019 when flow ceased in the riffle. The wetted-width-discharge relationship is reflective of site morphology and hydrology, and a simple polynomial fit provides a good approximation of the relationship ($r^2 = 0.74$). Analysis of paired wetted width and discharge data, which continue to be measured monthly at HS5, could be easily implemented to help understand how habitat availability changes with discharge.

Figure 27: Change in wetted width at HS5 as a function of discharge at HS5. Each point represents data from site visits.

For HS2, the wetted-width-discharge curve has an r^2 value of 0.0089. The poor fit results from there being little change in wetted width as discharge decreases to zero (Figure 28). As the pool habitat at HS2 is associated with relatively flat streambed morphology and is quite deep, the maintenance of wetted width at zero discharge reflects the maintenance of pool habitat through periods of flow cessation. This indication of habitation maintenance at zero discharge is biologically meaningful because previous studies have demonstrated that pool habitat likely prevents death and stranding of Nooksack Dace during periods of flow cessation and riffle drying (Avery-Gomm et al. 2014). Thus, wetted width at HS2 and HS5 are likely both useful parameters for continued monitoring at Otter Park.
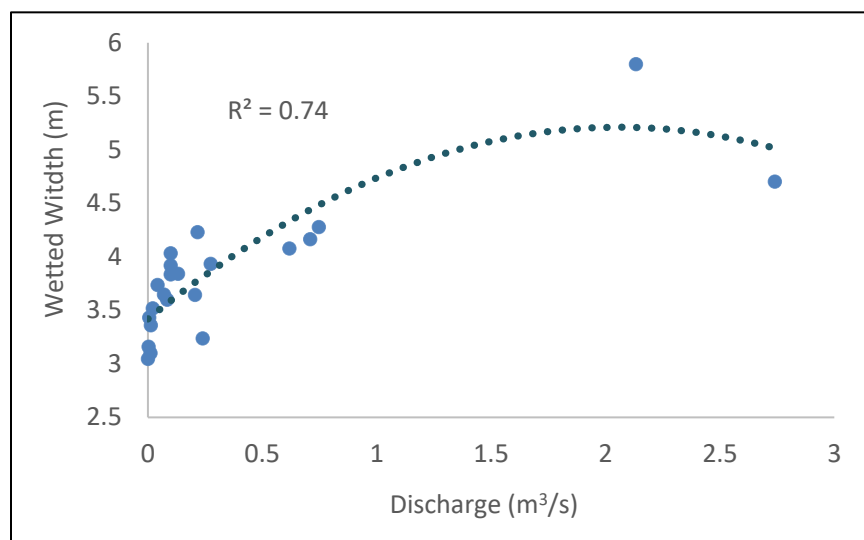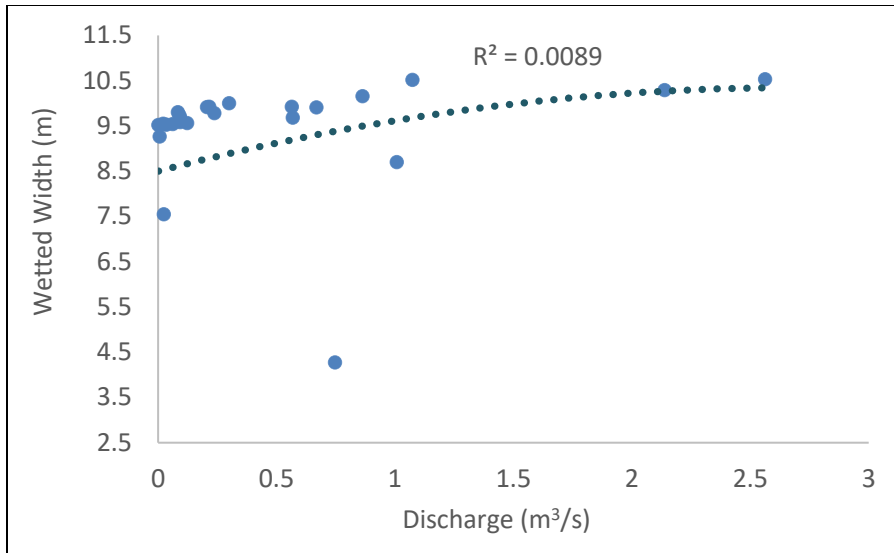
Figure 28: Change in wetted width at HS2 as a function of discharge at HS2. Each point represents data from site visits.

3.11 Streamflow Depletion Modeling

3.11.1 *Hunt (1999) Model Simulations*

The Hunt (1999) model for streamflow depletion was used to demonstrate how analytical streamflow depletion models can be linked with habitat models to estimate potential ecological impacts of groundwater pumping. This model was preferred over others because it contains a parameter for a 'clogging layer', also known as streambed impedance, which is a semipervious layer in the streambed with a lower hydraulic conductivity than the aquifer that impedes connectivity between the aquifer and the stream. A conceptual illustration of the aquifer-stream system used to frame the solution for streamflow depletion is shown in Figure 29.
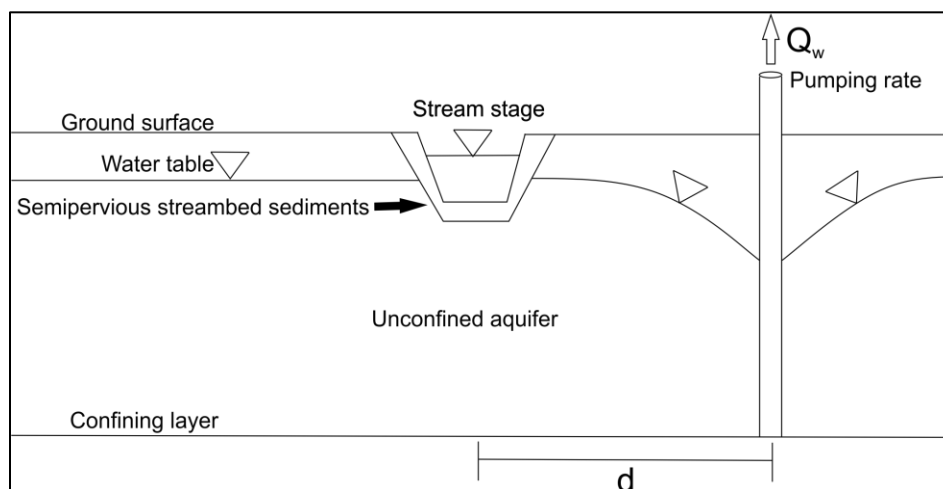
Figure 29: Conceptual model presented by Hunt (1999) frames the solution for streamflow depletion. Q_w is the groundwater pumping rate and d is the distance of the well from the stream.

Several assumptions are made in Hunt's (1999) streamflow depletion model:

1) Horizontal velocity components are much larger, so vertical components are effectively negligible;
2) The aquifer is horizontally homogenous, isotropic, and infinite in extent;
3) Equations can be linearized because drawdowns are negligible relative to the saturated thickness of the aquifer;
4) The streambed cross-section has horizontal and vertical dimensions that are small compared to the saturated aquifer thickness, and the stream extends from $y = -\infty$ to $y = +\infty$ along $x = 0$;
5) The pumping rate, Q_w, is constant;
6) Changes in stream stage are small relative to water table fluctuations;
7) Changes in head across the semi pervious layer are linearly correlated with changes in seepage flow rates between the river and the aquifer.

The Hunt model solves for the streamflow depletion rate (ΔQ_S) normalized to the pumping rate (Q_w) as a function of time (t) using Equation 6:

$$\frac{\Delta Q_S}{Q_w} = erfc\left(\sqrt{\frac{S_y d^2}{4Tt}}\right) - \exp\left(\frac{\lambda^2 t}{4S_y T} + \frac{\lambda d}{2T}\right) erfc\left(\frac{\lambda^2 t}{4S_y T} + \frac{\lambda d}{2T}\right) \tag{6}$$

with the parameters defined in Table 7. The values used for parameters in Equation 6 were consistent with those used in numerical model pumping simulations conducted by Nott and Allen (2021) to allow a comparison of these methods (see Section 3.11.2). Values for most parameters were based on the hydrogeological tests conducted at Otter Park (Allen et al. 2020). Specifically, the transmissivity (T) and specific yield (S_y) of the aquifer were calculated for each monitoring well using the Neuman method for analyzing the pumping data (Allen et al. 2020). The geometric mean values for T and S_y are reported in Table 7. Streambed hydraulic conductivity (K') was estimated from slug tests conducted in all the deep instream piezometers analyzed using both the Bower-Rice and Hvorslev methods. The geometric mean K' is reported in Table 7. The streambed conductance coefficient (λ) was calculated using:

$$\lambda = \frac{w\,K'}{b'} \tag{7}$$

Streambed conductance in the numerical model was calculated using:

$$C = \frac{K'\,x\,cell\,width\,x\,cell\,length}{b'} \tag{8}$$

with a model cell size of 25 m x 25 m.

Table 7: Variables for the Hunt (1999) model and their input values determined by Allen et al. (2020), which were used in the analytical streamflow depletion model (Equation 6). Parameters used in the numerical model by Nott and Allen (2021) are shown for comparison (see Section 3.11.2 for a description of the model).

Variable	Symbol	Units	Allen et al. (2020)	Nott and Allen (2021)
Pumping well distance from stream	d	m	15 – 401 m	15 – 401 m
Aquifer transmissivity	T	m^2/hr	3.28	3.28
Aquifer specific yield	S_y		0.272	0.272
Pumping rate	Q	m^3/hr	5.68	5.68
Streambed thickness	b'	m	1	1
Stream width	w	m	10	25 (grid size)
Streambed hydraulic conductivity (Maximum)	κ'	m/hr	5.92	5.92
Streambed conductance coefficient / conductance	λ or C	m/hr	1.71	1350 m^2/hr

For the Hunt (1999) simulations, the aquifer properties, the pumping rate, and the duration of pumping (132 days) were held constant while the distance of the pumping well from the stream (d in Equation 6) was incrementally increased from 15 m to 401 m to produce seven simulations. The model was implemented through a spreadsheet in Microsoft Excel Version 16.4. The seven functions depicting the change in streamflow depletion normalized to the pumping rate were plotted using *Matplotlib* (Hunter 2007) in Python. Model outputs for each simulation were converted to total streamflow depletion for the entire pumping period by solving for the area under each curve (i.e., integrating each function) using Simpson's Rule through *SciPy* (Virtanen et al. 2020) in Python, multiplying by the pumping rate, and dividing by the total time that the model was run (132 days). The resulting total streamflow depletion values were plotted as a function of distance of the pumping well from the stream.

The streamflow depletion vs. distance model was integrated with the WUW-discharge model with the best fit (i.e., highest r^2) to demonstrate how these models may be used as an integrative tool to evaluate potential ecological impacts of groundwater pumping. Assumptions and limitations of this approach are discussed in Section 4.3.

Using the Hunt (1999) model, seven streamflow depletion simulations were run by varying the distance of the pumping well to the stream while holding all other variables constant. Figure 30 shows the change in streamflow depletion rate (ΔQ_S) normalized to the pumping rate (Q_W), i.e. $\Delta Q_S / Q_W$, as a function of the duration of pumping for each of the seven simulations. As the distance of the pumping well from the stream increased, the total $\Delta Q_S / Q_W$ across the entire duration of the simulation decreased. The $\Delta Q_S / Q_W$ also increased more rapidly when the pumping well was closer to the stream.

Total streamflow depletion for each simulation was plotted as a function of the distance of the pumping well from the stream (Figure 31). In the next section, these results are compared with the numerical modeling. Streamflow depletion decreased with distance from the stream. The rate of change in streamflow depletion also decreased with distance from the stream. Streamflow depletion of 125 m^3/d resulted from the well positioned at just over 15 m from the stream. Increasing the distance by 375 m resulted in a decrease in total streamflow depletion to less than 10 m^3/d.
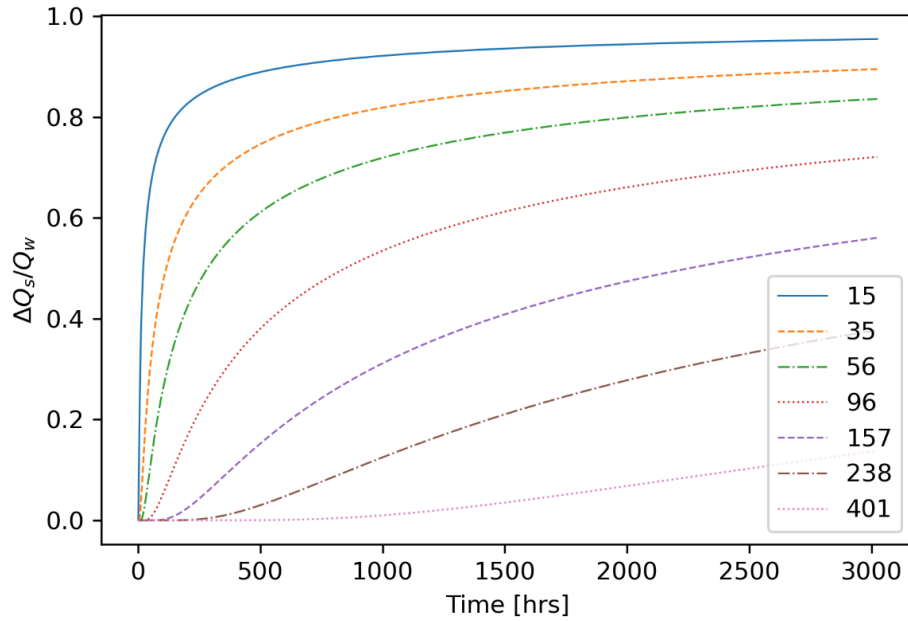
Figure 30: The change in streamflow depletion rate (ΔQs) normalized to the pumping rate (Qw) as a function of time for seven different simulations of groundwater pumping using the Hunt (1999) model. The distance from the well to the stream (in metres) for each function is indicated in the legend on the right.
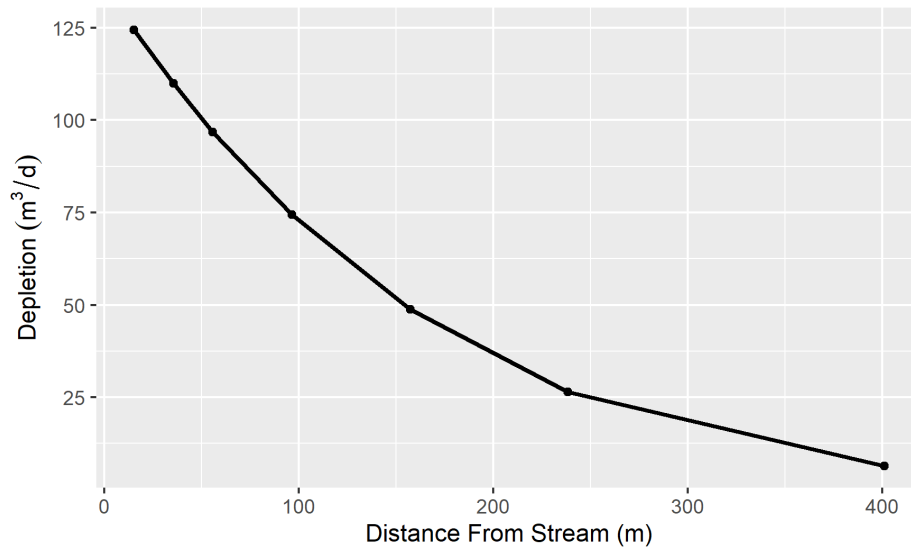
Figure 31: Total streamflow depletion as a function of the distance of the pumping well from the stream calculated from seven simulations of groundwater pumping using the Hunt (1999) model.

3.11.2 Numerical Pumping Simulations

A steady-state numerical groundwater flow model of the Bertrand Creek Watershed was developed by Nott and Allen (2020) to explore aquifer-stream exchange dynamics, including vertical flux as shown in Figure 3. The model was constructed using Visual MODFLOW Flex v6.1 (Waterloo Hydrogeologic Inc., 2019). Construction of the steady-state model is detailed in Nott and Allen (2020).

Nott and Allen (2021) used the steady-state model to explore the effects of pumping where seven pumping simulations were implemented in a transient model run for 100 years to reach quasi-steady-state. Like the Hunt (1999) model simulations detailed above in Section 3.11.1, the distance of the pumping well from the stream was increased in each consecutive simulation. These simulations were run within Otter Park, with the position of the pumping well in the second simulation (S02) corresponding to the location of PW01 (Figure 32). The pumping rate was set to that of a nearby unlicensed irrigation well, Well Tag Number 91148 (GWELLS, 2021), which has an estimated pumping rate of 5.68 m^3/hr. This pumping rate was used rather than the pumping rate employed in the Phase 2 constant discharge test at the site (324 US gpm or 73.6 m^3/hr) because the higher pumping rate caused the model to run dry.

Figure 32: Pumping well locations for pumping scenario 1 (S01) to scenario 7 (S07) are indicated by the blue circles. The distance of each well location is listed to the right of each well. The location of S02 corresponds to the location of PW01.

The numerical groundwater flow model incorporated different lithologies with heterogeneous hydraulic conductivity distributions as shown in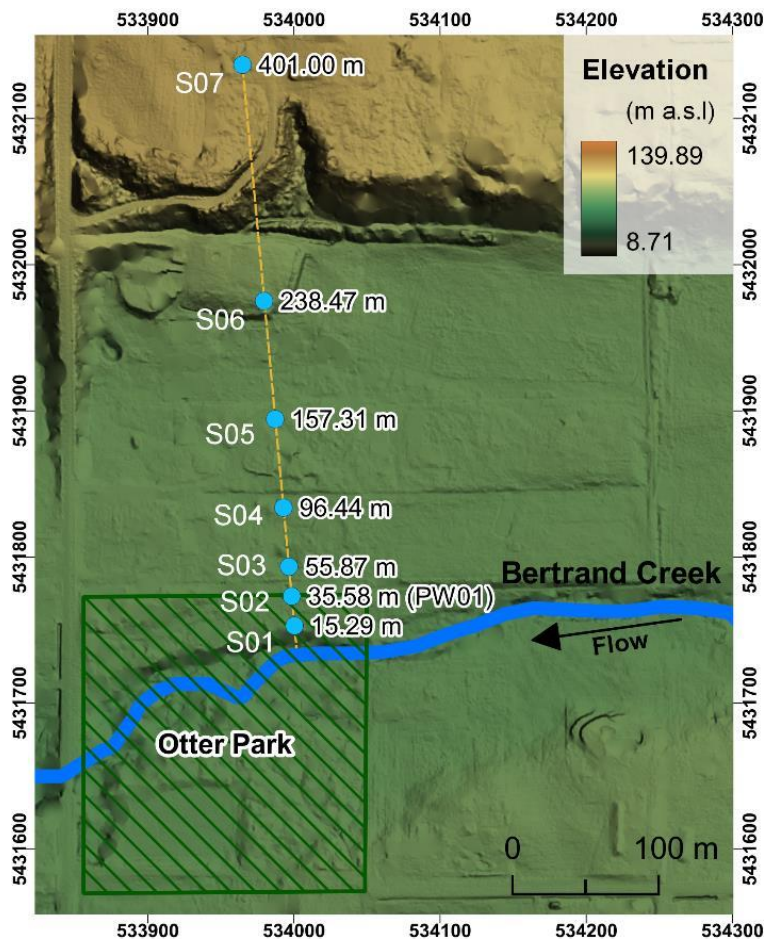 Figure 33. Therefore, the relationship between streamflow depletion and distance of the well from the stream was not smooth (Figure 33). An increase in distance from the stream of 100 m across the clay/till unit of the Fort Langley Formation resulted in a decrease in streamflow depletion roughly four times greater than that realized over a 150 m increase across the sand unit of the Sumas Drift. The slopes of the relationships between distance from the stream and streamflow depletion were similar for the gravel and sand units. Based on the streamflow depletion factor, as computed in Nott and Allen (2021), the number of days for streamflow depletion to initiate increases by roughly 160 days moving 100 m across the clay unit.

The numerical modeling results differ from the Hunt (1999) model results given above in Section 3.11.1. Proximal to the stream (~15 m), the Hunt model yields a streamflow depletion of 125 m^3/day while the numerical model yields 130 m^3/day, for a difference between models of 5 m^3/d. However, at a distance of 157 m, the results of the two models differ by roughly 70 m^3/d, due to the incorporation of lower conductivity clay-rich till in the numerical model (Figure 33). Therefore, the rate at which streamflow depletion reduces with distance from the stream is much higher in the Hunt model (Figure 31). These results suggest that either model is reasonable up to a distance where heterogeneity becomes important.
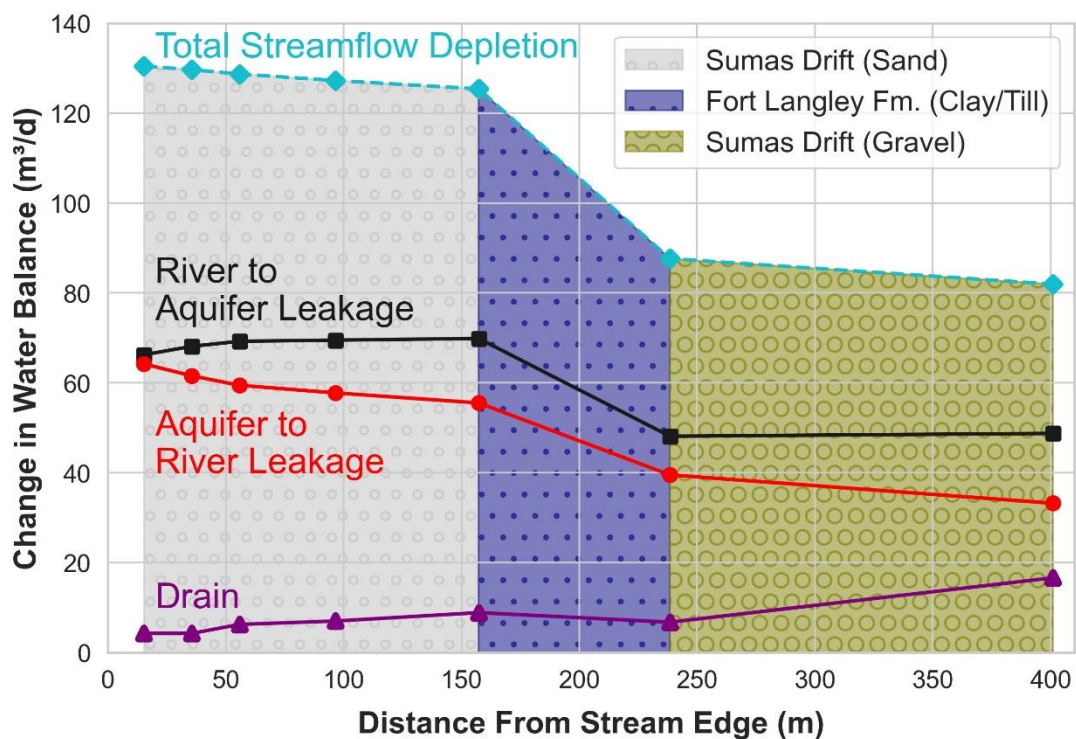

Figure 33: Numerical groundwater flow model water budget results showing the components of streamflow depletion (river to aquifer leakage and aquifer to river leakage) and the sum of those two components (total streamflow depletion) impacting Bertrand Creek during pumping. Material type varies with distance from Bertrand Creek.

3.12 Linking Pumping Models with Habitat Models

Analytical streamflow depletion models or pumping simulations from numerical groundwater flow models can be linked with habitat models, such as the WUW-discharge models (Figure 27 and Figure 28), to estimate potential ecological impacts of pumping. For example, we can estimate potential impacts on Nooksack Dace habitat at Otter Park from pumping 15 wells distanced 36 m from the stream. This is the distance of pumping well PW01 at Otter Park, which is just six metres short of the distance of the unlicensed irrigation well that was used to set the pumping rate for the numerical and analytical pumping simulations (Well Tag Number 91148; GWELLS 2021). Fifteen wells were used in this example to obtain habitat impacts that are visible on the resulting figure.

First, the depletion value corresponding to a distance of 36 m is obtained from the depletion-distance function (Figure 31) and multiplied by the number of wells to get the total depletion of 0.019 m^3/s. Using the WUW-discharge function (Figure 34), this depletion value is then used to obtain the change in WUW due to streamflow depletion, which is dependent on the initial non-pumping streamflow value selected by the user as input into the WUW-discharge function to obtain an estimate of the relative change in habitat for Nooksack Dace. For this example, the models suggest that streamflow depletion of 0.019 m^3/s would have a small positive impact on habitat at flows higher than 0.1 m^3/s (Figure 34). However, rapid habitat degradation would occur during non-pumping streamflows below 0.056 m^3/s. The same exercise could be performed using the results from the numerical groundwater flow model.
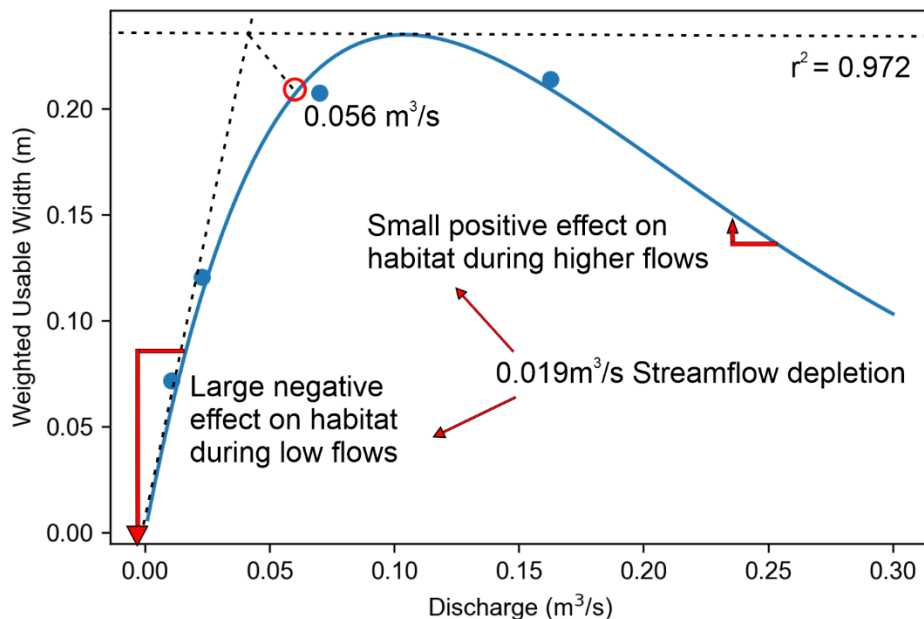
Figure 34: Example of how streamflow depletion output from the Hunt (1999) model can be used to estimate impacts on habitat using the WUW-discharge curve for Nooksack Dace fit using the equation for the Ricker Curve.

3.13 Well Counts Over Time

The cumulative number of wells in the Bertrand Creek Watershed increased consistently over each period from 1890 to 2023 based on GWELLS (2022) (Figure 35). The number of wells is likely an underestimate given that registration of wells was voluntary prior to 2016. Since the year 2000, 241 wells were added to the watershed. The largest growth in irrigation and commercial and industrial wells occurred from 1975 – 1999 with the addition of 36 and 18, respectively (Figure 36). Over time, the proportion of wells designated as water supply system wells also increased. At present day, the water use category associated with the greatest number of wells in the watershed is unknown, followed by private domestic wells. Most of the wells in close proximity to Bertrand Creek are of unknown water use or private and domestic.
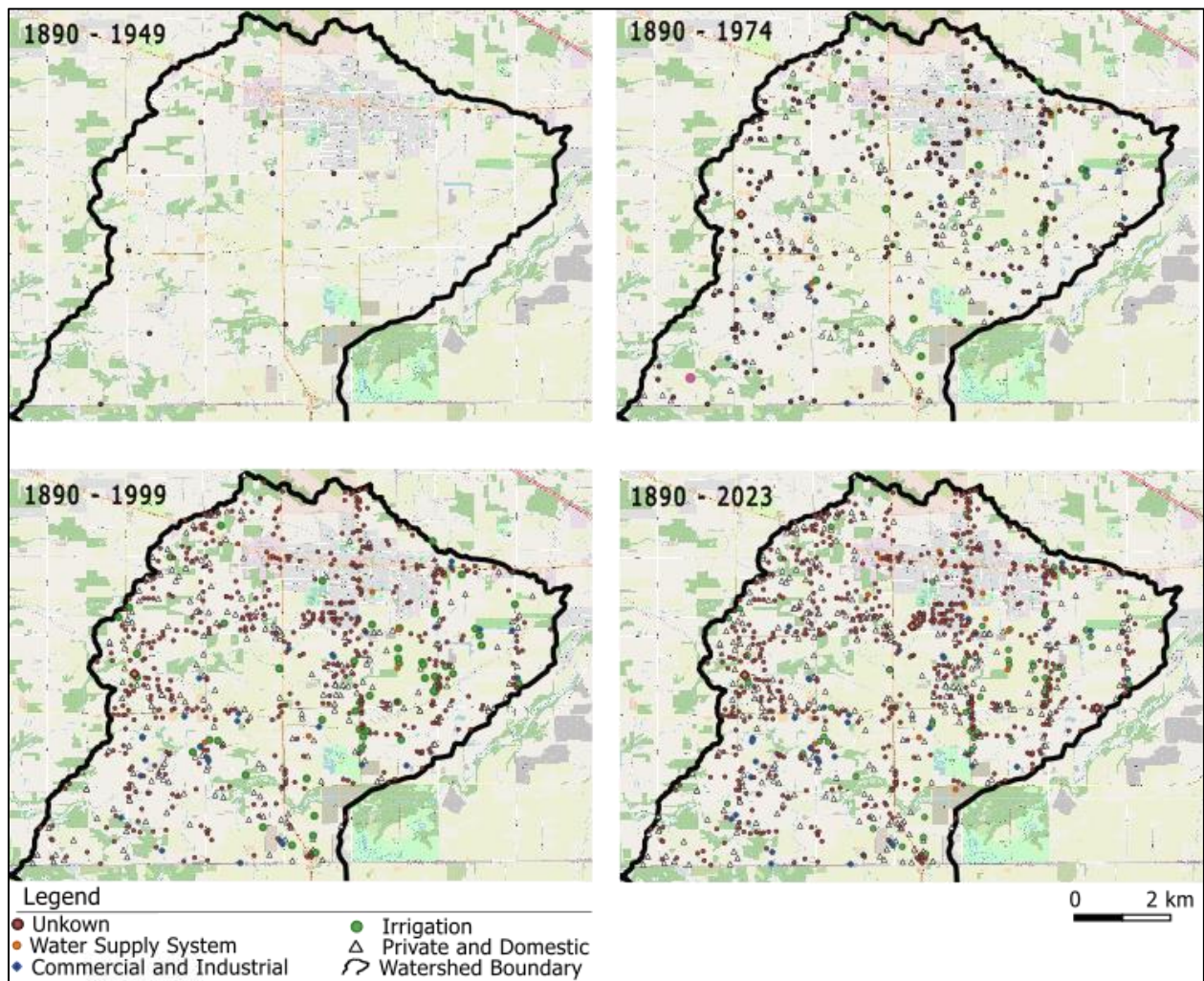
Figure 35. Cumulative number of groundwater wells in the Bertrand Creek Watershed associated with each specific water use designation for each time period.
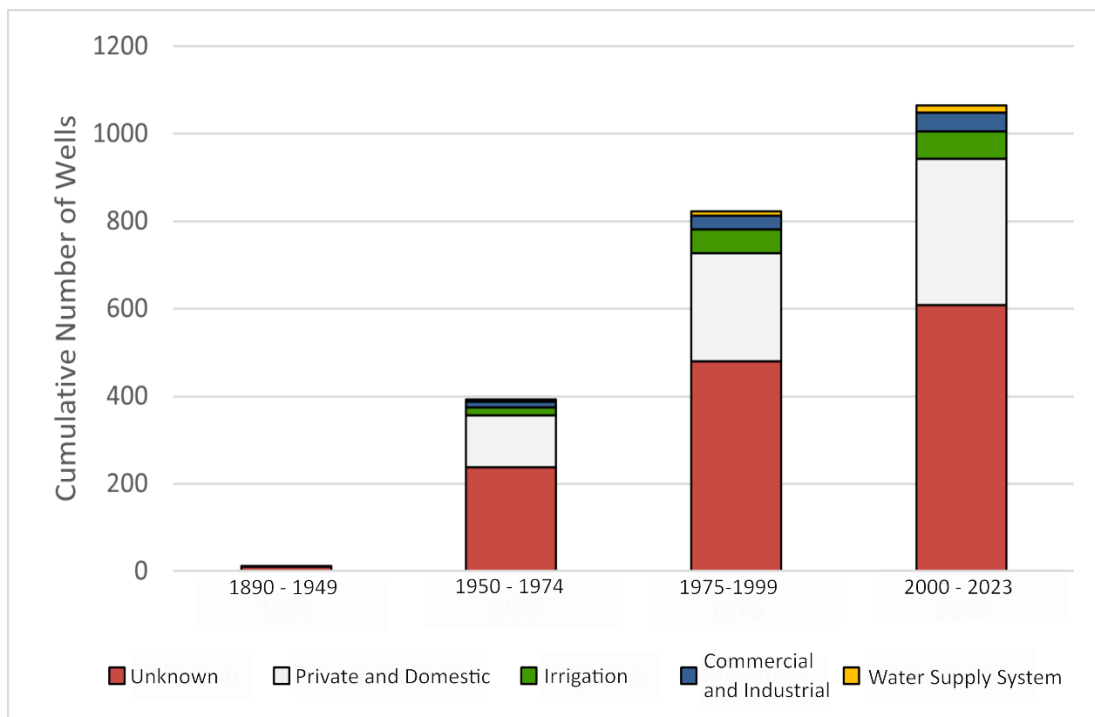
Figure 36. Cumulative number of groundwater wells for each time period in the Bertrand Creek Watershed associated with each specific water use designation.

While Figure 35 illustrates the increase in the number of wells in the watershed, it is much more difficult to estimate how much groundwater is being abstracted. Currently (as of July 2024), only 39 wells have been issued a water use license, and all are active. Using the priority date as an indication of when the well was first used and assuming the pumped volume has not changed, the total annual licensed amount of groundwater use from 1976 to 1999 was ~500,000 m³/year. From 1976 to present, the total annual licensed amount is 1,380,000 m³/year. Groundwater is pumped from five aquifers within Bertrand Creek Watershed: Aquifers 15, 27, 34, 35 and 1228.

Currently, 96 surface water licenses have been issued and all but 13 are active. Of these licenses, 32 indicate the source is Bertrand Creek itself, while the remaining are sourced from various streams including Pepin (8), Perry Homestead Brook (16), and several other small streams. Currently, 1,920,000 m³/year is licensed from all streams, with 368,000 m³/year from Bertrand Creek alone.

Between groundwater and surface water, currently ~3,300,000 m³/year is licensed, and this amount likely underestimates the total amount. Provincially, relatively few large users of groundwater have a license, although some have submitted applications. As well, a license is not required for domestic wells, and as shown in Figure 36, the largest proportion of known use is private domestic.

Ongoing research at SFU aims to simulate the incremental impacts of pumping and diversions on streamflow using an existing integrated hydrological model developed by Nott (2024).

4. DISCUSSION

4.1 Observed Hydrological Patterns

Although there were only four years of data for the hydrometric stations, streamflow patterns observed from 2018 – 2021 were relatively consistent with observations from previous reports. According to Avery-Gomm (2013), flow cessation has occurred at Otter Park during the summer since before 2010. For example, Berg and Allen (2007) reported that streamflow was near 0.1 m^3/s in June 2006 and decreased to values near 0.01 m^3/s by August at sites in Bertrand Creek. At their site, located roughly within 1 km downstream of Otter Park, pooling and overgrowth prevented a planned August streamflow measurement. The periods of flow cessation that were recorded at Otter Park from 2018 – 2021 at HS2 were characterized by the persistence of stagnant pools for variable durations. Summer low flows, flow cessation, and ponding have been known as threats to Nooksack Dace in Bertrand Creek since the early 2000s (Pearson 2000). The agreement between this study and previous studies suggests extremely low summer flows, flow cessation, and channel drying are fundamental components of the flow regime across this recent time frame (20 – 30 years).

The degree to which extremely low summer flows, flow cessation, and channel drying are naturally occurring or anthropogenically driven is an important question. Bertrand Creek's observed low flows, intermittency, and drying can likely be attributed to a mix of natural and anthropogenic factors. Naturally, Bertrand Creek, as a lowland stream, is predisposed to experience flow intermittency near its headwaters, especially during the drier summer months. However, anthropogenic activities have likely exacerbated these conditions. Groundwater abstraction, as evidenced by the steady-state numerical groundwater flow model constructed by Nott and Allen (2020), plays a role, redirecting more stream water into aquifers under pumping conditions and resulting in less groundwater discharge to the stream. Groundwater capture has the potential to exacerbate flow cessation and dry conditions in certain reaches of Bertrand Creek, especially upstream of Otter Park (Nott and Allen 2020). However, groundwater abstraction is not the only culprit. Changes in land use, channelization, dredging, and siltation have transformed Bertrand Creek's hydrological character over time. The cumulative impact of these activities, coupled with groundwater withdrawals, make it challenging to decouple and quantify their individual effects on streamflow. Without comprehensive and accurate water-use data, it becomes challenging to fully determine the quantitative impact of water withdrawals and to distinguish between natural and anthropogenic drivers of the observed streamflow alterations.

Regardless of the degree to which flow intermittency in Bertrand Creek at Otter Park is naturally or anthropogenically driven, evidence that flow cessation and drying are regular occurrences at Otter Park raise doubt of whether Bertrand Creek is a perennial stream as it has typically been labelled. Recently, the term "intermittent rivers and ephemeral streams" has been used increasingly to refer to any river or stream that ceases to flow at some point along its course (e.g., Datry et al. 2017; Stubbington et al. 2018; Borg Galea et al. 2019; Gómez-Gener et al. 2021). Following this understanding of terminology, the term "drought", which has been used to refer to the flow cessation and drying events in Bertrand Creek (e.g., Avery-Gomm et al. 2014), typically refers to a rare event of low water availability in a perennial stream, not a recurring event that is effectively a component of a stream's flow regime (Boulton 2003; Bonada 2006; Datry et al. 2014; 2017). While the exact terminology is not necessarily important, differentiating between a stream that experiences these events yearly versus every few years is critical because the regularity of flow cessation and drying is a fundamental control on how both habitat and biota fluctuate spatially and temporally (Boulton 2003; Datry et al. 2014; 2017). Thus, exploring how to characterize systems with these unique hydrological characteristics will likely be important for guiding and coordinating their management.

The temporal and spatial intermittence of streamflow characteristics of Bertrand Creek likely implies that not all hydroecological principles or management approaches used in perennial streams can be simply applied in Bertrand Creek, especially for the upper reaches such as near Otter Park. For streams in which flow cessation is spatially limited (i.e., spatially intermittent streams), fundamental ecological concepts like the River Continuum Concept (Vannote et al., 1980) may break down because they were modelled after perennial streams with year-round continuity in their longitudinal connectivity (Datry et al. 2017). The transferability of flow-ecology relationships and environmental flow assessment methodologies may also be limited in non-perennial systems because most have been developed in perennial streams (Buttle et al. 2012; Datry et al. 2014; 2017). While research on non-perennial systems is steadily growing (Datry et al. 2017), the spatial extent of research is limited, especially in Canada (Buttle 2012). This disparity in the representation of perennial versus non-perennial streams in the literature implies high uncertainty in the validity of traditional hydroecological models and management approaches for Otter Park, which likely precludes easy implementation of "rule-of-thumb" approaches used widely in environmental flow assessments. Moreover, these events will likely necessitate new strategies for long-term monitoring of hydrological variability and ecological outcomes of any decisions.

The observed effects of precipitation and temperature variability on flow persistence at Otter Park is one important consideration. On the one hand, the expected increase in the frequency of relatively wet years could decrease the number of years with flow cessation and/or drying events (B.C. Ministry of Environment (MOE) 2016). A significant increase in flow persistence can alter the state of ecosystems that are adapted to regular flow cessation and drying. However, increasing flow persistence is unlikely since streamflow in the region, especially summer flow, has been declining through time in response to increasing temperature (MOE 2016). High sensitivity of streamflow to temperature at Otter Park was evidenced by the longest and earliest onset of flow cessation occurring in 2021, despite 2018 being drier. This suggests that flow cessation and drying events at Otter Park will likely intensify with expected increases in summer temperatures and extreme temperature events (MOE 2016).

Characterization of aquifer-stream exchange is important for understanding variability in the direction and magnitude of exchange flow and thus how groundwater may buffer the effects of dry weather on instream habitat. The average upward vertical flow across the streambed (see Figure 9) suggests the stream was gaining groundwater for much of the 2019 focal period, and for the periods of time in 2020 near when flow cessation occurred later in the summer. This is supported by the fact that streamflow was maintained at the downstream hydrometric station, HS5, during periods when flow ceased at HS2 in 2020. Additionally, streamflow was maintained at HS5 during the entire 67-day period of flow cessation and drying at HS2 in 2021. Allen et al. (2020) also found that the stream was gaining at Otter Park in July 2018.

Conversely, the steady-state numerical groundwater flow model constructed by Nott and Allen (2020) suggests that most reaches in Bertrand Creek experience a net loss to the groundwater system on an average annual basis. However, the model also suggests Otter Park marks a transition zone where the occurrence of gaining reaches becomes more interspersed with losing reaches with increasing distance downstream (Nott and Allen, 2020). Thus, due to the high spatial variability in the direction and magnitude of flux between the aquifer and stream, and the fact that a steady-state model was used which represents mean annual groundwater conditions, the model results do not rule out the possibility that Otter Park receives groundwater input at some locations in the summer. Ultimately, the results of this study suggest that groundwater discharge to the stream serves as a buffer to the effects of dry weather patterns on instream conditions by aiding the persistence of standing pools in upstream segments and flow in downstream segments.

With groundwater likely playing an important ecological role, especially during low flows and periods of flow cessation, groundwater level decline would likely have adverse ecological impacts. The sensitivity of groundwater level in the aquifer adjacent to Otter Park to precipitation and temperature variability indicates the potential for groundwater levels to drop lower during summer dry periods if dry periods intensify. Reduced baseflows in Bertrand Creek have been attributed to both surface water and groundwater withdrawals (Golder Associates Ltd. 2005). In the United States portion of the Bertrand Creek Watershed, Pruneda et al. (2010) found that replacing some surface water withdrawals with groundwater would help improve summer flows. However, while supplementing water demands with groundwater may help, groundwater abstraction could exacerbate the losing nature of the stream (Nott and Allen 2020). Segments upstream of Otter Park are especially vulnerable to pumping-induced streamflow depletion and possibly flow cessation and drying events (Nott and Allen 2020). The pumping test conducted at Otter Park in 2018 demonstrated that pumping adjacent to Otter Park can induce streamflow depletion. Fortunately, in terms of recent groundwater level trends, only one (008) of five observation wells mapped to the Abbotsford-Sumas Aquifer exhibits a decreasing trend (AQ_00015_Aquifer_Factsheet.pdf). However, depending on how water depth and the area of wetted streambed respond to declining discharge in different habitat units and stream segments, localized pumping and the cumulative effects of pumping throughout the watershed could substantially alter the spatial and temporal variability in habitat availability and quality.

4.2   Hydraulic Habitat Variables

Characterization of variability in depth, velocity, and substrate in 2020 helped identify aspects of physical habitat heterogeneity that are likely ecologically important, including spatial variability in the change in hydraulic habitat variables with streamflow decline. The decline in depth with streamflow decline in riffle habitat to values near zero was expected because rapid drying of riffle habitat near the point of streamflow cessation is common for non-perennial and drought-stricken streams (Boulton and Lake 1990; Lake 2003; Avery-Gomm et al. 2013; Rosenfeld, 2017). Reflective of the relatively flat, even streambed topography in riffle habitat, the relationship between depth and discharge was nearly linear in riffles (see Figure 11b). Because the September macroinvertebrate sampling event occurred one day after a precipitation event that caused flow resumption, the sites in the upstream riffle habitat were only observed when wetted in 2020. However, the depths recorded at those sites, and the drying of other portions of the same riffle habitat suggest that these sites likely dried for some short period of time during the period of flow cessation.

Depth-discharge relationships in pools differed from riffles due to contrasts in streambed morphology between the two habitat types. The concave shape of pools, with the greatest depths in the center of the pool and shallower depths near the banks, explains the variation in discharge-depth relationships among individual sites within a given pool. Non-zero water depths in pools recorded at near zero discharge indicate the persistence of standing pools during non-flowing periods. Lower streambed elevations and finer sediments in pools relative to adjacent riffles are main reasons why pools persist while riffles dewater quickly following flow cessation. With more rapid loss of riffle habitat with streamflow decline and flow cessation, the maintenance of depth at pool sites throughout the entire period of flow cessation may have provided refuge for some aquatic organisms (Chester et al. 2010). For example, while Nooksack Dace growth is slower in these low-velocity pool habitats, the riffle-dwelling Nooksack Dace still use pools to avoid stranding and death during dry periods (Avery-Gomm et al. 2014). Therefore, the persistence of pools at Otter Park, even during periods of flow cessation, suggests that a discharge of zero does not imply a complete loss of habitat for all species. Thus, in the context of stream management, Otter Park reach should not be considered inactive during non-flowing periods, as has historically been assumed for intermittent reaches, because, for example, water abstraction during non-

flowing periods can still have negative ecological impacts by accelerating the contraction of pools impacted.

4.2.1   Water Quality Variables

Characterization of spatial and temporal variability in water quality variables helped identify variables of concern in terms of their relative likelihood to impact aquatic ecosystem health. DO values recorded at most sites in September 2020 were below 5 mg/L, which is the federal guideline for the protection of aquatic life (CCREM, 2015) and the target recommended for the recovery of Nooksack Dace (Fisheries and Oceans 2019). Stream temperature frequently exceeded the 18°C MWMT guideline at both hydrometric stations. Moreover, stream temperature neared 23°C, which is the lower bound of temperatures considered to be harmful for Nooksack Dace. These observations concur with previous reporting of low DO and elevated stream temperature being primary concerns for ecological health in Bertrand Creek. Therefore, DO and temperature should be considered primary water quality variables of concern.

As a low-gradient, intermittent stream, Bertrand Creek is prone to low DO during periods of hot and dry weather. As precipitation declines through the spring and summer months, Bertrand Creek is susceptible to DO losses with declining discharge because there is often little re-aeration that occurs by turbulent flow through riffle habitat in low gradient streams (Rosenfeld 2017). Moreover, streams that experience periods of flow cessation often experience extreme declines in DO due to the oxidation of organic matter that builds up in pools as flow ceases (Lake 2003; Datry et al. 2014). Oxidation of organic matter is likely an important cause of the low DO levels observed at most Otter Park sampling sites in September 2020, as thick deposits of leaf litter were observed on the streambed. The finding that only the two riffle sites with the highest stream velocity had DO levels above water quality guidelines may suggest that riffle aeration may play some local role in oxygenation exclusively during low flows when DO levels are already low, which could help maintain preferred habitat conditions for riffle-dwellers.

Just as hydraulic habitat variables in riffles were relatively sensitive to changing discharge, the high stream temperature variability at HS5 suggests that riffle habitat may be more sensitive to changes in air temperature. Greater water depths covering a larger proportion of the stream channel in the pool habitat at HS2, likely resulted in relatively less heating of streambed material compared to the riffle at HS5 (Poole and Berman 2001; Caissie 2006). Canopy cover, which can influence air movement and therefore convective heat transfer (Poole and Berman 2001) was similar at HS2 and HS5, so the amount of heat energy blocked by the riparian canopy at both sites was likely similar (Poole and Berman 2001; Caissie 2006). These complex interactions between climatic, hydrological, and habitat variables could enhance negative impacts of climate change on stream temperature. For example, increasing stream temperature in response to increasing air temperature would be amplified by decreased stream depth driven by the effect of lower precipitation on streamflow. Groundwater pumping may also impact stream temperatures. Groundwater discharge to streams moderates stream temperature fluctuations (Boulton and Handcock 2006); therefore, a reduction in groundwater discharge due to the capture of groundwater that would otherwise have discharged into the stream may also impact stream temperatures. Moreover, groundwater pumping may induce infiltration from the stream, thereby leading to streamflow depletion and, consequently, stream warming.

Differences in thermal sensitivity of habitat units may be useful for estimating potential impacts of temperature changes on different aquatic species and thus help inform stream management activities. For example, greater sensitivity of stream temperature in riffle habitat to air temperature changes may imply that air temperature increases will disproportionately impact riffle-dwelling species like Nooksack Dace. In turn, activities such as riparian enhancement could target areas adjacent to riffles. Although

Nooksack Dace are not likely to experience reduced fitness under historical temperature ranges (below 23C°), the potential for increased frequency of extreme high stream temperature due to climate change is an important consideration. Extreme temperatures exceeding 25 C° were recorded at HS5 during the 2021 heatwave. In addition to the direct effects of stream temperature on aquatic species, hotter stream temperatures will also negatively impact DO concentrations, potentially increasing the severity of hypoxia in Bertrand Creek. Careful DO and temperature monitoring will be important for understanding potential combinations of effects on stream biota and ecosystem health.

4.2.2 *Benthic Macroinvertebrates and Instream Habitat Variables*

The composition of the benthic macroinvertebrate assemblage constituted by all samples collected at Otter Park resembles invertebrate communities found at severely degraded sites (Hilsenhoff 1987; Barbour et al. 1999; Rosenberg et al. 1999). As Ephemeroptera, Plecoptera, and Trichoptera (EPT) taxa are relatively intolerant to poor water quality, the presence of only two EPT families across the study period would typically be attributed to degraded water quality related to contaminants associated with nearby land uses (Hilsenhoff 1987; Barbour et al. 1999; Rosenberg et al. 1999). This is also evidenced by the overwhelming dominance just four invertebrate families, which are all relatively tolerant (Simuliidae, Baetidae, Gammaridae, and Chironomidae (Hilsenhoff 1987; Barbour et al. 1999). Although chironomid dominance is sometimes interpreted as an indicator of degradation, it is normal for chironomids to dominate invertebrate communities, even in relatively pristine streams (Bouchard 2004). Yet, the large dominance of chironomids paired with the presence of few families and, which are in extremely low abundance, is not common for undisturbed stream systems sites (Hilsenhoff 1987; Barbour et al. 1999; Rosenberg et al. 1999). Although community assemblages vary between regions, common metrics such as the number of unique families and the number of EPT families were found to be strong predictors of biological impairment in the Pitt River and surrounding streams in southwest British Columbia (Rosenberg et al. 1999). Pappas (2008) frequently reported EPT richness values between 5 and 10 at sites impacted by agricultural and urban land use in the Salmon River Catchment, which neighbours Bertrand Creek. In comparison, just two EPT taxa were found at Otter Park. In another neighbouring stream, Pepin Brook, Avery-Gomm (2013), identified caddisflies and stoneflies in addition to mayflies in a study that was also carried out across the summer. Interestingly, Pepin Brook experiences many of the same water quality issues as Bertrand Creek, such as widespread hypoxia during summer low flows (Fisheries and Oceans Canada, 2020). Therefore, the macroinvertebrate communities at Otter Park can likely not be explained solely by poor water quality related to local land uses.

The recurrence of extremely low flows, flow cessation, and drying at Otter Park has likely shaped the Otter Park communities over time. The effects of these flow events and associated changes in habitat conditions on macroinvertebrate communities can be interpreted as anthropogenic contamination because taxa tolerant of the former are typically tolerant of the latter (Rose et al. 2008). In other streams with recurring periods of flow cessation and drying, relatively low EPT richness has been attributed to the effects of adverse changes in habitat conditions and declining habitat availability on intolerant taxa (Boulton, 2003; Lake 2003; Storey 2008; Feminella, 1996)). In turn, the dominance of just a few taxa can be explained by their characteristics, which allow them to persist through adverse changes in habitat conditions. The dominance of chironomids and gammarids and their persistence through the period of flow cessation is likely explained by their utilization of refuge habitats, such as pools or wetted interstitial spaces in the hyporheic zone (Boulton 1992; Dieterich & Anderson 2000; Poff et al. 2006; Stubbington et al. 2009; Datry et al. 2016; Vander Vorste et al. 2016). Year-round presence of chironomids in non-perennial streams has also been attributed in part to the short life cycles of many chironomid taxa. Black flies and baetid mayflies are often found in streams that experience flow

cessation because they possess traits that allow them to rapidly recolonize impacted reaches after flow resumption and drying (Mackay 1992; Robinson et al. 2003). Black flies are often abundant in non-perennial streams because they have desiccation resistant eggs, and some taxa also exhibit refuge seeking behaviour (Mackay 1992). Baetid mayfly abundance can be attributed in part to their strong swimming ability, which allows them to drift to downstream perennial reaches when streamflow ceases or habitat conditions become unfavourable in non-perennial reaches, and then swim back to recolonize non-perennial reaches after the resumption of streamflow (Mackay 1992). Baetids can successfully recolonize habitats immediately following flow resumption because they are able to feed on extremely thin layers of algae on rock, which are often all that is available after desiccation of algal layers in the open air (Mackay 1992). All four dominant taxa are in fact the most common first-arrivers on bare substrates in newly rewetted reaches (Mackay 1992). Given the strong resemblance of the benthic macroinvertebrate communities at Otter Park to communities at other non-perennial sites from previous studies, it is likely that the recurrence of flow cessation and drying at Otter Park since at least the late 2000s has strongly influenced the present-day taxanomic composition of the benthic macroinvertebrate assemblage at Otter Park.

Despite evidence that the dominant taxa at Otter Park are likely well adapted to deal with extreme changes in habitat conditions associated with regular flow cessation and drying events, the results of the analyses of macroinvertebrate and habitat data suggest that some macroinvertebrate taxa at Otter Park still have preferences for specific ranges of habitat variables. The GAM analysis revealed significant correlations between both Dace Prey abundance and total abundance with DO. Relationships between DO and benthic macroinvertebrate metrics vary widely throughout the literature. In a study of eight streams in Southwestern B.C., Reece and Richardson (2000) found significant positive correlations between abundance and a number of environmental variables, including conductivity and pH, but not DO. In a review by Davis (1975), minimum DO requirements were not defined for macroinvertebrates as they were for fish because of their ability to use anaerobic metabolism during periods of low DO. However, the minimum DO requirement of 5 mg/L suggested to protect Canadian fish species was recommended to also be applied to protect macroinvertebrates because shifts in typical DO patterns for a given stream would likely impact macroinvertebrate community composition. In a controlled laboratory experiment Kaller and Kelso (2007) also found that macroinvertebrates were able to tolerate sub-lethal effects of hypoxia. However, total abundance was higher for treatments with greater DO concentrations, and different taxa responded differently to declining DO, supporting the potential influence of DO on community composition. Ultimately, detailed multi-year analyses of macroinvertebrate-DO relationships are needed to accurately define macroinvertebrate-DO relationships for different taxa and the mechanisms underlying these relationships. However, the 5 mg/L guidelines used for many fish species across Canada, including Nooksack Dace, is likely adequate for the protection of macroinvertebrate communities at Otter Park and elsewhere in Bertrand Creek.

In contrast to DO, many studies have examined benthic macroinvertebrate-velocity relationships. The lower uncertainty and greater magnitude of the velocity effect in both the total abundance and Dace prey abundance GAMs suggests velocity was the most significant driver of variability. Velocity is often found to be one of the most important predictors of benthic macroinvertebrate distributions (Statzner et al. 1988; Bonada 2006; Monk et al. 2018). The concentration of most black flies and baetid mayflies at R3 and R4 with velocities of roughly 0.3 – 0.6 m/s agrees with the velocity preference values of just over 0.4 m/s derived from the Canadian Aquatic Biomonitoring Network (CABIN) database (Armanini et al. 2011). Chironomids and gammarids are typically more evenly distributed between riffles and pools, which explains the lack of strong relationships with these taxa and velocity in their respective GAMs. However, slightly higher abundances of these taxa in higher velocity riffle sites resulted in a strong correlation between velocity and total abundance. A strong correlation was also found for velocity and

Dace prey abundance, which is the metric primarily constituted by gammarids, black flies, and baetid mayflies. While gammarids and chironomids are typically more evenly distributed among riffle habitat and pool habitat, strong velocity preferences have been documented for certain species of gammarids and chironomids in other studies, which may help account for higher abundances in riffles (Burgazzi et al., 2020). In addition to velocity driving spatial variability in abundance for baetid mayflies and black flies, declining velocity with discharge likely played a key role in driving the elimination of these taxa because declining velocity is often associated with marked increases in the numbers of these taxa drifting downstream, likely to sites of greater flow persistence with more favourable velocity conditions (James et al. 2008). Maintenance of velocities typically associated with riffle habitat is therefore likely critical for maintaining macroinvertebrate biodiversity, as well as the abundance of invertebrates in riffles, which is especially important for their riffle-dwelling Nooksack Dace predators. However, potential sources of uncertainty in the modelled effects of both velocity and DO and their implications for Dace prey availability should be considered. These are discussed below with the discussion of HSI curves to better demonstrate how these different models compare in their strengths and weaknesses.

4.3   Habitat Models

Relative to building GAMs, construction of HSI curves was quick and required little background knowledge. In addition to the lower effort requirement, the HSI and subsequent WUW modelling procedure was attractive because it produced firm discharge values, which are typically used to set minimum flow requirements. However, the resulting threshold depended on which curve-fitting method was used. The Ricker curves suggest a negative impact on habitat suitability of flows higher than 0.1 m^3/s, while the log-normal curves suggest WUW steadily increases with discharge past 0.1 m^3/s. Both curves suggest a decrease in habitat suitability below 0.1 m^3/s, but the discharge thresholds suggested by the tangent method differed between the Ricker curve and log-normal curve. For both Nooksack Dace and Dace prey, the application of the tangent method using the Ricker curves suggested that 0.056 m^3/s is the threshold below which habitat degrades rapidly. Conversely, application of the tangent method using the log-normal curve suggested a threshold of 0.029 m^3/s for Dace prey and 0.032 m^3/s for Nooksack Dace. Although Lewis et al. (2004) demonstrated that the WUW-discharge relationship for steelhead trout juveniles followed a log-normal curve, and while the Okanagan Nation Alliance (2020) used a Ricker curve model the WUW-discharge relationship for steelhead, manual selection of one of the curves leaves too much to professional judgement. To truly evaluate which model best estimates the true fish-habitat or invertebrate-habitat relationship, the model results should be evaluated against some biological rate, such as growth, or a population-level metric, such as population change (Bovee 1986). Therefore, a conclusion as to which model is best cannot be made without further study, but it is clear that the choice of curve-fitting method can greatly impact the WUW-discharge relationship and the results of the tangent method.

While the quality of the WUW-discharge models cannot be properly evaluated, some comparisons can be made against results of Avery-Gomm's (2013) study of Nooksack Dace in Bertrand Creek. Although not a WUW-discharge relationship, Avery-Gomm's (2013) WUA-discharge relationship resembled a log-normal curve more than a Ricker curve. The discharge (0.12 m^3/s) at which the tangent method indicated a rapid decline in weighted usable area (WUA) for Nooksack Dace (Figure 3.3 in Avery-Gomm, 2013) was double the value of 0.056 m^3/s associated with the Ricker curves for both Nooksack Dace and Dace prey and nearly quadruple the value of 0.032 m^3/s associated with the log-normal curves in this study. Avery-Gomm (2013) did in fact find a positive relationship between biomass and WUA for Nooksack Dace in Bertrand Creek, which is a key underlying assumption of these habitat simulation EFMs (Bovee 1986). However, the relationship was weak, which suggests there was high uncertainty of how Nooksack Dace would be impacted at higher flows. Because the higher flows are where the Ricker

and log-normal curves differ most significantly, Avery-Gomm's (2013) results do not provide any means with which to evaluate which curve is best. However, the higher confidence in the WUA-biomass relationship at lower flows found by Avery-Gomm (2013) provides some evidence that habitat for the Nooksack Dace declines with discharge, but the accuracy of the specific discharge values at which thresholds in habitat are crossed are highly uncertain.

An interesting point to consider is whether the intercepts of these habitat models are appropriate if Nooksack Dace can still occupy standing pool habitats when discharge is zero (Avery-Gomm et al. 2014). Although biomass was lower for Nooksack Dace that had to rely on standing pools to survive flow cessation, the availability of some habitat, although lower quality, might be important to capture in the habitat models (Avery-Gomm et al. 2014). As the use of standing pools by fish and insects as refuge habitat during dry periods is a common phenomenon in streams that experience flow cessation. Thus, non-zero y-intercepts may be a key characteristic to capture in the habitat models for certain species in these systems. Alternatively, certain species may require two separate models, one with discharge as the independent variable, and one with water level as the independent variable. Either way, examinations of how to quantify and portray biotic responses to changing habitat conditions during non-flowing phases would greatly improve our ability to estimate ecological responses across the complete spectrum of hydrological variability in non-perennial systems.

Approaches involving HSI models have been heavily criticized in the literature. Yet, while GAMs are more highly regarded, they do not necessarily outperform HSI models in every scenario to render them obsolete (Jowett and Richardson 2007). For example, a common criticism of HSI models is that each habitat variable (i.e., depth, velocity, substrate) is treated as equally important instead of there being a variable selection process like is often performed using GAMs. Yet, Jowett and Richardson (2007) found that this did not have a major impact on the results of HSI models relative to GAMs. They also found that the benefit of being able to include interaction terms in GAMs was limited because typically just the basic single predictors were found to be significant (Jowett and Richardson 2007). Interaction terms are also hard to interpret and can cause issues of multi-collinearity. Consequent of the expertise required to safely model complex interactions, the time and budget constraints typical of most professional settings likely diminish the value of the interaction modelling feature. Without interaction terms, GAMs remain more challenging to learn than HSI modelling. However, with the complexity of GAMs comes their flexibility, and in turn, models that better capture the natural contouring of data (Jowett and Richardson 2007). In contrast, the binning approach used to construct the HSI curves effectively alters the curvature of the data. As such, binning imposes a coarser resolution at which you may identify critical thresholds of habitat change, with the resolution determined by the bin size. Binning can also lead to unequal variances across bins, especially when the sample sizes associated with each bin are highly variable. However, if constructing an HSI curve from a large number of samples, procedures detailed by Bovee and Cochnauer (1977) can be followed to minimize variance. Low sample size and uneven sample size across bins resulted in the deviation of the GAM and HSI model results at the highest velocity values. However, both models captured the general preference of Dace prey for higher velocities. The HSI models can be improved by constructing the curves from larger sample size, preferably with samples covering a greater range of discharge values and a greater number of sites in different locations throughout the stream or stream reach (Bovee 1986; Bovee and Cochnauer 1977; Inglis 1994; Avery-Gomm 2013).

Another limitation is that WUW and WUA cannot be readily measured in the field, which limits verification of habitat simulation results and makes it difficult for decision makers unfamiliar with habitat simulation methodologies to interpret the results and their consequences for the target organisms being modelled (Jowett and Davey 2007). Therefore, as Jowett and Davey (2007) highlight,

modelling approaches that produce a measurable output, such as GAMs of fish or macroinvertebrate abundance as functions of habitat variables, may be better alternatives. WUW and WUA output may also not be of appropriate spatial scale for certain target organisms (Manly et al. 2002). WUW represents habitat as a portion of a single transect drawn perpendicular to flow (Lewis et al. 2004), while WUA represents habitat as a cell that constitutes some area of the streambed (Bovee 1986). For larger aquatic species with large habitat ranges, representing their habitat-discharge relationships using data from a few transects across a reach only metres in length is unlikely to truly capture how their habitat changes with discharge, especially in a stream where hydraulic habitat variables such as depth and velocity vary widely between the transects that are being used as proxies (Manly et al. 2002; Lewis et al. 2004). Likewise, trying to represent their habitat in cells of a few square metres in area does not agree with the spatial scales at which they seek their prey (Manly et al. 2002). However, the same arguments of inappropriate scale may also apply to the use of GAMs if the input for the predictor (i.e., habitat) variables is obtained by measuring those variables over a small area. Mesohabitat models or models of different scales may therefore be more useful in many instances (Parasiewicz 2001, Manly et al. 2002). For macroinvertebrates and their small drift-feeding predators, Nooksack Dace, WUW models or local-scale GAMs may be more suitable than for larger fish (Manly et al. 2002). If the spatial scale is suitable for both the fish and its prey, both habitat-discharge relationships might be modelled with the inclusion of the predator-prey relationship, potentially improving the model (Jowett 1998; Rosenfeld 2017). However, as Rosenfeld (2017) asserts, the scale at which predator-prey relationships occur can greatly impact the accuracy of the habitat-discharge relationship. The example given by Rosenfeld (2017) is that drift-feeding fish that occupy low velocity pools often rely on invertebrate drift from high velocity riffles, so while WUA or WUW will be maximized for the fish when low-velocity habitats are maximized (i.e., at low discharge), the prey availability will actually be lower. Therefore, if prey availability is limiting to a target organism, it is important to consider how differences in habitat preferences and different scales of habitat use by predator and prey might impact the habitat modelling results. Nooksack Dace are riffle specialists and the majority of their prey occupy riffle habitats, so WUW and WUA will increase with velocity for both predator and prey to some point as demonstrated in the HSI curves presented in this study (Avery-Gomm 2014; Champion 2016; Fisheries and Oceans Canada 2019). However, the foraging efficiency of Nooksack Dace decreases with velocity (Champion 2016), so the effect of habitat variables on the ability for a predator to capture its prey is important even if predator and prey occupy the same habitat and have similar HSI curves. Ultimately, while the appropriateness of scale of the habitat models is likely not an issue for macroinvertebrates and potentially less problematic for Nooksack Dace relative to larger fish, considerations of the appropriateness of scale will likely be critical for other studies looking to apply these methods.

Some other fundamental assumptions involved with the construction of these habitat model curves may also limit their applicability. Neither type of model developed for Dace prey accounted for the availability of habitat, which means that the apparent preferences of Dace prey for certain habitat characteristics may be due to the fact that other habitat characteristics were less available (Bovee 1986). Accounting for habitat availability in future studies could therefore improve the GAMs and WUW models (Bovee 1986). As Beecher et al. (2010) demonstrated, the apparent preference of certain species and life stages may also be impacted by the behaviour of certain individuals. Beecher et al. (2010) found that two types of behaviour of Coho salmon smolts resulted in different HSI curves, and therefore they recommended that habitat simulation methodologies were ultimately not suitable for modelling habitat-discharge relationships for Coho salmon smolts. In part due to the other limitations discussed above, these model curves are generally not representative of populations and therefore limit the use of these models for making population-level predictions (Railsback 2016). In fact, habitat simulation methodologies routinely perform poorly in evaluations of their power for predicting population-level

responses (Railsback 2016). In this study, the HSI curves and GAMs have not been verified against biological rates or population-level responses (Inglis et al. 1994). The data are also from one single year of field study, so they are likely biased by environmental conditions at the time of study (Bovee 1986; Inglis et al. 1994).

Future work should include measurement of substrate size each month along with substrate embeddedness. While substrate size (i.e., intermediate axis length) distributions may have been relatively static over the study period, substrate embeddedness could have been impacted by the deposition of fine particles associated with declining streamflow (Fisheries and Oceans Canada 2019). Substrate embeddedness can impact the flow forces experienced by macroinvertebrates and can increase their exposure to predators, such as Nooksack Dace (Champion 2016). Second, sample locations could be rearranged to cover a greater longitudinal distance of the stream. Although Otter Park was the focus of the study, sampling in upstream and downstream reaches would provide valuable context for how Otter Park compares to the rest of the watershed and would aid in identifying how different taxa move throughout the stream during streamflow decline and flow cessation. Future work could also consider changes to streambed morphology. The baseline streambed topography dataset (Appendix A) would be useful for tracking changes in streambed topography over time.

5. CONCLUSIONS

5.1 Flow Cessation and Drying are Fundamental Characteristics of the Flow Regime

Bertrand Creek, particularly at Otter Park, is an intermittent stream, often experiencing periods where it dries up. This pattern has been consistent for over two decades. However, it is unclear how much of this dryness is due to natural cycles versus human activities because we lack detailed data on water use and historical streamflow records at Otter Park.

Our research and that of Allen et al. (2020), including pumping tests and analytical and numerical models, indicates that groundwater pumping near the stream reduces the amount of water that would naturally discharge into the stream. This captured groundwater is crucial for maintaining healthy stream habitat, especially during dry periods. While it is evident that groundwater pumping has some negative effects on these habitats, the lack of water use data prevented us from quantifying the exact impact of the current groundwater pumping on the stream's ecosystems. This underscores the need for more data to better understand and protect the habitats within Bertrand Creek.

5.2 Consequences of Flow Intermittency for Instream Habitat

Our study highlights that habitat changes in Bertrand Creek are not uniform; different sections respond differently to environmental shifts. Riffles, or the shallow, fast-moving sections, are particularly sensitive. Not only do they dry out faster, but they are also more responsive to temperature changes in the atmosphere and can reach extreme temperatures that pose a threat to local species, such as the Nooksack Dace. Depth and velocity declined far more rapidly in riffle habitat than in pool habitat, suggesting a higher likelihood of adverse ecological impacts due to streamflow decline, especially since many riffle-dwelling taxa have strong velocity preferences. At least for Nooksack Dace, these velocities are needed to sustain growth. Sensitivity of stream temperature to air temperature change was also greater in riffle habitat, with water quality guidelines being exceeded more frequently. Exceedance of stream temperature in riffle habitat past the 25°C guideline for Nooksack Dace protection during the 2021 heatwave demonstrates the thermal sensitivity in riffle habitat, which may increase in severity with expected increases in mean temperatures and more frequent extreme temperature events.

In contrast, pool habitats, the deeper and slower-moving sections, tend to persist longer even after riffles have dried up. However, isolated pools quickly experience increasing stream temperature and decreasing DO, creating challenging living conditions for aquatic life until the flow is restored. Despite these challenges, pools are crucial for the survival of both fish and benthic macroinvertebrates, serving as refuge habitats during dry spells. Even the wetted spaces between sediment particles can house macroinvertebrates, keeping the streambed biologically active even when water is not flowing above. This is a vital insight, as groundwater pumping can hasten the drying of pools and streambed sediments, negatively impacting these refuge habitats. Recognizing that intermittent streams like Bertrand Creek are not biologically inactive even when they are not flowing challenges traditional assumptions and underscores the need for careful water management during both flowing and non-flowing periods to protect the stream's diverse and vital ecosystems.

5.3   Flow Methodologies

Since many environmental flow assessment methodologies were designed and tested in perennial streams, flow cessation and drying can limit, if not preclude, their use in systems with intermittent streamflow. The failure of the WUW models to capture and convey the maintenance of habitat as standing pools exemplifies how unique characteristics of hydrological variability in non-perennial systems can impact the use of certain methods. However, as discussed above, these models may be adaptable for use in non-perennial streams. Investigations of new and modified approaches for environmental flow assessments in non-perennial streams will be crucial for their proper management. We stress the urgency of initiating such investigations due to the time required for developing and testing new methodologies relative to the rapid rate at which these sensitive non-perennial systems could be degraded due to improper management, climate change, and other potential anthropogenic impacts.

6.   MANAGEMENT IMPLICATIONS

This study underscores streamflow, dissolved oxygen, and stream temperature as crucial variables needing urgent attention for effective water management in Bertrand Creek. A consistent pattern of flow cessation during summer months has been observed for at least the past two decades, often leading to the drying of riffle habitat at Otter Park. This riffle habitat is classified as critical habitat for the endangered Nooksack Dace, emphasizing the critical need for thoughtful and proactive management approaches.

Given the frequent and long periods of flow cessation and drying at Otter Park, the streamflow of 0.12 m³/s identified as optimal for Nooksack Dace by Avery Gomm et al. (2013) appears unattainable during Otter Park's summer months. Therefore, a focus on enhancing baseflows, for example by reducing diversions and groundwater pumping during critical periods, is a more realistic and immediate target. Achieving this would not only support the recovery of Nooksack Dace but also positively influence dissolved oxygen levels and temperature conditions within the stream.

Restoring baseflows would enhance aeration through riffle habitats, prevent overheating in stagnant pools, and reduce the accumulation of leaf litter and algae that contribute to low dissolved oxygen levels during periods of extremely low flow or no flow. It is imperative that any further water abstraction, either from the stream itself or from groundwater wells situated upstream of Otter Park, be meticulously assessed and managed. Any additional abstraction is likely to hinder progress towards restoring baseflows, subsequently impeding the recovery efforts for the Nooksack Dace.

Therefore, management strategies need to be reviewed and adjusted to protect and restore the delicate ecosystems within Bertrand Creek. A commitment to avoiding further depletion of streamflow, coupled with efforts to restore baseflows, will provide a more supportive environment for the endangered species reliant on these habitats, while also maintaining healthier dissolved oxygen and temperature conditions crucial for the overall wellbeing of the stream's diverse aquatic life.

7. RECCOMMENDATIONS FOR FUTURE WORK

7.1 Intermittent Streams

Future research should focus on developing a comprehensive inventory of intermittent streams (or stream reaches) within the South Coast Region. Ideally, this initiative should also aim to identify and understand the key explanatory factors and predictors of flow intermittency (e.g., topography, geology, and drainage area). Characterizing the variability in the timing and duration of flow cessation is crucial for a deeper understanding of the hydrological dynamics of these streams. This characterization will provide valuable insights into the streams' seasonal behavior, response to climatic events, and potential environmental stressors, thereby offering a basis for more informed water resource management.

A significant challenge in this endeavor is that many intermittent streams in the region are ungauged, leaving a gap in the data necessary for thorough analysis and understanding. To address this, following an initial inventory and assessment of gauged streams and their key factors, a systematic plan should be devised for visual checks of nearby ungauged streams. These checks could be strategically integrated into field visits conducted during summer months when the streams are most likely to exhibit intermittent behavior. This approach will enable researchers to identify and predict which ungauged streams are likely to be intermittent based on the assessed key factors, effectively expanding the inventory and improving the accuracy of intermittency predictions.

Lastly, it would be advantageous not only to identify streams experiencing flow intermittency, but also to distinguish between streams that go completely dry and those that only undergo temporary flow cessation. Such distinctions can be made through careful visual assessments during site visits. Understanding the degree and nature of flow intermittency in these streams is vital, as it influences the habitat availability and water quality, thereby affecting the overall aquatic and riparian ecosystems. Therefore, adding this level of detail to the inventory will significantly enhance its utility as a tool for water management in the South Coast Region.

7.2 Water Use Data and Improved Models / Ability to Naturalize Flows

Improving water management and conservation practices in the South Coast Region necessitates more detailed water use information on both surface water and groundwater licenses. Acquiring precise data on water usage, including volume and timing, would greatly enhance the accuracy of naturalizing streamflow records – a process critical for understanding the intrinsic behaviour of our water systems. Naturalized streamflow records represent the hydrologic conditions of streams without human interference, providing a baseline that is crucial for differentiating natural intermittency from interruptions driven by water use.

The benefit of acquiring granular water use data is multifold. First, it facilitates a clear differentiation between natural stream intermittence and drying events that are directly attributable to human water consumption. A precise understanding of this dynamic is pivotal, as it sheds light on the degree to which human activities are influencing water availability and stream ecology. Understanding whether streams are naturally intermittent, or if their flow patterns are significantly altered by water extraction, is

essential for implementing effective water management policies and practices aimed at sustainable use and conservation.

Furthermore, with detailed water use data in hand, researchers and policymakers are better positioned to evaluate the impact of other anthropogenic influences on water systems, including land use changes, channelization, and development activities. Without an accurate baseline, it becomes challenging to assess the additional stress these factors impose on our water resources. For example, modifications in land use can alter the natural runoff patterns, while channelization can change the streamflow velocity and capacity, each imposing its unique influence on water availability and quality.

In a region where water resources are under continual stress from various anthropogenic and natural factors, a robust understanding of the actual versus naturalized streamflows is not just beneficial but imperative. It supports the development and implementation of more informed, adaptive, and resilient water management strategies that effectively address contemporary challenges while safeguarding the region's water resources for future generations. Having precise data enables more nuanced understanding and decision-making, providing a foundation for policies that are responsive to both the needs of the human population and the ecological systems dependent on these vital water resources.

7.3 Flow Intermittence Affects the Applicability of Common Environmental Flow Assessment Methods

Consider the development of regional environmental flow management approaches/frameworks. Despite being in their infancy, the Functional Flows Approach used in the California Environmental Flows Framework and the approaches used in Ecological Limits of Hydrological Alteration (ELOHA) have yielded promising results. Regional characterization of fundamental ecohydrological characteristics facilitates the development of living conceptual models for each major stream type in the region. The models are essentially neatly packaged information regarding the dominant attributes of components such as physical catchment characteristics, climate, and identifying components of the flow regime that are strongly associated with the maintenance of some aspect of aquatic ecosystems. Forming characterizations is beneficial even during the early stages of data collection because quantitative ecohydrological relationships can simply be treated as testable hypotheses, allowing easy integration of new information and facilitating the identification of key factors influencing spatial and temporal variability. In theory, the return on regional scale investigations such as these should be profitable because regional scale studies facilitate more rapid and accurate site-specific assessments.

REFERENCES

Allen, D. M., Johnson, B., Garnet, A., Howe, K., Lepitre, M., and Simpson, M. 2020. Assessment of Aquifer-Stream Connectivity Related to Groundwater Abstraction in the Lower Fraser Valley: Phase 2 Field Investigation at Otter Park, Langley. B.C. Water Science Series 2020-03. Victoria: Province of British Columbia.

Armanini, D. G., Horrigan, N., Monk, W. A., Peters, D. L., and Baird, D. J. 2011. Development of a benthic macroinvertebrate flow sensitivity index for Canadian rivers. River Res. Applic. 27, 723–737. doi:10.1002/rra10.1002/rra. 1389

Arthington, A. H., Bhaduri, A., Bunn, S. E., Jackson, S. E., Tharme, R. E., Tickner, D., Young, B., Acreman, M., Baker, N., Capon, S., Horne, A. C., Kendy, E., McClain, M. E., Poff, N. L. R., Richter, B. D., & Ward, S. 2018. The Brisbane Declaration and Global Action Agenda on Environmental Flows (2018). Frontiers in Environmental Science, 6(JUL), 1–15. https://doi.org/10.3389/fenvs.2018.00045

Avery-Gomm, S. 2013. Determining the Impacts of Hydrological Drought on Endangered Nooksack Dace (Rhinichthys Cateractae) at the Population and Individual Level: Implications for Minimum Environmental Flow Requirements. [Vancouver, B.C.]: University of British Columbia. [master's thesis].

Avery-Gomm, S., Rosenfeld, J. S., Richardson, J. S., and Pearson, M. 2014. Hydrological drought and the role of refugia in an endangered riffle-dwelling fish, Nooksack Dace (Rhinichthys Cataractae Ssp.). Can. J. Fish. Aquat. Sci. 71, 1625–1634. doi:10.1139/cjfas-2013-0585

Barbour, M.T., J. Gerritsen, B.D. Snyder, and J.B. Stribling. 1999. Rapid Bioassessment Protocols for Use in Streams and Wadeable Rivers: Periphyton, Benthic Macroinvertebrates and Fish, Second Edition. EPA 841-B-99-002. U.S. Environmental Protection Agency; Office of Water; Washington, D.C.

Beecher, H. A., Caldwell, B. A., DeMond, S. B., Seiler, D., and Boessow, S. N. 2010. An empirical assessment of PHABSIM using long-term monitoring of coho salmon smolt production in Bingham Creek, Washington. North Am. J. Fish. Manag. 30, 1529–1543. doi:10.1577/M10-020.1.

Berg, M. A., and Allen, D. M. 2007. Low flow variability in groundwater-fed streams. Can. Water Resour. J. 32, 227–246. doi:10.4296/cwrj3203227.

Bonada, N., Rieradevall, M., Prat, N., and Resh, V. H. 2006. Benthic macroinvertebrate assemblages and macrohabitat connectivity in mediterranean-climate streams of Northern California. J. North Am. Benthol. Soc. 25(1), 32-43. doi:10.1899/0887-3593(2006)25[32]2.0.co;2

Bolker, B. 2007. Ecological Models and Data in R. Princeton University Press doi:10.1086/644667.

Borg Galea, A., Sadler, J. P., Hannah, D. M., Datry, T., and Dugdale, S. J. 2019. Mediterranean intermittent rivers and ephemeral streams: challenges in monitoring complexity. Ecohydrology 12. doi:10.1002/eco.2149

Bouchard, R. 2004. Guide to aquatic macroinvertebrates of the Upper Midwest. St. Paul, Minnesota: Water Resources Center, University of Minnesota.

Boulton, A. and Hancock, P. 2006. Rivers as groundwater-dependent ecosystems: a review of degrees of dependency, riverine processes and management implications. Aust. J. Bot. 54, 133-144.

Boulton, A. J. 2003. Parallels and contrasts in the effects of drought on stream macroinvertebrate assemblages. Freshwater Biology, 48(7), 1173-1185.

Bovee, K. D. 1986. Development and Evaluation of Habitat Suitability Criteria for Use in the Instream Flow Incremental Methodology. https://pubs.usgs.gov/publication/70121265 [Accessed July 29, 2024, 2019]

Bovee, K. D., and Cochnauer, T. 1977. Development and Evaluation of Weighted Criteria, Probability-Of-Use Curves for Instream Flow Assessments: Fisheries. Instream Flow Information Paper 3. U.S.D.I. Fish and Wildlife Service, Office of Biological Services. FWS/OBS-77/63.

Bovee, K. D., and Milhous, R. 1978. Hydraulic Simulation in Instream Flow Studies: Theory and Techniques. Instream Flow Information Paper 5. U.S.D.I. Fish and Wildlife Service, Office of Biological Services. FWS/OBS-78/33.

British Columbia Ministry of Environment and Climate Change Strategy (ECCS). 2019. British Columbia Approved Water Quality Guidelines: Aquatic Life, Wildlife & Agriculture, Summary Report. Available at: https://www2.gov.bc.ca/gov/content/environment/air-land-water/water/ water-quality/water-quality-guidelines/approved-water-quality-guidelines (Accessed September 2020).

British Columbia Ministry of Environment and Climate Change Strategy (ECCS). 2020. B.C. Source Drinking Water Quality Guidelines: Guideline Summary. Water Quality Guideline Series, WQG-01. Prov. B.C., Victoria B.C.

British Columbia Ministry of Environment and Climate Change Strategy (ECCS). 2021. British Columbia Approved Water Quality Guidelines: Aquatic Life, Wildlife & Agriculture - Guideline Summary. Water Quality Guideline Series, WQG-20. Prov. B.C., Victoria B.C

Brunke, M., and Gonser, T. 1997. The ecological significance of exchange processes between rivers and groundwater. Freshw. Biol. 37, 1–33. doi:10.1046/j.1365-2427.1997.00143.x.

Burgazzi, G., Laini, A., Ovaskainen, O., Saccò, M., Stubbington, R., and Viaroli, P. 2020. Communities in high definition: Spatial and environmental factors shape the micro-distribution of aquatic invertebrates. Fresh. Biol. 65, 2053–2065. doi:10.1111/fwb.13599.

Buttle, J. M., Boon, S., Peters, D. L., Spence, C., van Meerveld, H. J., and Whitfield, P. H. 2012. An overview of temporary stream hydrology in Canada. Can. Water Resour. J./Revue canadienne des ressources hydriques 37, 279–310. doi:10.4296/cwrj2011-903

Caissie, D. 2006. The thermal regime of rivers: a review. Freshw. Biol 51, 1389–1406. doi:10.1111/j.1365-2427.2006.01597.x

Canadian Council of Ministers of the Environment [CCME]. 1999. Canadian Water Quality Guidelines For the Protection of Aquatic life: Dissolved Oxygen (freshwater). In: Canadian Environmental Quality Guidelines, 1999, Canadian Council of Ministers of the Environment, Winnipeg.

Canadian Council of Ministers of the Environment [CCME]. 2012. Canadian water quality guidelines for the protection of aquatic life: Nitrate ion. In Canadian environmental quality guidelines, 1999. Canadian Council of Ministers of the Environment. https://ccme.ca/en/summary-table

Canadian Council of Resource and Environment Ministers [CCREM]. 2014. Canadian water quality guidelines. Canadian Council of Resource and Environment Ministers, Ottawa. Available from http://ceqg-rcqe.ccme.ca/en/index.html#void.

Cardenas, M. B., Wilson, J. L., and Zlotnik, V. A. 2004. Impact of heterogeneity, bed forms, and stream curvature on subchannel hyporheic exchange. Water Resour. Res. 40, 1–14. doi:10.1029/2004WR003008.

Champion, J. M. 2016. Determining the effects of sediment deposition on the growth, survival, and foraging efficiency of the endangered Nooksack dace (Rhinichthys cataractae sp. cataractae), and on the abundance, distribution, and community structure of their invertebrate prey.

(Thesis). University of British Columbia. Retrieved from https://open.library.ubc.ca/collections/ubctheses/24/items/1.0300476

Champion, J. M., Rosenfeld, J. S., and Shadwick, R. 2018. Effects of water velocity and substrate composition on foraging efficiency of an endangered benthic cyprinid, Nooksack Dace (Rhinichthys Cataractae Subsp. Cataractae). Hydrobiologia 805, 231–243. doi:10.1007/s10750-017-3304-2

Chester, E.T., & Robson, B.J. 2011. Drought refuges, spatial scale and recolonisation by invertebrates in non-perennial streams [Article]. Freshwater Biology, 56(10), 2094–2104. https://doi.org/10.1111/j.1365-2427.2011.02644.x

Datry, T., Bonada, N., and Boulton, A. 2017. Intermittent Rivers and Ephemeral Streams. San Diego: Elsevier Science & Technology.

Datry, T., Larned, S.T., and Tockner, K. 2014. Intermittent Rivers: A challenge for Freshwater Ecology. BioSci 64, 229–235. doi:10.1093/biosci/bit027

de Graaf, I.E.M., Gleeson, T., van Beek, L.P.H., Sutanudjaja, E.H., and Bierkens, M.F.P. 2019. Environmental flow limits to global groundwater pumping. Nature 574, 90–94. doi:10.1038/s41586-019-1594-4

Davis, J. 1975. Minimal dissolved oxygen requirements of aquatic life with emphasis on Canadian species: A review. J. Fish. Res. Board Can. 32, 2295-231

Dieterich, M., and Anderson, N. H. 2000. The invertebrate fauna of summer-dry streams in western Oregon. Archiv fur Hydrobiologie 147, 273–295.

Environment Canada. 2011. Canadian Aquatic Biomonitoring Network Field Manual - Wadeable Streams. Available at: https://publications.gc.ca/site/eng/ 422979/publication.html (Accessed 20th August, 2019).

Feminella, J. W. 1996. Comparison of benthic macroinvertebrate assemblages in small streams along a gradient of flow permanence. J. N. Am. Benthol. Soc. 15(4), 651-669.

Fisheries and Oceans Canada. 2008. Final Revised Recovery Strategy for the Nooksack Dace (Rhinichthys cataractae) in Canada. https://www.canada.ca/en/environment-climate-change/services/species-risk-public-registry/recovery-strategies/revised-nooksack-dace-rhinichthys-cataractae-proposed-2008.html [Accessed July 29, 2024].

Fisheries and Oceans Canada. 2019. Recovery Strategy for the Nooksack Dace (Rhinichthys Cataractae Ssp.) in Canada, 2019 (Proposed). Species Risk Act Recover. Strateg. Ser. Available at: https://www.canada.ca/en/environment-climate-change/services/species-risk-public-registry/recovery-strategies/nooksack-dace-2019-proposed.html [Accessed July 29, 2024].

Fisheries and Oceans Canada. 2020. Action Plan for the Nooksack Dace (Rhinichthys cataractae ssp.) and the Salish Sucker (Catostomus sp. cf. catostomus) in Canada [Proposed]. 1st amendment. Species at Risk Act Action Plan Series. Fisheries and Oceans Canada, Ottawa. v + 21 pp.

Fox, J., & Weisberg, S. 2019. An {R} companion to applied regression (3rd ed.). Sage Publications. https://CRAN.R-project.org/package=car

Gippel, C. J., and Stewardson, M. J. 1998. Use Of wetted perimeter in defining minimum environmental flows. River Res. Appl. 14, 53–67. doi:10.1002/(sici)1099-1646(199801/02)14:1<53::aid-rrr476>3.0.co;2-z.

Golder Associates Ltd. 2005. Final Report: Comprehensive Groundwater Modelling Assignment. Prepared for the Township of Langley, 94p.

Gómez-Gener, L., Siebers, A. R., Arce, M. I., Arnon, S., Bernal, S., Bolpagni, R., et al. 2021. Towards an improved understanding of biogeochemical processes across surface-groundwater interactions in intermittent rivers and ephemeral streams. Earth-Science Rev. 220, 103724. doi:10.1016/J.EARSCIREV.2021.103724

Hall, G., Allen, D.M., Simpson, M., Tolera, H., Jackson, B., Middleton, M.A., and Lepitre, L. 2017. Assessment of Aquifer-Stream Connectivity Related to Groundwater Abstraction in the Lower Fraser Valley: Phase 1 Field Investigation. Water Science Series, WSS2017-02. Prov. B.C., Victoria B.C, 76 pp.

Harvey, J. W., and Bencala, K. E. 1993. The effect of streambed topography on surface-subsurface water exchange in mountain catchments. Water Resour. Res. 29, 89–98. doi:10.1029/92WR01960

Harris C.R., Millman, K.J., van der Walt, S.J., et al. 2020. Array programming with NumPy. Nature. 585, 357–362. DOI: 10.1038/s41586-020-2649-2.

Haywood, G. P., and R. W. Drinnan (Dobrocky Seatech Ltd.). 1983. A Literature Review and Report on Barium Toxicity in Freshwater, In Relation to the Monkman Coal Project, February, 1983, 49 p. (Prepared for: Petro-Canada Exploration Ltd.).

Hilsenhoff, W. L. 1987. An improved biotic index of organic stream pollution. Gt. Lakes Entomol. 20, 31–40. doi:10.1016/S0025-326X(01)00271-5.

Hunt, B. 1999. Unsteady stream depletion from ground water pumping. Ground Water, 39(1), 98-102.

Hunter, J.D. 2007. Matplotlib: A 2D Graphics Environment. Comput. Sci. Eng. 9(3), 90-95, doi: 10.1109/MCSE.2007.55.

Inglis, S., and Pollard, S. M. 1994. Distribution and Habitat of Nooksack Dace (Rhinichthys Sp.) in Canada. B.C. Regional Fisheries Report No. LM237.

Inglis, S., Pollard, S. M., and Rosenau, M. L. 1994. Distribution and habitat of Nooksack dace (Rhinichthys sp.) in Canada. Regional Fisheries Report, B.C. Ministry of Environment, Lands and Parks, Surrey.

James, A.W., Dewson, Z.S., and Death, R.G. 2008. The effect of experimental flow reductions on macroinvertebrate drift in natural and streamside channels. River. Res. Appl. 24(1), 22–35, doi: 10.1002/rra.1052.

Johnston, N. T., and Slaney, P. A. 1996. Fish Habitat Assessment Procedures: Watershed Restoration Technical Circular No. 8. Ministry of Environment, Lands and Parks and Ministry of Forests.

Jowett, I. G., Richardson, J., Biggs, B. J. F., Hickey, C. W., and Quinn, J. M. 1991. Microhabitat preferences of benthic invertebrates and the development of generalised deleatidium spp. habitat suitability curves, Applied to Four New Zealand Rivers. New Zealand J. Mar. Freshw. Res. 25, 187–199. doi:10. 1080/00288330.1991.9516470

Jowett, I. G., & Biggs, B. J. F. 2006. Flow Regime Requirements and the Biological Effectiveness of Habitat-Based Minimum Flow Assessments for Six Rivers. International Journal of River Basin Management. 4. 179-189. 10.1080/15715124.2006.9635287.

Jowett, I. G., & Richardson, J. 2007. Habitat use by New Zealand fish and habitat suitability models. NIWA Science and Technology Series No. 55. National Institute of Water and Atmospheric Research.

Kaller, M. D., Kelso, W. E. 2007. Association of macroinvertebrate assemblages with dissolved oxygen concentration and wood surface area in selected subtropical streams of the southeastern USA. Aquatic Ecol. 1, 95–110. https://doi.org/10.1007/s10452-006-9046-2

Kerr Wood Leidal Associates LTD. 2009. Bertrand Creek Integrated Stormwater Management Plan (ISMP). Prepared for the Township of Langley.

Kløve, B., Ala-Aho, P., Bertrand, G., Gurdak, J. J., Kupfersberger, H., Kværner, J., Muotka, T., Mykrä, H., Preda, E., Rossi, P., Bertacchi Uvo C., Velasco, E., Pulido-Velazquez, M. 2014. Climate change impacts on groundwater and dependent ecosystems. Journal of Hydrology, 518, Part B, 250-266.

Knief, U., and Forstmeier, W. 2018. Violating the normality assumption may be the lesser of two evils. BioRxiv. doi:10.1101/498931

Lake, P.S. 2003. Ecological effects of perturbation by drought in flowing waters. Freshwater Biology, 48: 1161-1172. https://doi.org/10.1046/j.1365-2427.2003.01086.x

Lewis, A., Hatfield, T., Chilibeck, B., and Roberts, C. 2004. Assessment Methods for Aquatic Habitat and Instream Flow Characteristics in Support of Applications to Dam, Divert, or Extract Water from Streams in British Columbia.http://www.env.gov.bc.ca/wld/documents/bmp/assessment_methods_instreamflow_in_bc.pdf [Accessed February 19th 2020].

Linnansaari, T. 2012. The application of habitat simulation methods in setting environmental flows: A review of past practices and suggestions for new direction. Canadian Rivers Institute.

Mackay, R. 1992. Colonization by lotic macroinvertebrates: A review of processes and patterns. Can. J. Fish. Aquat. Sci. 49, 617-628.

Mangiafico, S. 2020. rcompanion: Functions to support extension education program evaluation. R package version 2.3.25. https://CRAN.R-project.org/package=rcompanion

Mangiafico, S. S. 2016. Summary and Analysis of Extension Program Evaluation in R. version 1.18.8. Available at: rcompanion.org/handbook/. (Accessed January 20th, 2021).

Marra, G., and Wood, S. N. 2011. Practical variable selection for generalized additive models. Comput. Stat. Data Anal. 55, 2372–2387. doi:10.1016/j.csda. 2011.02.004.

Monk, W. A., Compson, Z. G., Armanini, D. G., Orlofske, J. M., Curry, C. J., Peters, D. L., et al. 2018. Flow velocity–ecology thresholds in Canadian rivers: A comparison of trait and taxonomy-based approaches. Fresh. Biol. 891–905. doi:10.1111/fwb.13030.

Neuwirth, E. 2014. RColorBrewer: ColorBrewer palettes. R package version 1.1-2. https://CRAN.R-project.org/package=RColorBrewer

Nott, A.H. 2024. Groundwater Response to Extreme Weather Events in Various Hydrogeological Regimes across Southern British Columbia. MSc thesis, Simon Fraser University.

Nott, A.H. and Allen, D.M. 2020. Quantifying Aquifer-Stream Exchanges Along Bertrand Creek, British Columbia and Washington State, Using a Numerical Groundwater Flow Model. Water Science Series, WSS2020-06. Province of British Columbia, Victoria. Available from https://a100.gov.bc.ca/pub/acat/public/viewReport.do?reportId=59013

Nott, A.H. and Allen, D.M. 2021. Modelling stream sensitivity to Pumping in the Bertrand Creek Watershed, British Columbia and Washington State. Proceedings of GeoNiagara 2021, Niagara Falls, Ontario, September 2021.

Okanagan Nation Alliance. 2020. Environmental Flow Needs Assessment In The Okanagan Basin. Prepared for B.C. Ministry of Forests, Lands, Natural Resource Operations and Rural Development & the Okanagan Basin Water Board.

Pappas, S. 2008. An Assessment of Historical Changes in Aquatic Biota Water and Sediment Quality Within A Catchment at a Developing Urban Front. [Vancouver, B.C.]: University of British Columbia. [master's thesis].

Parasiewicz, P. 2001. MesoHABSIM: A concept for application of instream flow models in river restoration Planning. Fish. 26, 6–13.

Peel, M. C., Finlayson, B. L., and McMahon, T. A. 2007. Updated world map of the Köppen-Geiger Climate Classification. Hydrol. Earth Syst. Sci. 11, 1633–1644. doi:10.5194/hess-11-1633-2007

Platts, W. S., Armour, C., Booth, G. D., Bryant, M., Bufford, J. L., Cuplin, P., Jensen, S., Lienkaemper, G. W., Minshall, G. W., Monsen, S. B., Nelson, R. L., Sedell, J. R., Tuhy, J. S., & Van Sickle, V. A. 1983. Methods for evaluating stream, riparian, and biotic conditions. USDA Forest Service, Intermountain Forest and Range Experiment Station, Ogden, Utah, General Technical Report INT-138.

Poff, N. L., Allan, J. D., Bain, M. B., Karr, J. R., Prestegaard, K. L., Richter, B. D., et al. 1997. The natural flow regime. BioScience 47, 769–784. doi:10.2307/ 1313099

Poff, N. L., Olden, J. D., Vieira, N. K. M., Finn, D. S., Simmons, M. P., et al. 2006. Functional trait niches of North American lotic insects: Traits-based ecological applications in light of phylogenetic relationships. Journal of the North American Benthological Society, 25(4), 730-755. https://doi.org/10.1899/0887-3593(2006)025[0730:FTNONA]2.0.CO;2

Poole, G. C., and Berman, C. H. 2001. An ecological perspective on in-stream temperature: natural heat dynamics and mechanisms of human-caused thermal degradation. Environ. Manage. 27, 787–802. doi:10.1007/s002670010188

Pruneda, E., Barber, M., Wu, J. and Allen, D.M. 2010. Use of stream response functions to determine impacts of replacing surface-water use with groundwater withdrawals. Hydrogeology Journal, 18(5), 1077-1092. DOI 10.1007/s10040-010-0591-3.

R Core Team. 2020. R: A Language and Environment for Statistical Computing. Vienna, Austria: R Foundation for Statistical Computing. https://www.R- project.org/.

Railsback, S. F. 2016. Why it is time to put PHABSIM out to pasture. Fisheries 41, 720–725. doi:10.1080/03632415.2016.1245991.

Reece, P.F. and Richardson, J.S. 2000. Benthic macroinvertebrate assemblages of coastal and continental streams and large rivers of southwestern British Columbia, Canada. Hydrobiologia 439(1), 77–89. doi: 10.1023/A:1004105820586.

Robinson, C. T., Uehlinger, U., & Monaghan, M. T. 2003. Effects of a multi-year experimental flood regime on macroinvertebrates downstream of a reservoir. Aquatic Sciences, 65(3), 210–222. https://doi.org/10.1007/s00027-003-0663-8

Rose, P., Metzeling, L., & Catzikiris, S. 2008. Can macroinvertebrate rapid bioassessment methods be used to assess river health during drought in south eastern Australian streams? Freshwater Biology, 53(12), 2626–2638. https://doi.org/10.1111/j.1365-2427.2008.02074.x

Rosenberg, D. M., Reynoldson, T. B., & Resh, V. H. 1999. Establishing reference conditions for benthic invertebrate monitoring in the Fraser River catchment, British Columbia, Canada (Catalogue No. En14-183/1999E-PDF). Environment Canada.

Rosenfeld, J. S. 2017. Developing flow-ecology relationships: implications of nonlinear biological responses for water management. Freshw. Biol. 62(8), 1305-1324.

Simpson, G. L. 2019. Model Selection with GAM in R. https://stats.stackexchange. Available at: https://CRAN.R-project.org/package=gratia

SonTek. 2019. FlowTracker2 handheld ADV: User manual (Version 2.0). SonTek, a Xylem brand.

Sophocleous, M. 2002. Interactions between groundwater and surface water: the state of the science. Hydrogeology J. 10, 52–67. doi:10.1007/s10040-001-0170-8

Stubbington, R., Wood, P. J., & Boulton, A. J. 2009. Low flow controls on benthic and hyporheic macroinvertebrate assemblages during supra-seasonal. Hydrological Processes, 23, 2252–2263. https://doi.org/10.1002/hyp

Tang, Y., Horikoshi, M., & Li, W. 2016. ggfortify: Data visualization tools for statistical analysis results. R Journal, 8(2), 478-489. https://doi.org/10.32614/RJ-2016-060

Tharme, R. E. 2003. A global perspective on environmental flow assessment: Emerging trends in the development and application of environmental flow methodologies for rivers. River Research and Applications, 19(5-6), 397-441. https://doi.org/10.1002/rra.736

Vander Vorste, R., Mermillod-Blondin, F., Hervant, F., Mons, R., Forcellini, M., and Datry, T. 2016. Increased depth to the water table during river drying decreases the resilience of Gammarus Pulex and alters ecosystem function. Ecohydrol. 9, 1177–1186. doi:10.1002/eco.1716

Vannote, R. L., Minshall, G. W., Cummins, K. W., Sedell, J. R., & Cushing, C. E. 1980. The River Continuum Concept. Canadian Journal of Fisheries and Aquatic Sciences, 37(1), 130-137. https://doi.org/10.1139/f80-017

Virtanen, P., Gommers, R., Oliphant, T.E., et al. 2020. SciPy 1.0: fundamental algorithms for scientific computing in Python. Nat. Methods. 17(3), 261–272. doi: 10.1038/s41592-019-0686-2.

Wickham, H. 2016. ggplot2: Elegant graphics for data analysis (2nd ed.). Springer-Verlag. https://ggplot2.tidyverse.org

Wickham, H., François, R., Henry, L., & Müller, K. 2020. dplyr: A grammar of data manipulation. R package version 1.0.0. https://CRAN.R-project.org/package=dplyr

Wickham, H., & Seidel, D. 2020. Scales: Scale Functions for Visualization. R package version 1.1.1. Available at: https://CRAN.R-project.org/package=scales

Wickham, H. 2021. tidyr: Tidy messy data. R package version 1.1.4. https://CRAN.R-project.org/package=tidyr

Wood, S. N. 2017. Generalized Additive Models: An Introduction with R. Boca Raton, Florida: CRC Press.
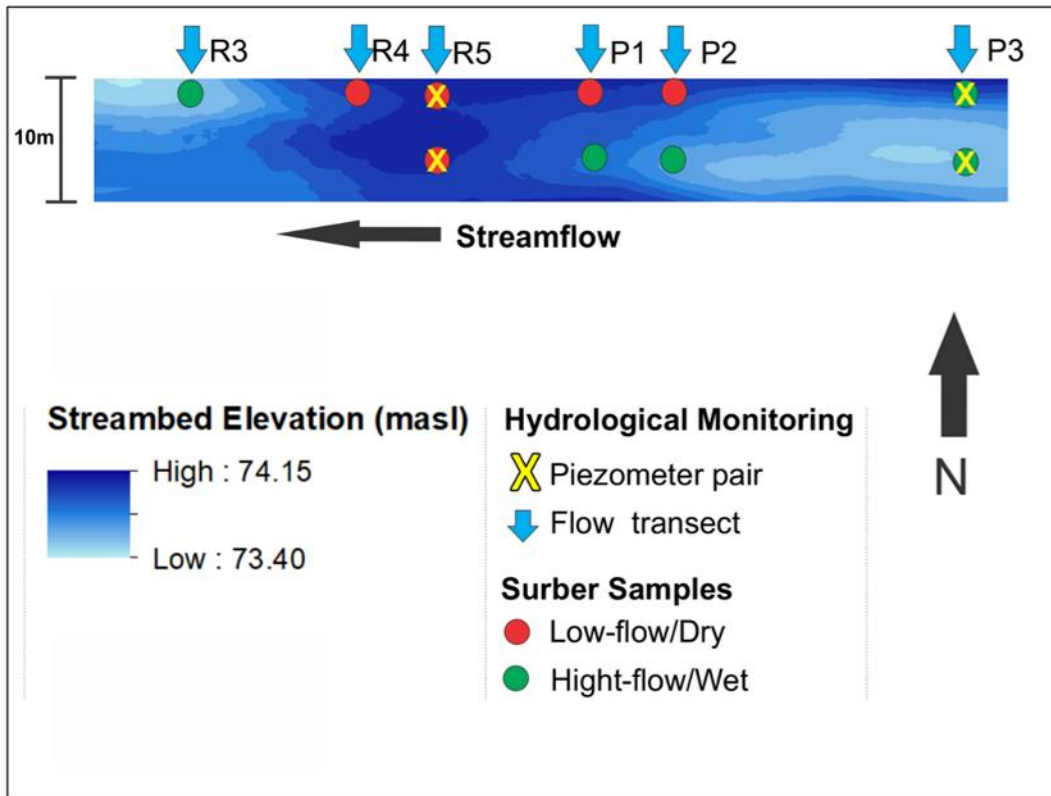
Figure A1: Streambed elevation in metres above sea level (masl) for the upstream segment of the Otter Park study reach in May 2020. Map created in ArcMap from streambed elevation data. Sites were classified by drying potential, based on streambed elevations. Numbers above arrows indicate transect number.

Figure A2: Stagnant pool in the upstream segment of the Otter Park study reach during the 2018 period of flow cessation.

Figure A3: Stagnant pool in the upstream segment of the Otter Park study reach during the 2021 period of flow cessation.

Figure A4: Deep, seemingly stagnant pool located a few metres downstream of HS5.

APPENDIX B. HYDRAULIC GRADIENT CALCULATIONS

Calculation of vertical hydraulic gradients involved multiple steps. Each step is detailed below:

Step one:

The difference in hydraulic head between piezometers of each nested pair was calculated from manual water level measurements made using a water level tape on 19/09/2019, 11/05/2020, and 17/09/2020 using:

$$dh_{m_{i,t}} = \left(ETOC_{D_i} - DTW_{D_{i,t}}\right) - \left(ETOC_S - DTW_{S_{i,t}}\right) \tag{B1}$$

where:

$dh_{M_{i,t}}$ = the difference in hydraulic head from manual measurements for piezometer pair *i* at time *t.*

$ETOC_{D_i}$ = the elevation of the top of the casing in metres above sea level (surveyed 05/2019) of the deep piezometer of piezometer pair *i.*

$DTW_{D_{i,t}}$ = the depth to water from the top of the deep piezometer casing measured with a water level tape for piezometer pair *i* at time *t.*

$ETOC_{S_i}$ = the elevation of the top of the casing in metres above sea level (surveyed 05/2019) of the shallow piezometer of piezometer pair *i*

$DTW_{S_{i,t}}$ = the depth to water from the top of the deep piezometer casing measured with a water level tape for piezometer pair *i* at time *t.*

Step two:

The vertical separation between loggers of pair *i* at time *t*, $dz_{i,t}$, was then calculated from $dh_{m_{i,t}}$ using:

$$dz_{i,t} = dh_{M_{i,t}} - \left(WL_{D_{i,t}} - WL_{S_{i,t}}\right) \tag{B2}$$

where:

$WL_{D_{i,t}}$ = the water level recorded by the data logger in the deep piezometer of piezometer pair i at the same time t as the corresponding $DTW_{D_{i,t}}$ value.

$WL_{S_{i,t}}$ = the water level recorded by the data logger in the shallow piezometer of piezometer pair i at the same time t as the corresponding $DTW_{S_{i,t}}$ value.

Step three:

$dz_{i,t}$ values were compiled for each nested pair and averaged to get a representative vertical separation value, dz_{F_i} (Table B1).

Table B1. $dz_{i,t}$ values averaged to get a final dz_F for each piezometer pair. *Asterisk indicates an anomalous value thus omitted from the average.*

Pair	dz$_i$ 19/09/2019	dz$_i$ 19/09/2019	dz$_i$ 19/09/2019	dz$_F$ Average
D39/D40	-0.322	-0.289	-0.274	-0.295
D23/D24	-0.636	-0.584	-0.603	-0.608
D7/D8	-0.008*	-0.550	-0.615	-0.582
D41/D42	-0.625	-0.648	-0.644	-0.639
D43/D44	-0.615	-0.691	-0.677	-0.661
D9/D10	-0.614	-0.637	-0.588	-0.613

Step four:

dz$_i$ was assumed to be equal to the difference in bottom depths of the piezometers of each pair i because the loggers were resting at the bottom of the piezometers. Thus, the hydraulic gradient was calculated at each 15-minute time step from the continuous water level data recorded by each logger of pair i according to Equation B3:

$$\frac{dh}{dl}_{i,t} = \frac{\left(WL_{D_{i,t}} + dz_i\right) - WL_{S_{i,t}}}{dz_i} \qquad (B3)$$

where:

$\frac{dh}{dl}_{i,t}$ = the hydraulic gradient for pair *i* at time *t.*

$WL_{D_{i,t}}$ = the water level recorded by the data logger in the deep piezometer of piezometer pair *i* at time *t.*

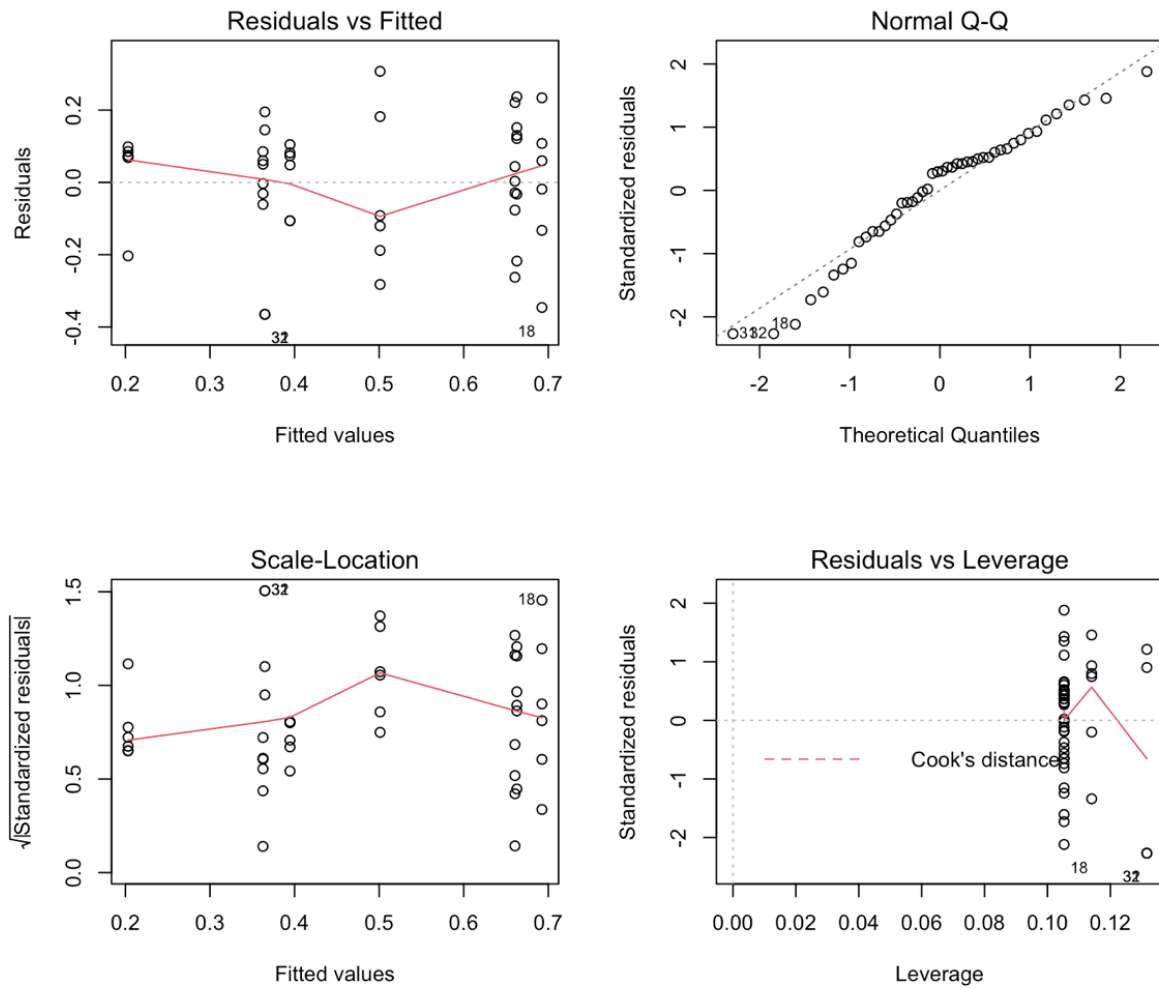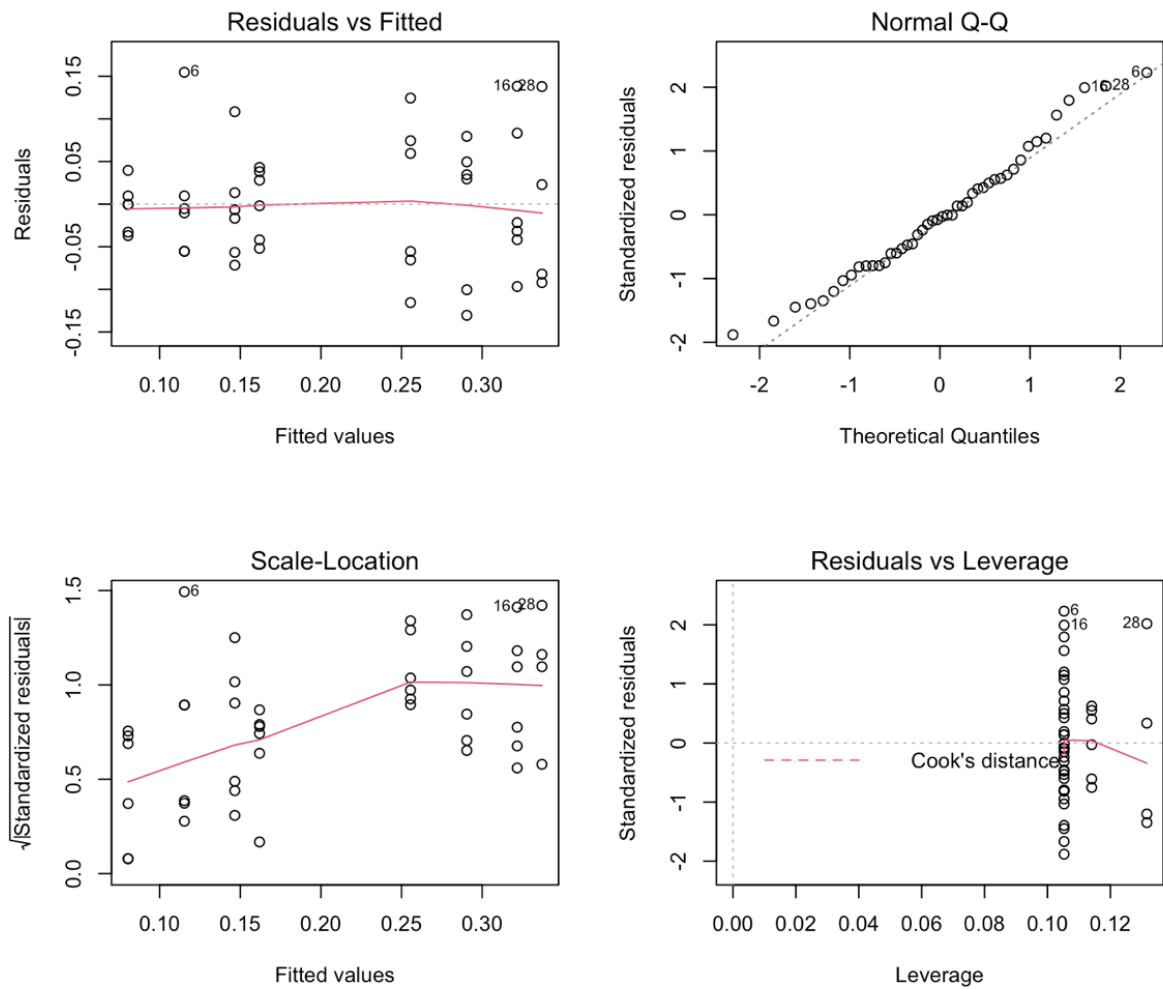dz_{F_i} = the final vertical separation between loggers of pair *i,*

Figure C1. Diagnostic plots for a two-way ANOVA model of velocity as a function of site type and month.

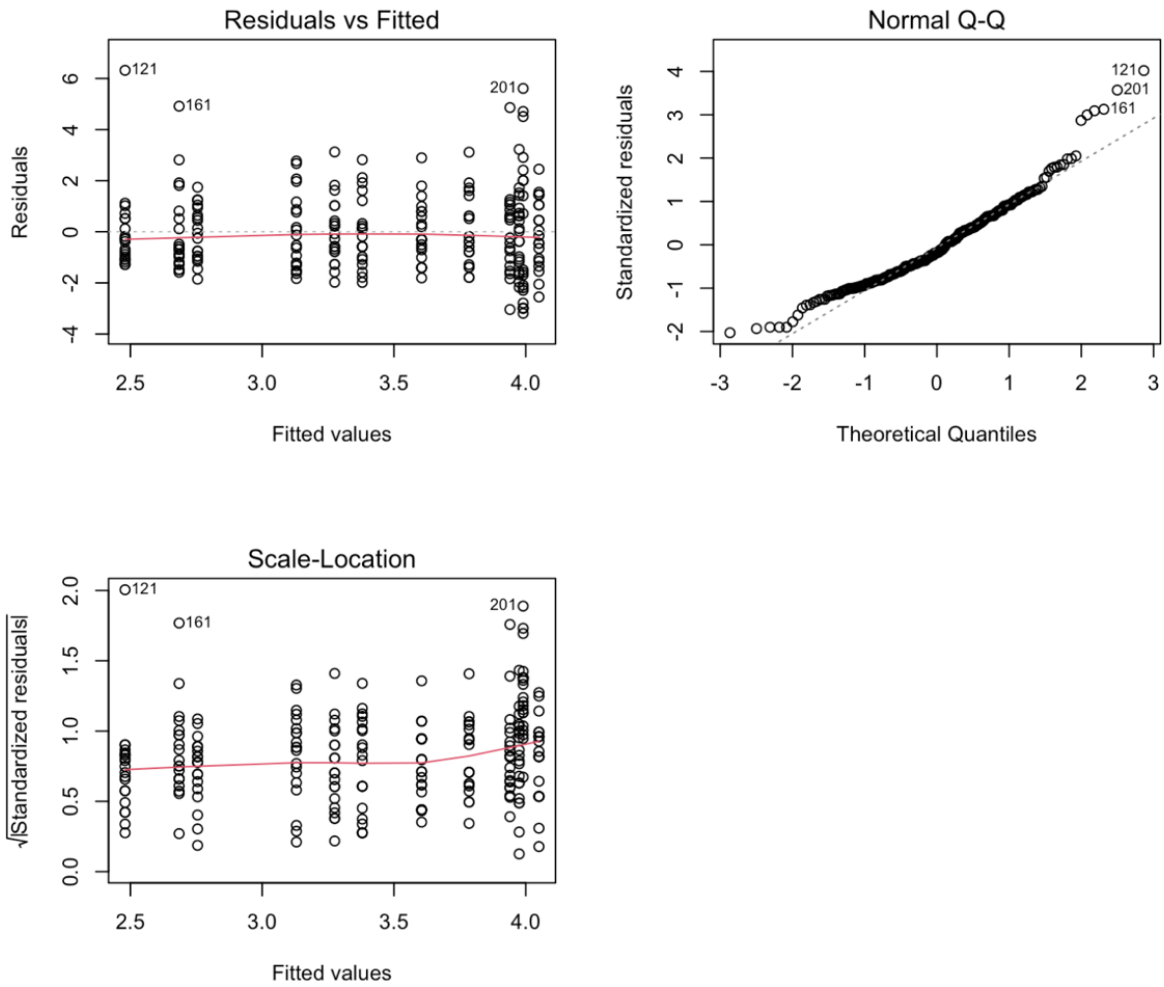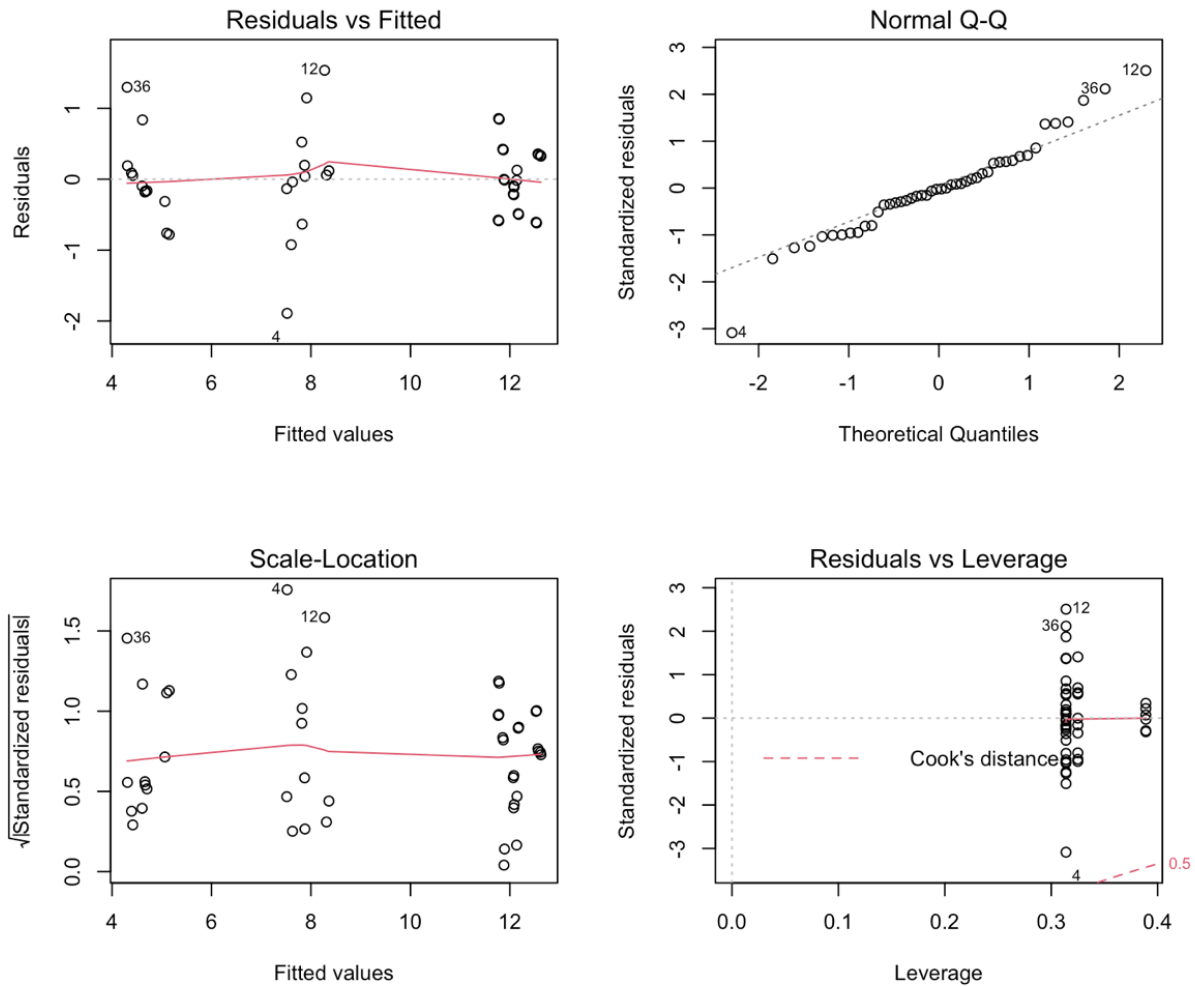*Figure C2. Diagnostic plots for a two-way ANOVA model of depth as a function of site type and month.*

Figure C3. Diagnostic plot for a one-way ANOVA model of substrate as a function of site.

Figure C4. Diagnostic plots for a two-way ANOVA of dissolved oxygen as a function of site and month.
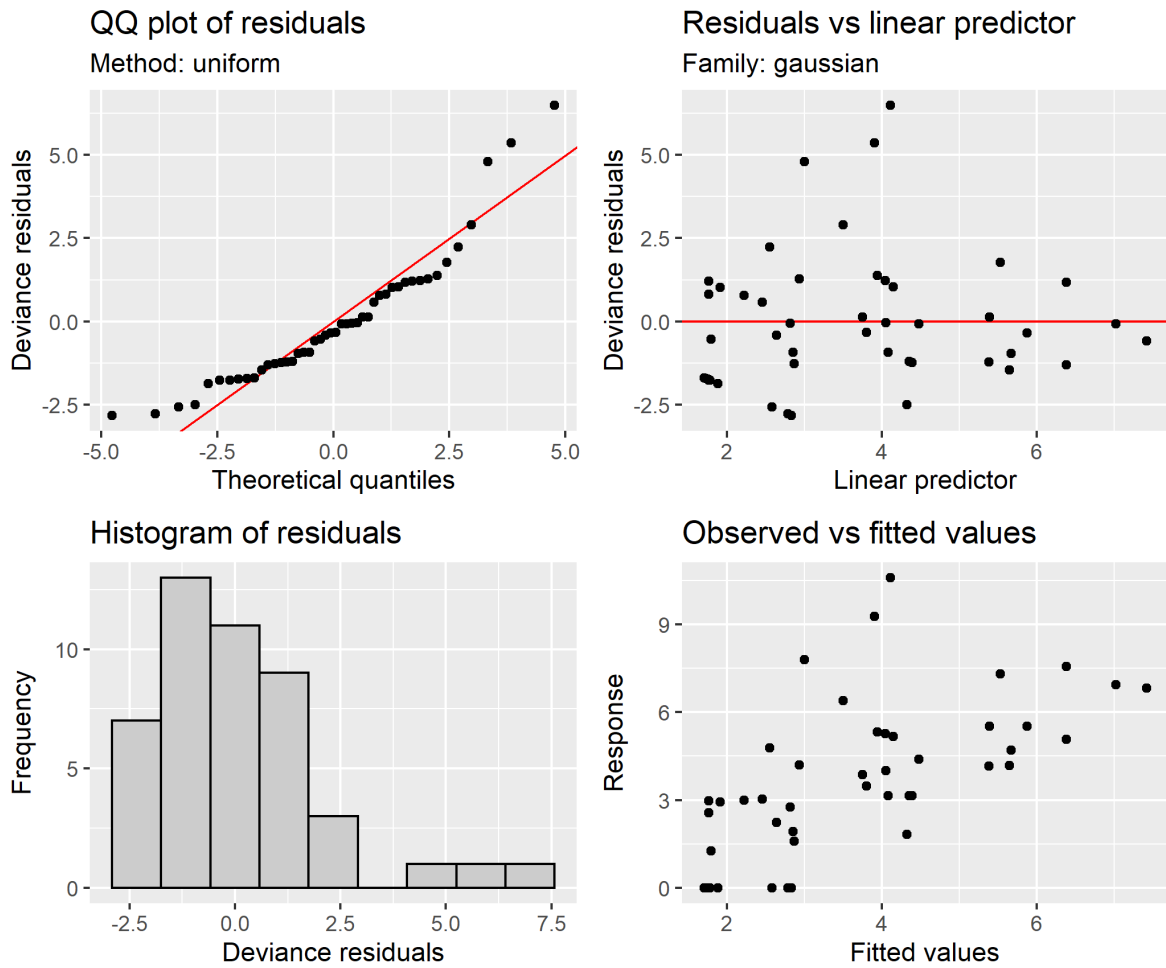
Figure C5. Diagnostic plots for a generalized additive model of total macroinvertebrate abundance as a function of depth and velocity. Total abundance was cube-root transformed to better satisfy test assumptions.
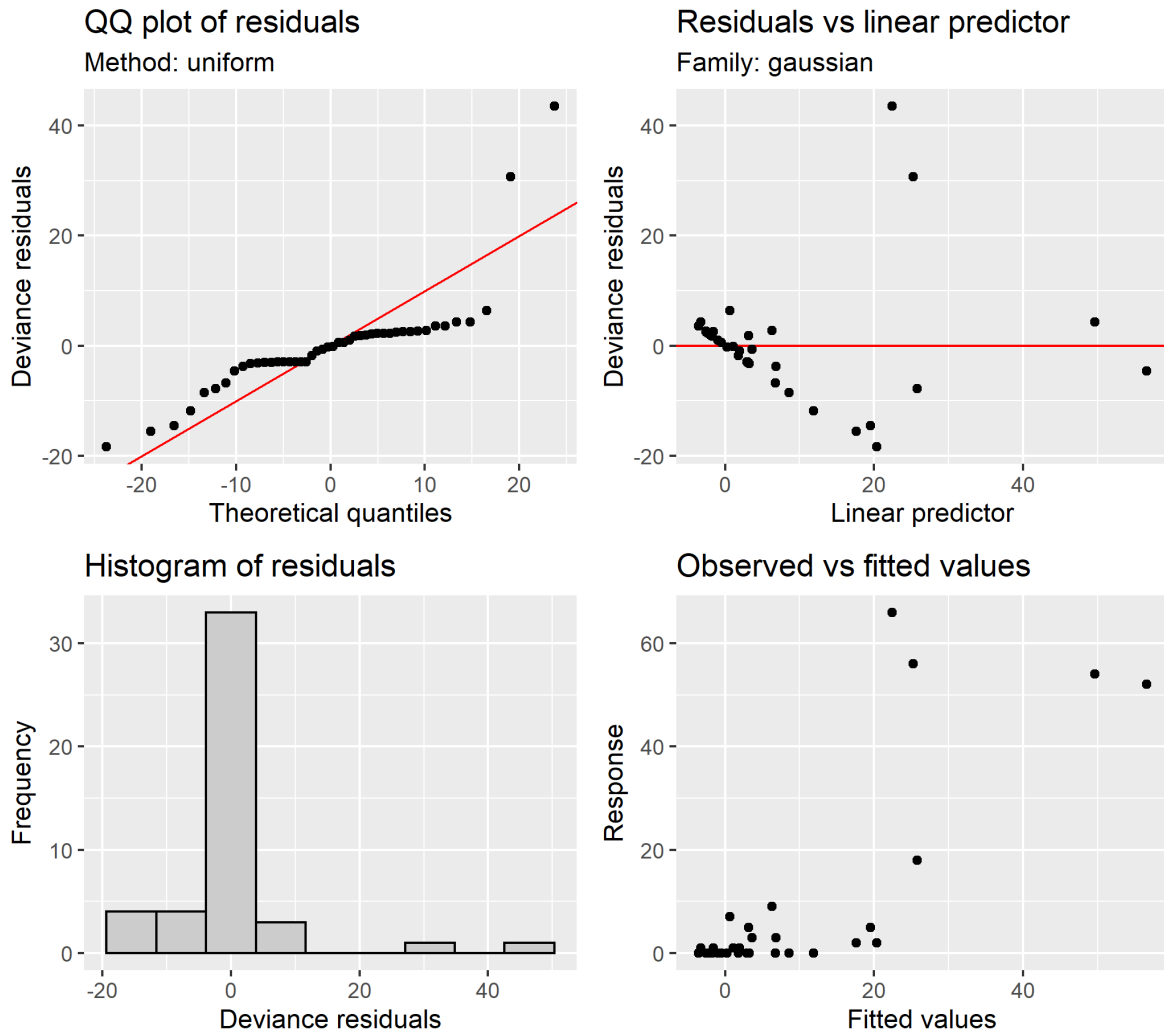
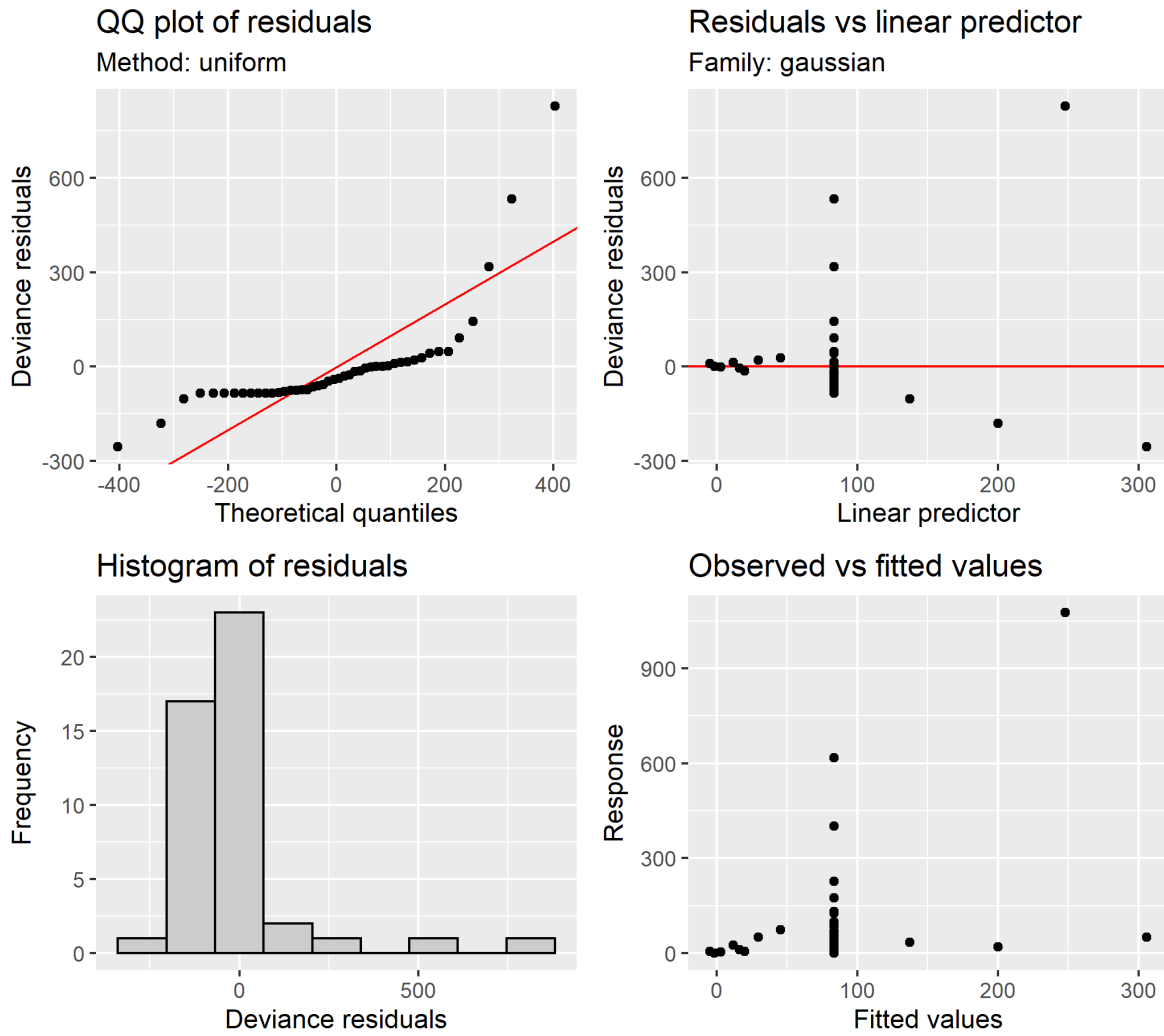*Figure C6. Diagnostic plot for a GAM of Baetidae abundance as a function of velocity each month.*

Figure C7. Diagnostic plot for a GAM of Chironomidae abundance as a function of velocity each month.
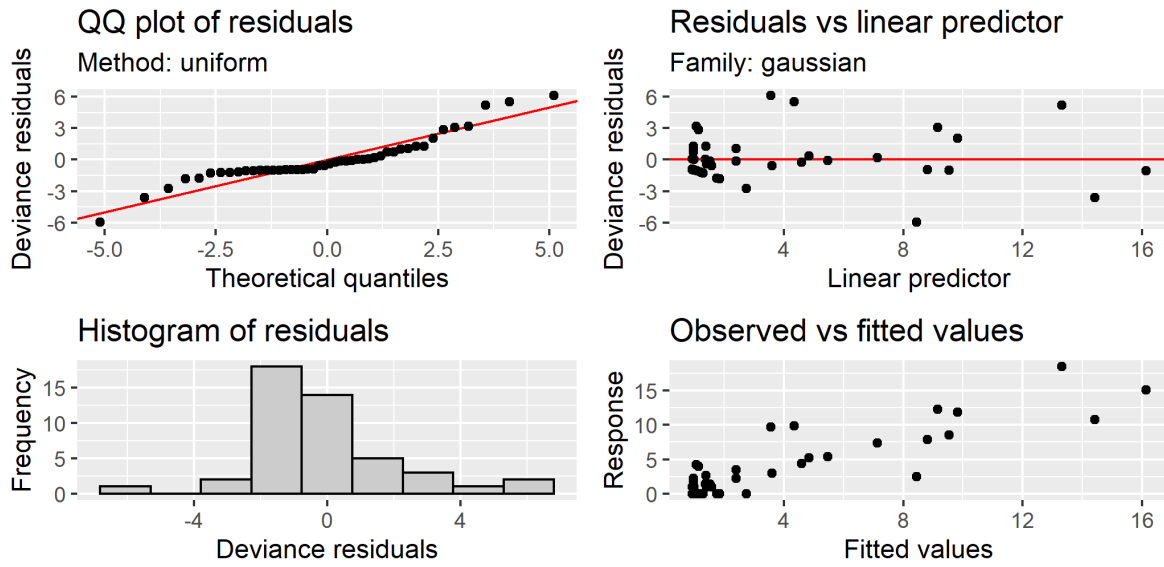
Figure C7. Diagnostic plot for a GAM of Dace Prey abundance as a function of depth and velocity.
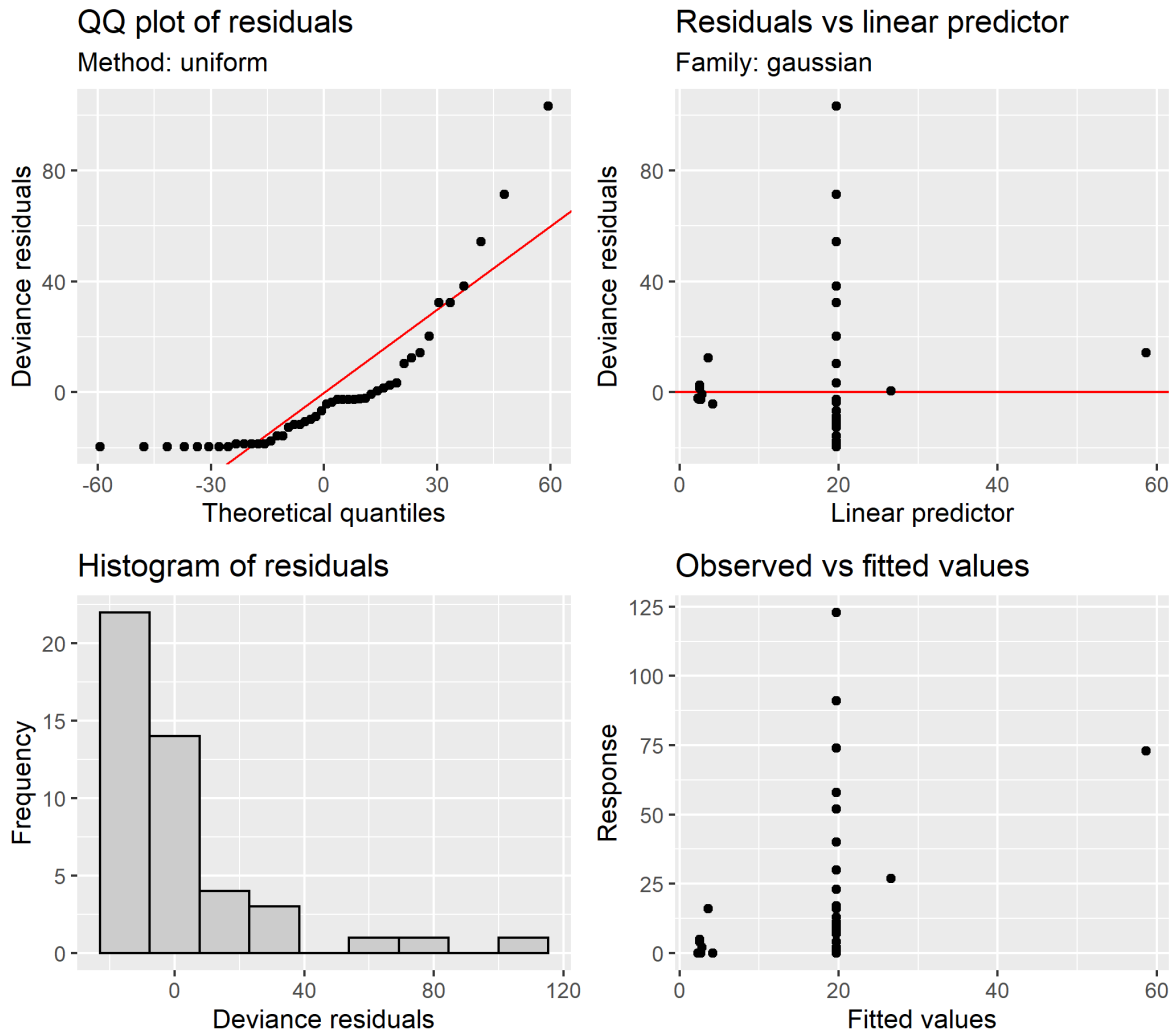
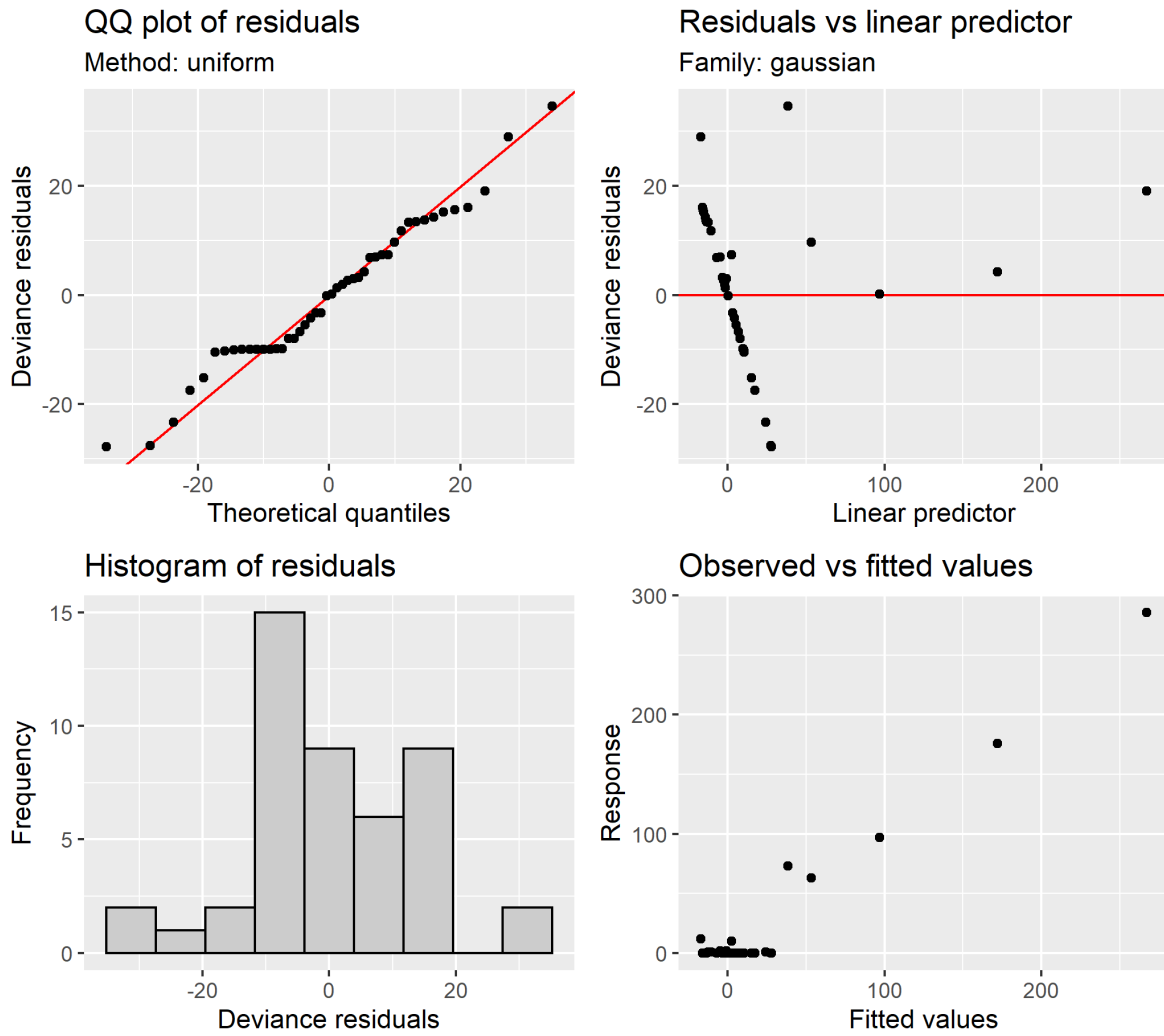*Figure C8. Diagnostic plot for a GAM of Chironomidae abundance as a function of velocity each month.*

Figure C9. Diagnostic plot of Gammaridae abundance as a function of velocity each month.

APPENDIX D. GENERALIZED ADDITIVE MODEL CONSTRUCTION

The GAMs for total macroinvertebrate abundance and Dace Prey abundance were built using Equation D1:

$$Y \sim s(x_1) + s(x_2) + s(x_3) + s(x_4) \qquad \text{(D1)}$$

The initial models were constructed by selecting the predictors and making a reasonable estimate of the functional form of their relationship to the response variable (i.e., Dace Prey abundance or total abundance). The $s(x_i)$ terms in Equation (D1) are smooth functions of the predictor variables included in the model, velocity (x_1), depth (x_2), substrate (x_3), and dissolved oxygen (x_4). The GAMs were fit using Reduced Maximum Likelihood (REML) smoothing parameter estimation, which is considered to be the most stable method (Wood, 2017). The distributional family, which defines the distribution of the response conditional on the covariates, was set as Gaussian. While Poisson and quasi-Poisson distributions are often used to model count data, consequences of violating these distributions are severe, whereas Gaussian models are more robust to violations (Hoef and Boveng, 2007; Knief and Forstmeier, 2018). The double penalty approach was used to identify important model variables (Marra and Wood, 2011; Simpson, 2019). In the GAM results, variables with flat horizontal functions (i.e., effective degrees of freedom equal to zero), were effectively removed from the model because the simpler model was better at explaining stream temperature patterns (Marra and Wood, 2011; Simpson, 2019).